REPORT NO.
UC SESM 74-5

STRUCTURES AND MATERIALS RESEARCH
DEPARTMENT OF CIVIL ENGINEERING

STRUCTURAL BEHAVIOR OF A CURVED TWO SPAN REINFORCED CONCRETE BOX GIRDER BRIDGE MODEL

VOL. I – DESIGN, CONSTRUCTION, INSTRUMENTATION AND LOADING

by

A. C. SCORDELIS
J. G. BOUWKAMP
P. K. LARSEN

In cooperation with the State of California, Business and Transportation Agency, Department of Transportation and the U. S. Department of Transportation, Federal Highway Administration.

SEPTEMBER 1974

COLLEGE OF ENGINEERING
OFFICE OF RESEARCH SERVICES
UNIVERSITY OF CALIFORNIA
BERKELEY CALIFORNIA

Structures and Materials Research
Department of Civil Engineering
Division of Structural Engineering
and
Structural Mechanics

UC-SESM Report No. 74-5

STRUCTURAL BEHAVIOR OF A CURVED TWO SPAN REINFORCED CONCRETE BOX GIRDER BRIDGE MODEL

VOL. I - DESIGN, CONSTRUCTION, INSTRUMENTATION AND LOADING

by

A. C. Scordelis
J. G. Bouwkamp
Professors of Civil Engineering

and

P. K. Larsen
Assistant Research Engineer

In cooperation with

State of California
Business and Transportation Agency
Department of Transportation
Under Research Technical Agreement
No. 13945-14647
and
U.S. Department of Transportation
Federal Highway Administration

College of Engineering
Office of Research Services
University of California
Berkeley, California

September 1974

TECHNICAL REPORT STANDARD TITLE PAGE

1. Report No.	2. Government Accession No.	3. Recipient's Catalog No.

4. Title and Subtitle	5. Report Date
STRUCTURAL BEHAVIOR OF A CURVED TWO SPAN REINFORCED CONCRETE BOX GIRDER BRIDGE MODEL, VOL. I - DESIGN, CONSTRUCTION, INSTRUMENTATION AND LOADING	September 1974
	6. Performing Organization Code
7. Author(s)	8. Performing Organization Report No.
A. C. Scordelis, J. G. Bouwkamp, P. K. Larsen	UCSESM 74-5
9. Performing Organization Name and Address	10. Work Unit No.
Department of Civil Engineering University of California Berkeley, California 94720	11. Contract or Grant No. HPR - 1 (12) D04110
	13. Type of Report and Period Covered
12. Sponsoring Agency Name and Address	Final Report
California Department of Transportation Sacramento, California 95807	14. Sponsoring Agency Code RTA 13945 - 14647

15. Supplementary Notes

Prepared in cooperation with the State of California, Business and Transportation Agency, Department of Transportation and the U.S. Department of Transportation, Federal Highway Administration.

16. Abstract

This is the first of a three volume sequence as follows: Vol. I - Design, Construction, Instrumentation and Loading; Vol. II - Reduction, Analysis and Interpretation of Results; and Vol. III - Detailed Tables of Experimental and Analytical Results. In the present volume a detailed study of the instrumentation, construction and testing of a large scale, horizontally curved, two span, four cell, reinforced concrete box girder bridge model is presented. The selection of the model scale, the choice and location of instrumentation, and the system of data acquisition are discussed. The reinforcement and the dimensions of the model are given. A complete description of the experimental program is presented. A loading schedule incorporating the various types of loading, support conditions and stress levels is described. Results of control tests on steel and concrete are given.

17. Key Words	18. Distribution Statement
Curved box girder bridge; continuous box girder; reinforced concrete model; large scale model; experimental study; dead load; live load; overloads; ultimate strength; measurement of reactions, deflections and strains.	Unlimited

19. Security Classif. (of this report)	20. Security Classif. (of this page)	21. No. of Pages	22. Price
Unclassified	Unclassified	136	

Form DOT F 1700.7 (8-69)

DISCLAIMER

The contents of this report reflect the views of the authors who are responsible for the facts and the accuracy of the data presented herein. The contents do not necessarily reflect the official views or policies of the State of California or the Federal Highway Administration. This report does not constitute a standard, specification or regulation.

ABSTRACT

This is the first of a three volume sequence as follows: Vol. I - Design, Construction, Instrumentation and Loading; Vol. II - Reduction, Analysis and Interpretation of Results; and Vol. III - Detailed Tables of Experimental and Analytical Results. In the present volume a detailed study of the instrumentation, construction and testing of a large scale, horizontally curved, two span, four cell, reinforced concrete box girder bridge model is presented. The selection of the model scale, the choice and location of instrumentation, and the system of data acquisition are discussed. The reinforcement and the dimensions of the model are given. A complete description of the experimental program is presented. A loading schedule incorporating the various types of loading, support conditions and stress levels is described. Results of control tests on steel and concrete are given.

KEYWORDS

Curved box girder bridge; continuous box girder; reinforced concrete model; large scale model; experimental study; dead load; live load; overloads; ultimate strength; measurement of reactions, deflections and strains.

TABLE OF CONTENTS

LIST OF TABLES

LIST OF FIGURES

1. INTRODUCTION

1.1 Objective

The objective of the investigation was the construction, instrumentation and testing of a horizontally curved, continuous, two span, four cell, reinforced concrete box girder bridge model, Fig. 1.1, so as to produce reliable experimental data on curved box girder bridge behavior, with emphasis on load distribution among girders, and to compare these findings with results from analytical studies to evaluate the validity of analytical methods used for design. In order to ascertain the effect of the curvature on the structural response,the results were also to be compared with the experimental results from a similar straight box girder bridge previously tested and reported on in detail [9, 10, 11]. The effects of several loading and support conditions and the importance of a midspan diaphragm with reference to load distribution characteristics were also to be assessed.

These studies were to be carried out for dead load,for point loads placed over the girder webs at selected locations, and for vehicle type loads. The point loads were to be applied after the bridge model had been subjected to working load stresses as well as high levels of overload. A final loading to failure was to be applied to study ultimate strength behavior and modes of failure.

The adequacy of existing design procedures for box girder bridges was to be evaluated on the basis of the results of the investigation and suggested improvements were to be made in these procedures where deemed appropriate.

The present volume is the first of a three volume sequence on the "Structural Behavior of a Curved Two Span Reinforced Concrete Box Girder Bridge Model." The material included in each volume is as follows:

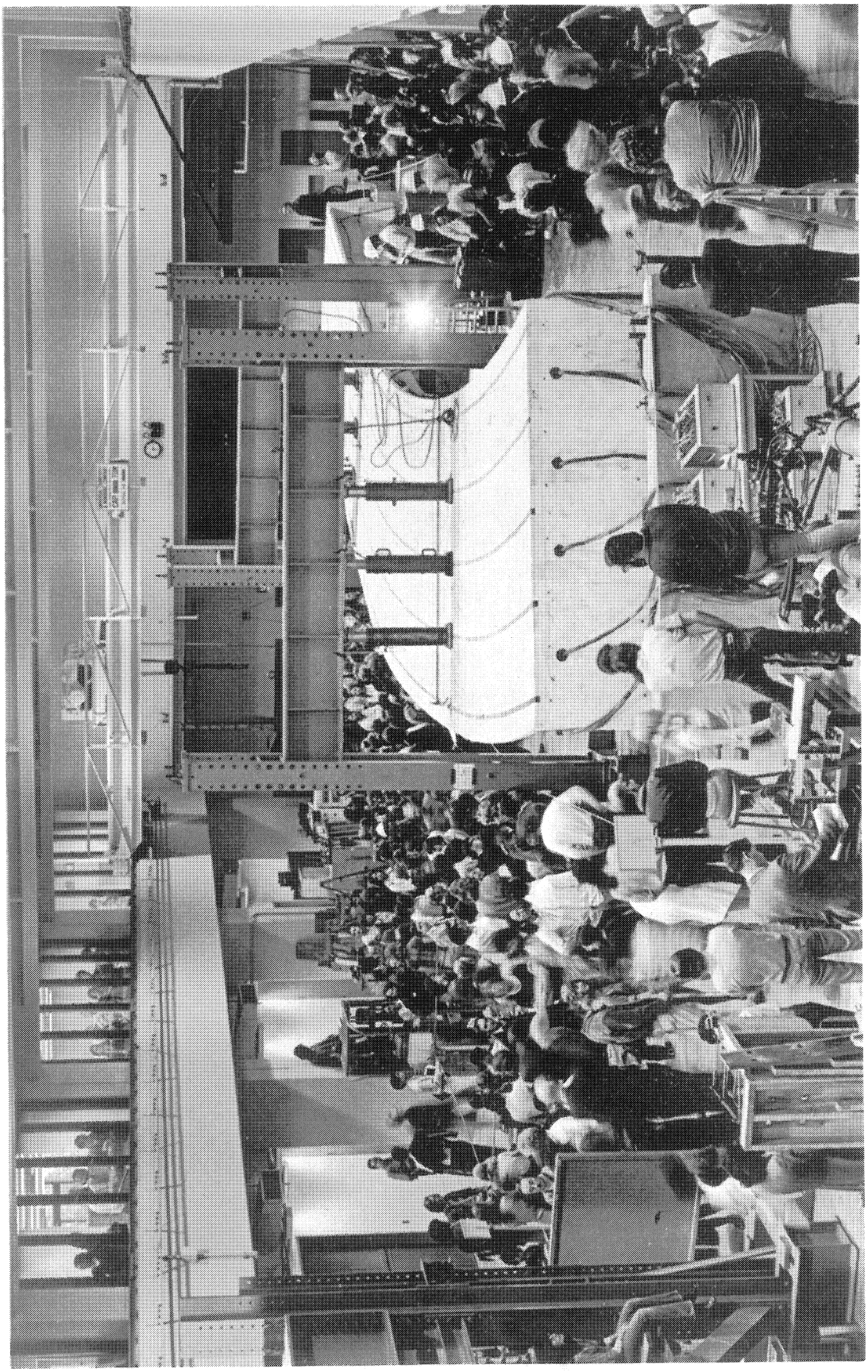

FIG. 1.1 FINAL LOAD TEST ON CURVED BOX GIRDER BRIDGE MODEL

Vol. I - Design, Construction, Instrumentation and Loading.

Vol. II - Reduction, Analysis and Interpretation of Results.

Vol. III - Detailed Tables of Experimental and Analytical Results.

1.2 General Remarks

Bridge systems of various types are extensively used in the highway network of California, the United States and elsewhere. The reinforced concrete box girder or hollow girder type of bridge began to be employed some thirty years ago in Europe where materials, as opposed to labor, were then relatively expensive. The use of intricate formwork enables the connection of plate-like elements to obtain a cellular or box-like structure, Fig. 1.2, that is rigid and has a high resistance to torsional moments. Through extensive use, the box girder bridge has become economically competitive and is at the same time aesthetically attractive in appearance. The latter fact is of importance especially when freeways and highway systems penetrate populated industrial and residential districts. The box girder bridge is a smooth, functional structure with the added asset of providing space within itself to carry utilities safely. It also can easily be adapted to the complex geometry required from the design of the highway itself.

As a natural development of all these qualities, the use of box girder bridges in reinforced and prestressed concrete has increased tremendously, particularly throughout California where contractors have acquired familiarity with their construction. In the span ranges between 60 ft. and 100 ft., reinforced concrete bridges are used, while for the longer spans becoming more prevalent today, post-tensioned prestressed bridges are used extensively. In terms of the total bridge deck area built in California each year, the percentage for cast-in-place, reinforced plus prestressed,

box girder bridges was 66%, 66%, 78%, 84% for 1968, 1969, 1970, 1971 respectively.

A typical concrete box girder bridge, Fig. 1.2, consists of a top and bottom slab monolithically joined to each other by vertical webs to form a box-like or cellular structure. Most box girder bridges are also provided with transverse diaphragms at the ends and at points of interior support. Other structural characteristics include interior diaphragms between supports and sloping or rounded exterior webs. Plan geometries may be straight, curved, skew or of an arbitrary nature to adapt to the highway alignment.

Continuous bridges are often improved in appearance by the provision of single column bents at the interior supports.

A study of over 200 box girder bridges in California [1] reveals that the majority of the bridges had a depth-span ratio ranging from 0.050 to 0.065, a top slab-thickness of 6 to 7 in., a bottom slab thickness of 5 1/2 in. and web thicknesses of 8 in. Typical cell widths were between 7 and 9 ft., with most bridges possessing 3 to 9 cells.

In spite of the variety of box girder bridges in use, most design calculations for these bridges depend on simple empirical formulas that do not always reflect the true behavior of the structural system. Thus, current design methods for continuous box girder bridges of the type built and tested in this investigation are based on considering either typical repeating units of the cross-section as independent continuous beams or the entire cross-section as a whole unit. For transverse and longitudinal slab moments, as well as for the study of wheel loads on bridge decks, empirical expressions are used. The effect of the curvature in the horizontal plane is in many cases neglected, or included by using approximations or engineering judgement only.

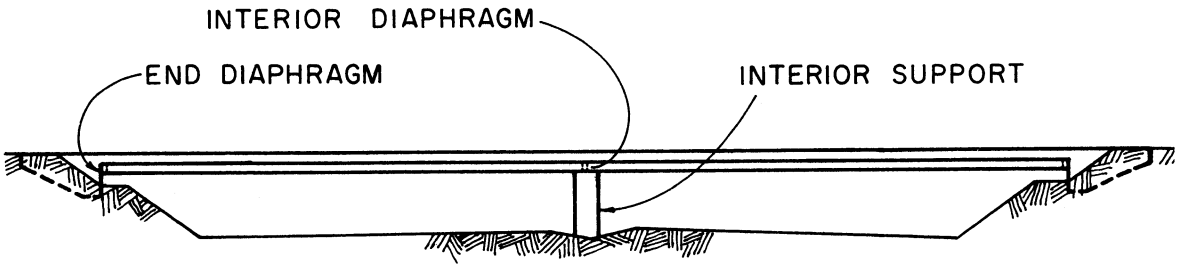

a) ELEVATION OF TYPICAL CONTINUOUS BOX GIRDER BRIDGE

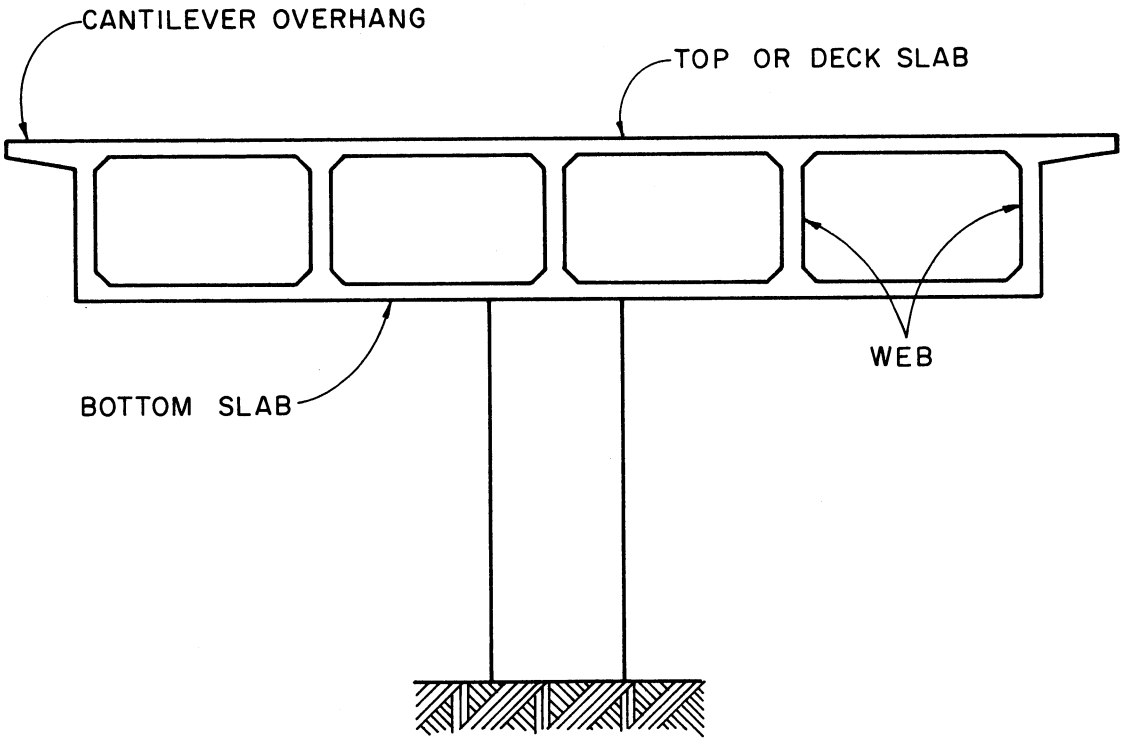

b) CROSS-SECTION OF BOX GIRDER BRIDGE WITH INTERIOR SUPPORT

FIG. 1.2 MULTI-CELL REINFORCED CONCRETE BOX GIRDER BRIDGE

In view of the above, it is evident that for considerations of efficiency and economy, theoretical and experimental work dealing with curved box girder bridges is necessary to improve the design of this important bridge type.

1.3 Previous Studies

Because of their widespread use in California, a continuing program of research on box girder bridges has been conducted at the University of California at Berkeley for several years. A systematic plan was initially developed to study successively straight, simple and continuous bridges, skew bridge and curved bridges. For each of these configurations the approach has been to: (1) study the available literature; (2) develop analytical methods and general computer programs; (3) perform experimental studies on elastic models to verify the analytical methods developed if deemed necessary; (4) make analytical parameter studies; (5) test large scale reinforced concrete models or prototypes; and (6) develop recommended design procedures. The results of this research have been reported in a series of research reports [1 - 16] and technical papers [17 - 27].

Of particular interest to the present study are references 6, 7, 8 and 12, which describe analytical methods and computer programs which can be used to analyze curved box girder bridges. Reference 8 presents a comprehensive study of the analysis and design of curved box girder bridges. It describes the following subjects: (1) bridge geometric parameters as governed by highway design; (2) methods of analysis; (3) computer programs for analysis; (4) structural behavior of curved box girder bridges based on the analysis of bridges with various parameter changes; and (5) tentative design recommendations. Reference 16 presents the results of a detailed experimental study of six small scale aluminum models of a

four cell curved box girder bridge. Several spans and midspan diaphragm conditions were investigated. Experimental results from these elastic models were compared with analytical results to verify the methods of analysis previously developed for uncracked homogeneous systems. In the present study, a large scale curved reinforced concrete model was tested to evaluate the validity of these same analytical methods in predicting the structural response of an actual structure, which experiences cracking and is non-homogeneous, being composed of concrete and steel reinforcement.

Few comprehensive experimental and analytical studies of reinforced concrete box girder bridges have been made to date. For straight bridges, results presented by Davis et al [28], and in the work by Scordelis et al [9, 10, 11], which preceded the present investigation, gave valuable information on the behavior of straight box girder bridges both at the working stress level and at failure.

Because of the large increase in highway construction in the United States during the past decade, an extensive nationwide program of research on the structural behavior of various types of bridges has been undertaken at a number of other institutions in addition to the University of California. Investigations at various institutions have tended to concentrate on bridge types common to the local state or area. A comprehensive investigation of curved girder bridges (primarily steel) is being conducted by a Consortium of University Research Teams (CURT) consisting of Syracuse University, Carnegie Mellon University, University of Rhode Island, and University of Pennsylvania. No attempt will be made herein to review the many excellent publications that have resulted from these investigations since they are not directly pertinent to the subject of this report.

1.4 Present Design Methods

The present method of box girder design for live loads employs the AASHO standard HS 20-44 truck with a width of 10 ft. For the purpose of most studies, the spacing between axles is taken as 14 ft. to produce maximum stress. In each span of the box girder bridge, one HS 20-44 truck is placed per traffic lane in a position that will produce maximum stress.

The 1973 AASHO Specifications [29] specify a design method wherein a box girder bridge is considered to be made up of a number of identical I-shaped interior girders plus two exterior girders that lack half a bottom flange each, as in Fig. 1.3. According to these specifications, each girder is designed as a separate member by applying to it a certain fraction of a single longitudinal line of wheels from the standard truck. This fraction, known as the number of wheel loads N_{WL}, is given by the relations

$$N_{WL} = S/7 \quad \text{for interior girders} \tag{1.1}$$

and

$$N_{WL} = S_1/7 \quad \text{for exterior girders} \tag{1.2}$$

S is the flange width in feet of the interior girder, which is also equal to the average width of the cell, and S_1 is the top flange width in feet of the exterior girder, which is also equal to half the cell width plus the cantilever overhang.

In December 1967 the State of California put forward a design specification in which the distinction between S_1 and S was abolished and the total value of the distribution factor N_{WL} for the "whole-width unit" was given by

$$N_{WL}\ (\text{total}) = \frac{\text{Deck width in feet}}{7} \tag{1.3}$$

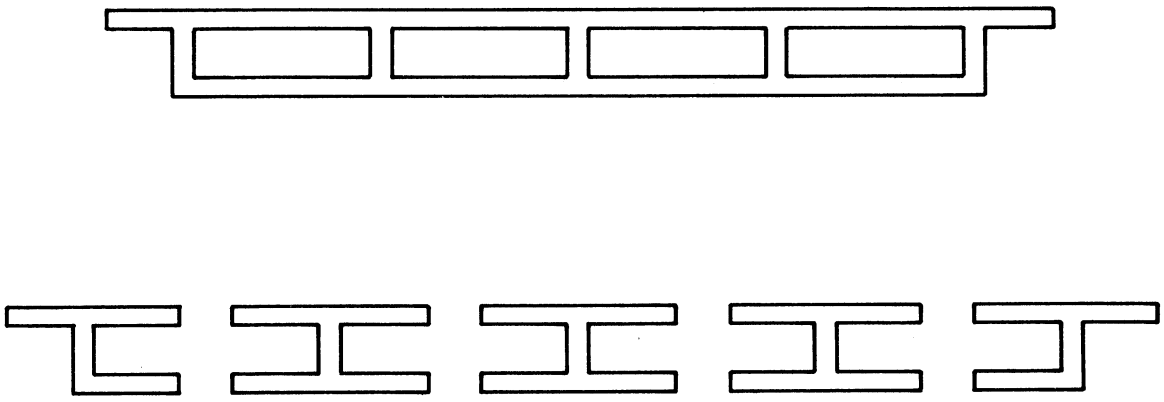

FIG. 1.3 DESIGN MODEL FOR BOX GIRDER BRIDGE

These changes were indications of the recognition of the structural efficiency of the box girder section, but they also called into question the whole process of bridge design based on distribution factors. Scordelis and Meyer [3] have pointed out that the most important variable not taken into account by the AASHO specifications is the number of traffic lanes on the bridge, and have demonstrated that a two-lane box girder bridge of conservative design could be changed into an unconservatively designed three-lane bridge by minor adjustments in the widths of the barrier curbs alone. Other factors such as span, total width, number of cells and continuity or fixity at the supports also influence the load distribution and should be considered. A tentative empirical design formula incorporating these factors for straight box girder bridges was proposed by Scordelis and Meyer [3] based on the analysis of a large number of bridges for which important parameters were varied.

A comprehensive study of the distribution of wheel loads on all types of highway bridges has been made by Sanders and Elleby [30]. Their study was restricted to straight bridges of short to intermediate span length (20 to 130 ft.). For concrete box girder bridges, they used the computer programs developed at the University of California [1, 2] to analyze a large number of straight box girder bridges in which the following variables were studied: (1) span length; (2) overall width; (3) overall depth of the cross section; (4) number of girders or cells; (5) number of transverse diaphragms; (6) thickness of webs and flanges; and (7) edge conditions. On the basis of these studies they have recommended that the present AASHO formula for live load distribution, Eq. (1.1), be replaced by a more realistic, but more complex, empirical formula incorporating many of the parameters described in the preceding paragraph.

It should be noted that the AASHO design specifications do not make any distinction between straight and curved box girder bridges. The effect of the curvature on the transverse distribution of load to each girder must therefore be decided by the designer, based on a more exact analysis, approximations or engineering judgement.

Both analysis and design find their ultimate confirmation in the behavior of a real structure. The shortcomings of the design procedures for concrete box girders having been briefly touched upon, some consideration must also be given to the present state of the analytical methods. The theoretical approaches referred to earlier incorporate highly sophisticated analytical models, which necessitate the use of large capacity electronic computers to obtain solutions for displacements and internal forces and moments.

The analytical model, however, assumes that the plates forming the box girder are elastic isotropic and homogeneous, and that a linear relationship between forces and deformations exists. The true response for a concrete box girder bridge is highly complicated, and involves a non-homogeneous structure made up of two materials, concrete and steel. Under increasing load the concrete cracks and stress redistributions occur. Time dependent effects such as shrinkage and creep in the concrete also affect displacements and internal stresses and are a function of the environment of the prototype.

Only by experimental observations of the behavior of actual reinforced concrete box girder bridges under controlled conditions can it be ascertained if the proposed analytical methods, based on the assumed analytical model described above, adequately predict the load distribution properties, the magnitudes of displacements, internal forces and moments, and the effects of interior diaphragms.

For curved reinforced concrete box girder bridges, however, no experimental data is available at the present time. It is therefore the purpose of the present investigation to provide such experimental data that will permit the structural behavior of this class of bridges to be more fully understood under loadings in the elastic, inelastic and ultimate ranges.

1.5 Scope of Present Investigation

This investigation was concerned with all phases of a large scale,horizontally curved, continuous, two-span, four cell, reinforced concrete box girder bridge model including the planning, construction, instrumentation and testing. The bridge model had two 36 ft. spans and thus had a total length of 72 ft. measured along the center line. It was 12 ft. wide and had a depth of 1 ft. 8-9/16 in. The center line radius of curvature in the horizontal plane was 100 ft. The model to prototype geometric scale was 1:2.82. Therefore, the prototype bridge had two 101.5 ft. spans and overall dimensions of 203 ft. long, 34 ft. wide , 4 ft. 10 in. in depth and a radius of curvature of 282 ft.

The prototype chosen was a typical two-lane bridge with a single column bent at the center providing interior support. Many reinforced concrete box girder bridges of this kind are in actual service in California as part of the highway network, and span distances of up to 200 ft.

In order to study the history of the bridge model from the dead load condition through service loads into the ultimate load range, the model was instrumented during construction. Steel tensile strains were measured by 144 weldable waterproofed strain gages and concrete compressive strains were registered by 72 concrete strain meters. For the measurement of loads and reactions, 20 load cells were used, and 24

linear potentiometers measured vertical deflections of the bridge at various locations.

The proper simulation of prototype dead load behavior was accomplished by the placing of steel billets of the required weight within the cells of the box girder model. The variation in strains and reactions prior to the removal of shoring was monitored by means of SR-4 indicator boxes and switching units. This procedure allowed an evaluation of the effect of differential shrinkage and creep during the construction and curing phases.

The loading schedule for the box girder bridge model consisted of loading patterns to provide information on different aspects of structural behavior. Live load distribution properties of the box girder section were evaluated by point loads singly and in several combinations at each girder. Scaled-down models of trucks and heavy construction vehicles, and a moving load were also used. Multiple and symmetrical loads were applied to test the validity of the principle of superposition. Special attention was paid to the successive deterioration of the structure under phases of loadings inducing stresses higher than the allowable design stresses. Loading of the box girder bridge model to failure was also studied.

For the application of the live loads, two load frames were designed and constructed. Subsequently, one was assembled at each midspan and enabled live loads to be applied by means of jacks in various combinations.

For each of the above loading cases, signals from the measuring gages and meters were fed into the S.E.S.M. Low Speed Scanner, consisting of a portable computer of 8k storage, a digital voltmeter unit, a teletype and four terminal boxes. Each terminal box contained dummy

resistors to balance the gage circuits, as well as a channel to which a standard resistor of invariable resistance was hooked to provide a check on the system.

The portable computer was programmed for strain, deflection and reaction calculations so that at every loading step each gage or meter was scanned five times and the readings averaged. The data difference from the pre-load condition was obtained in print through a teletype and also recorded on punched paper tape. A total of 450 sets of scanner readings was taken during the experimental program.

The data reduction operations consisted of organizing and editing the measured values of strains, reactions and deflections by means of computer programs before quantities of interest, e.g. moments, forces were calculated systematically.

The comparison of these quantities with theoretical values based on existing analyses was carried out, and discrepancies were studied.

The accuracy and extent to which the bridge model simulated the prototype was examined. Independently, crack propagation and time-dependent effects were also observed.

Underlying the present investigation in all its aspects was the desire to interpret all the information from the point of view of better design, or at least to obtain the information for this goal.

2. DESCRIPTION OF MODEL

2.1 Advantages of Model Testing

Model testing of structures in the laboratory is superior to the testing of prototypes in several ways. Large scale models (between quarter and half scale) are particularly useful because their behavior can duplicate prototype behavior to a high degree of accuracy.

The testing of a box girder bridge model in the laboratory eliminates the uncertainties and lack of precision that characterize field testing. Temperature and humidity conditions are stable, and there is no interruption from traffic or other sources.

Smaller live loads are required to produce large stresses in models, and because testing models to destruction is normal routine, the behavior of the structure in the post-service range, its deterioration and ultimate load characteristics can be observed. Often the construction and testing of a model is more economical when all factors are considered than the instrumentation and testing of a prototype.

As opposed to these advantages, the simulation of the dead load effects of the prototype requires the addition of a large amount of extra dead weight to the model if the response under working load conditions with simulated live loads is to be studied.

2.2 Dimensional Analysis

For the dimensional analysis of a structure, the independent or basic dimensions must first be selected. All significant variables are then represented in terms of these dimensions.

For problems of structures where static loading and testing are involved, the force dimension F and the characteristic dimension of

length L are usually chosen as basic dimensions. Other variables of interest can be tabulated thus:

Variable	Notation	Dimension in Terms of F and L
Deflection	δ	L
Strain	ε	0
Poisson's ratio	ν	0
Elastic Modulus	E	$F\,L^{-2}$
Moment of Inertia	I	L^4
Area	A	L^2
Unit weight of material	γ	$F\,L^{-3}$

It is to be noted that depending on their significance in the model study, variables may be added to or omitted from the above list.

According to the Buckingham Pi theorem, dimensionless terms formed from the above variables must be equal for both the model and the prototype if a true model is to be obtained. In the present case the dimensionless Pi terms are as follows:

$$\pi_1 = \delta/L \qquad \pi_5 = I/L^4$$

$$\pi_2 = \varepsilon \qquad \pi_6 = A/L^2$$

$$\pi_3 = \nu \qquad \pi_7 = \gamma/(F\,L^{-3})$$

$$\pi_4 = E/(F\,L^{-2})$$

The condition for true representation of prototype properties by the model can therefore be stated in the form

$$\pi_{im} = \pi_{ip} \quad \text{where} \quad i = 1, 2 \ldots 7$$

2.3 Selection of Scale and Design of Model

The box girder bridge model of the present investigation was a "direct method" model with a linear scale relationship $L_m:L_p = 1:2.82$, where the subscripts m and p stand for model and prototype respectively. The direct method model allows the determination of forces, moments or stresses in the prototype under a certain load directly from a study of the model, the load on the model in this case being, of course, appropriately scaled down. The "indirect method" of model testing commonly uses distorted models and only the elastic behavior of a structure can be fully investigated. The direct method is especially suitable for the determination of the ultimate load carrying capacity of the prototype structure, as the behavior of the structure in the elastic and post-elastic states can be examined.

The linear scale of 1:2.82 was chosen for the box girder bridge model so as to enable the use of standard high strength steel deformed bars as reinforcement, in place of annealed wire commonly used in small scale models. The scale was determined by replacing the standard longitudinal reinforcement of an actual box girder bridge, i.e. a No. 11 deformed bar of nominal cross-sectional area 1.56 sq. in. by a No. 4 deformed bar of nominal cross-sectional area 0.20 sq. in. in the model. Then the relation $L_m:L_p = \sqrt{A_m}:\sqrt{A_p}$ provided the scale 1:2.82.

An advantage of using standard reinforcing bars in place of steel wire is that bond behavior is realistically represented by the reinforcing bars. Bonding in reinforced concrete is a complex phenomenon based on adhesion and the resistances to slip produced by the lugs on a deformed reinforcing bar. In some models where steel wire is used to represent deformed reinforcing bars, a process of corrosion is employed

to obtain a pitted surface on the wire, but this is a costly and unsatisfactory process.

A reduction in the number of reinforcing bars is often made in models when the reinforcement becomes very fine. In the present case this was not adopted, the attempt throughout being at a scaling down of an actual box girder bridge.

The large scale enabled the use of concrete rather than a mortar mix as the model material; the emphasis, once again, being on an accurate simulation of the prototype. It was thus possible to satisfy the relations $E_m = E_p$ and $\nu_m = \nu_p$ for the model and prototype to a reasonable degree.

It can be observed that the equations connecting the chosen variables for the box girder bridge model and the prototype were the following:

$$\delta_m = \delta_p/2.82 \qquad I_m = I_p/64$$

$$\varepsilon_m = \varepsilon_p \qquad A_m = A_p/8$$

$$F_m = F_p/8 \qquad \gamma_m = 2.82\ \gamma_p$$

Given all the above conditions, equal strains and stresses would be obtained at homologous (i.e. corresponding) points in the prototype and the model.

The only difficulty in satisfying these relations lay in having to make the unit weight of the model equal to 2.82 times that of the prototype while keeping the elastic modulus and Poisson's ratio unchanged. The best solution was the artificial addition of extra dead weight which, added to the weight of the model, would result in 2.82 times the weight of the model itself. Various schemes of realizing this considerable load-

ing (equivalent for the model bridge in the present study to an extra weight of about 1.57 kips/ft.) were examined in detail. It was decided that the most convenient and least expensive way of providing the extra dead load for proper simulation of prototype conditions lay in renting steel billets of approximately 9 in. x 9 in. x 65 in. dimensions from a local manufacturer and placing these suitably within the cells of the box girder bridge model during its construction. This method had been used successfully in testing a similar straight bridge previously [9].

2.4 Basic Dimensions of Prototype and Model

The box girder bridge prototype was a curved two-span structure, 203 ft. long along the longitudinal center line, 34 ft. wide and 4 ft. 10 in. in depth with a radius of curature of 282 ft. It had four cells, a center bent with a circular column support, two end diaphragms and a diaphragm at one midspan. The dimensions of a typical cross-section of the prototype are given in Fig. 2.1. The basis for the selection of the prototype lay in its being a typical two lane box girder bridge of the kind extensively used in the California highway system.

The box girder bridge model was identical to the prototype in shape but not in size, being 72 ft. long along the longitudinal center line, 12 ft. wide and 1 ft. 8 9/16 in. in depth, with a radius of curvature of 100 ft.

For convenience of access and observation, it was decided to fix the height of the model so that the distance of the soffit from the level of the test floor was about 5 ft. This was done to allow unimpeded views of crack formations in the tensile zones, which could also be easily marked, at any stage of the loading.

The abutments at each end provided for the simply supported end

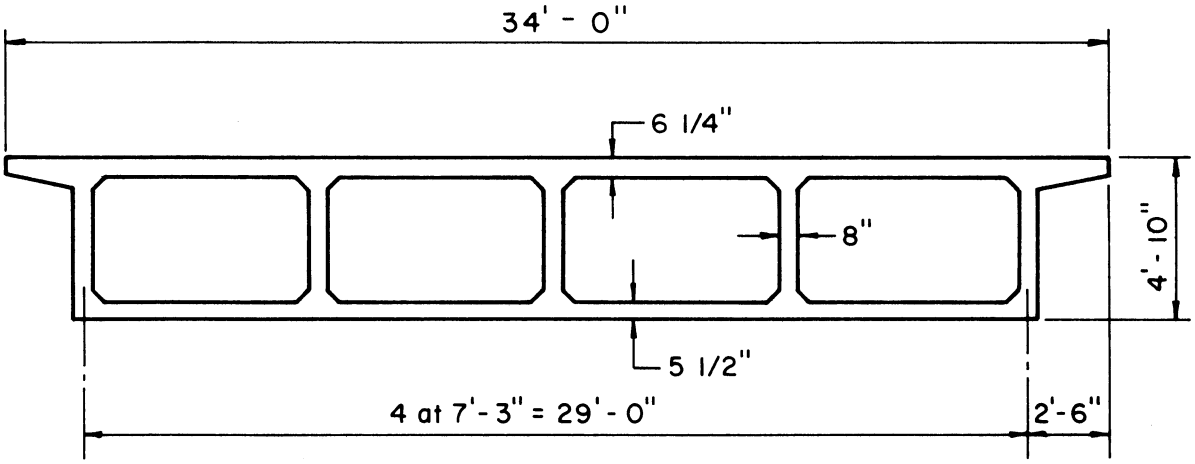

FIG. 2.1 DIMENSIONS OF TYPICAL PROTOTYPE CROSS-SECTION

condition and if desired, for restraint against longitudinal movement. Both the abutments and the square footing of the central column were anchored to the test floor by means of prestressed steel rods.

2.5 Detailed Drawings of Model

A complete set of the detailed design drawings used as part of the bidding documents for the construction of the model is given for reference in Appendix A.

The elevation, plan and typical section of the box girder bridge model with relevant dimensions are shown in Figs. 2.2 and 2.3. These figures also contain views of the end abutments and designations for significant longitudinal and transverse sections. Thus, the girders of the bridge model are identified as girders 1 to 5, with girder No. 1 taken to be on the concave (inner) side of the bridge closest to the center of horizontal curvature. For purposes of identifying locations at midbays and quarter bays, longitudinal sections between girders had also to be created. The longitudinal sections at the cantilever edge were identified as 0 and 6 respectively.

Transverse Sections A and D are locations at sections of maximum positive moment under the dead load, while Sections B and C on either side of the center bent diaphragm are in the region of maximum negative moment. Sections X and Y are the midspan sections, while Section Z is the bridge centerline. Quarter span sections are designated in accordance with proximity to another transverse section; thus QA is the quarter span section nearest Section A. Sections E and W represent sections through the East and West ends of the box girder bridge model. F denotes the square footing of the interior support as a location.

The two spans of the bridge model are designated Span I and

Span II respectively. Span I has a midspan diaphragm at Section X, while Span II has no midspan diaphragm at Section Y.

The nominal specified concrete strength f'_c was 3000 psi. A summary of actual measured properties of the concrete from control tests is given in Chapter 6. These tests indicated actual 28-day f'_c strengths ranging from 3500 to 4100 psi.

No. 2, 3 and 4 reinforcing bars with standard deformations and No. 2 plain bars without deformations were used in the construction of the model. The No. 2 undeformed plain bars were used because of the limited available supply of No. 2 deformed bars.

The nominal specified yield stress for the No. 2, 3 and 4 deformed bars was 40, 60 and 60 ksi respectively, while for the No. 2 undeformed bars it was 45 ksi. A summary of actual measured properties of these bars from control tests is given in Chapter 6. These tests indicated an actual average yield stress of 38, 61 and 70 ksi for the No. 2, 3 and 4 deformed bars respectively and 47 ksi for the No. 2 undeformed bars.

The main longitudinal reinforcement in the maximum positive moment regions consisted of 55 - No. 4 bars in the bottom slab of each span, and the main longitudinal reinforcement in the negative moment region consisted of 82 - No. 4 bars in the top slab over the center bent. As shown in the schematic drawings, Figs. 2.4a and 2.4b, some of these No. 4 bars were cut off at various distances from the midspan Section X or Y, Fig. 2.4a, or the support Section Z, Fig. 2.4b. Some additional No. 3 bars were added in the bottom and top slabs as shown in Figs. 2.4a and 2.4b. Not shown in Fig. 2.4b are 12 - No. 3 longitudinal bars continuous over Sections B, Z, C which were added at the quarter points

between webs for strain measuring purposes. This gave a total negative reinforcement over Section Z of 82 - No. 4 bars plus 12 - No. 3 bars.

Transverse reinforcement in the top and bottom slabs consisted of No. 3 bars placed in top and bottom face of each slab. Web longitudinal reinforcement consisted of continuous No. 3 bars, and the stirrups were made from No. 2 bars, both deformed and undeformed. The No. 2 deformed bars were used for the stirrups in the zones along the span where the shear forces were the highest.

Detailed drawings of all reinforcement placement may be found in Appendix A. Schematic drawings for the reinforcement in the end, midspan and center diaphragms are given in Fig. 2.5 and reinforcement for the center column and footing are shown in Fig. 2.6.

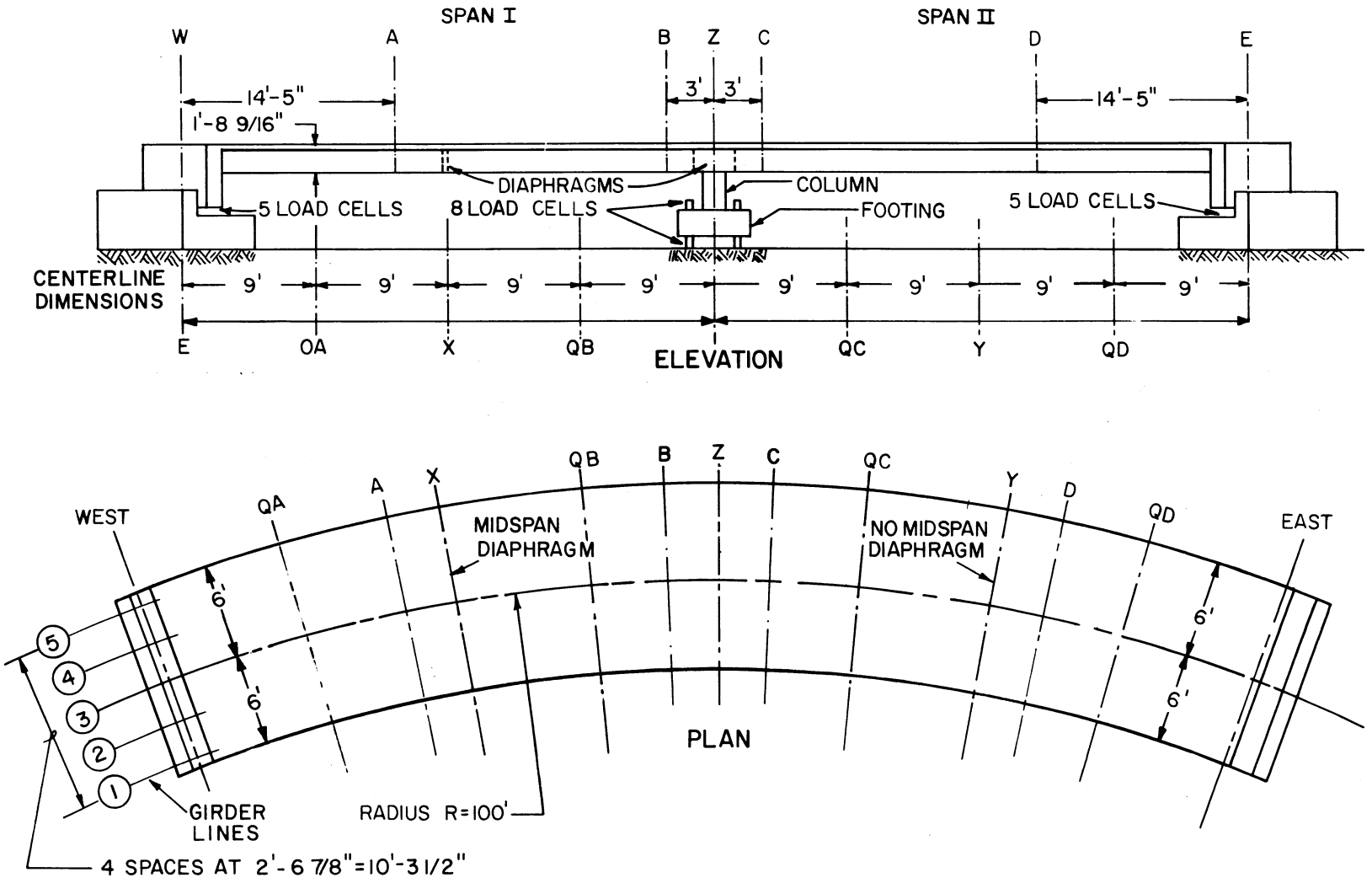

FIG. 2.2 DIMENSIONS OF BOX GIRDER BRIDGE MODEL WITH LOCATIONS OF TRANSVERSE SECTIONS AND LONGITUDINAL GIRDER LINES

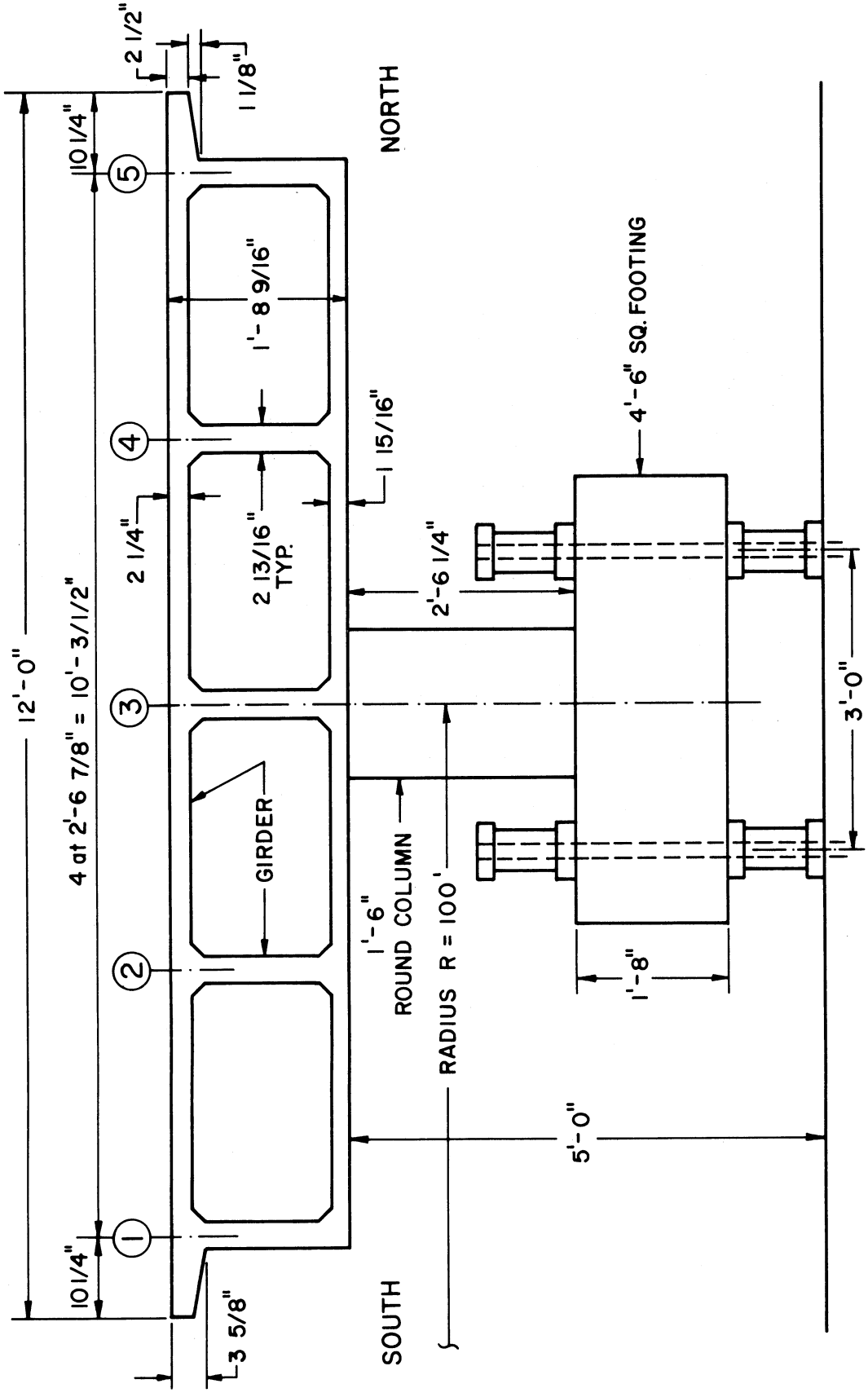

FIG. 2.3 TYPICAL SECTION OF BOX GIRDER BRIDGE MODEL

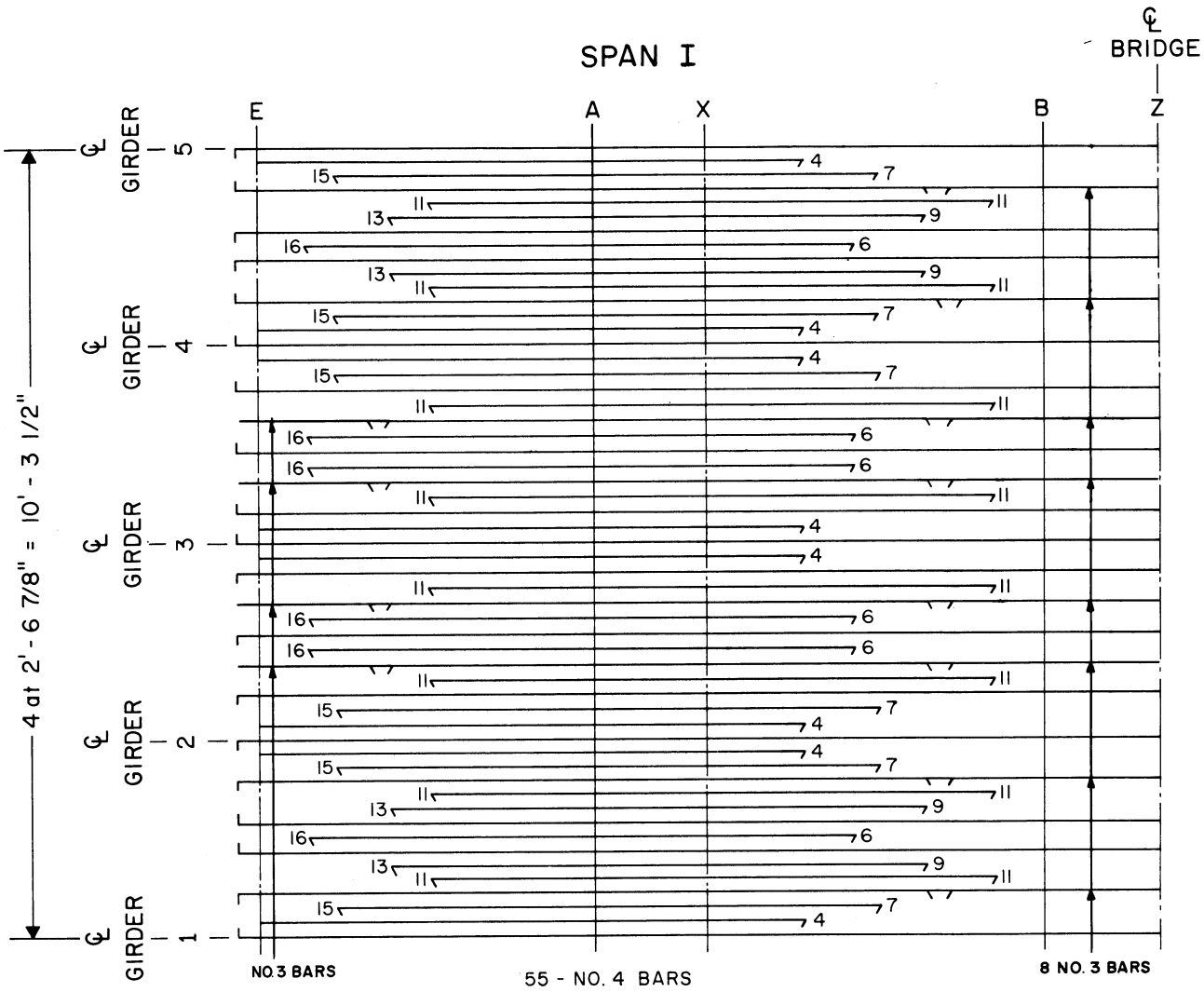

NUMBERS AT ENDS OF BARS INDICATE DISTANCE FROM MIDSPAN SECTION X IN FEET

(SPAN II REINFORCEMENT IDENTICAL)

NOT TO SCALE

CURVATURE NOT SHOWN

FIG. 2.4a BOTTOM SLAB MAIN LONGITUDINAL REINFORCEMENT

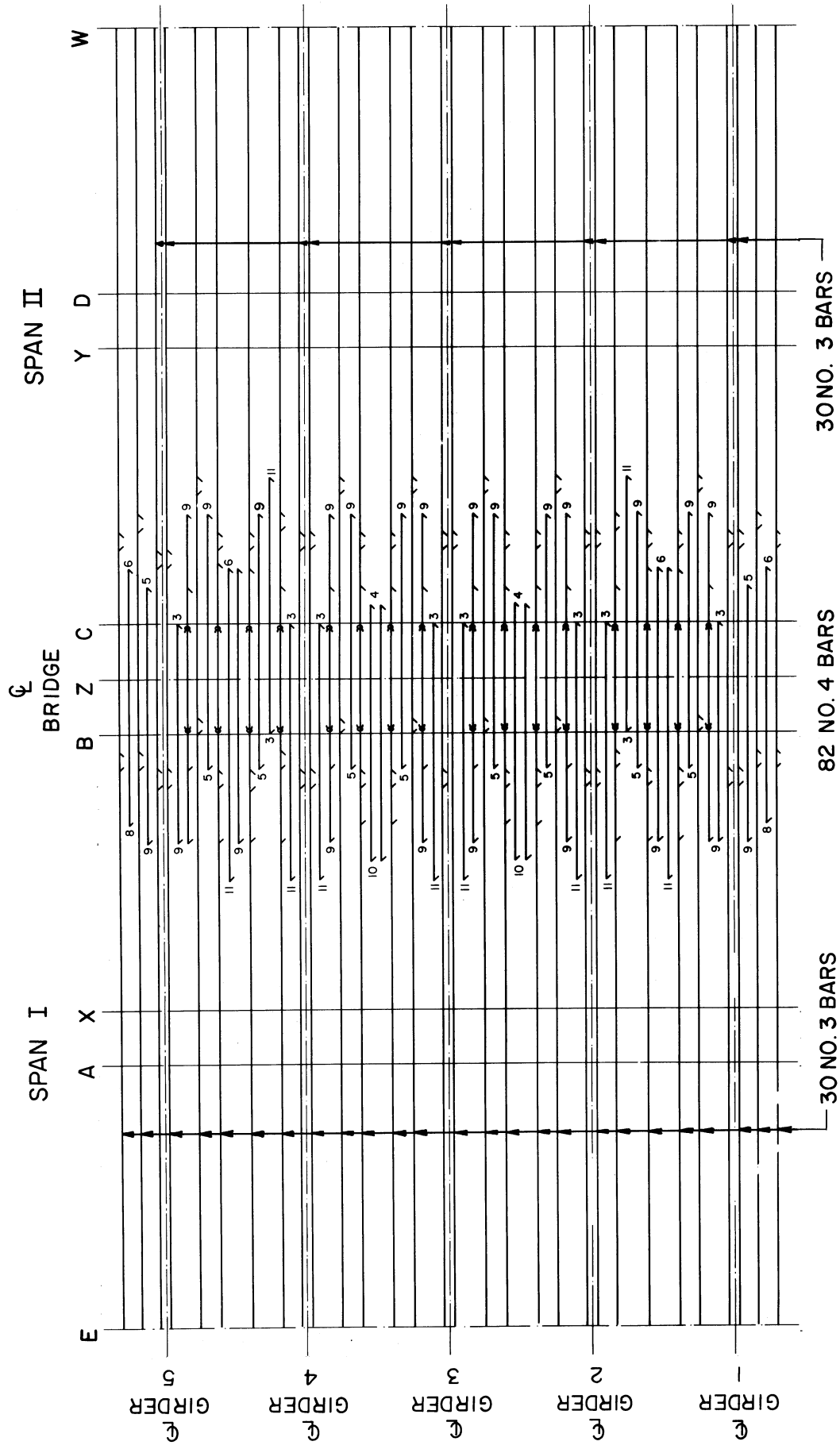

NUMBERS AT ENDS OF BARS INDICATE DISTANCE FROM BRIDGE CENTERLINE Z IN FT.

INDICATES TWO BUNDLED NO. 4 BARS

NOT TO SCALE – CURVATURE NOT SHOWN

FIG. 2.4b TOP SLAB MAIN LONGITUDINAL REINFORCEMENT

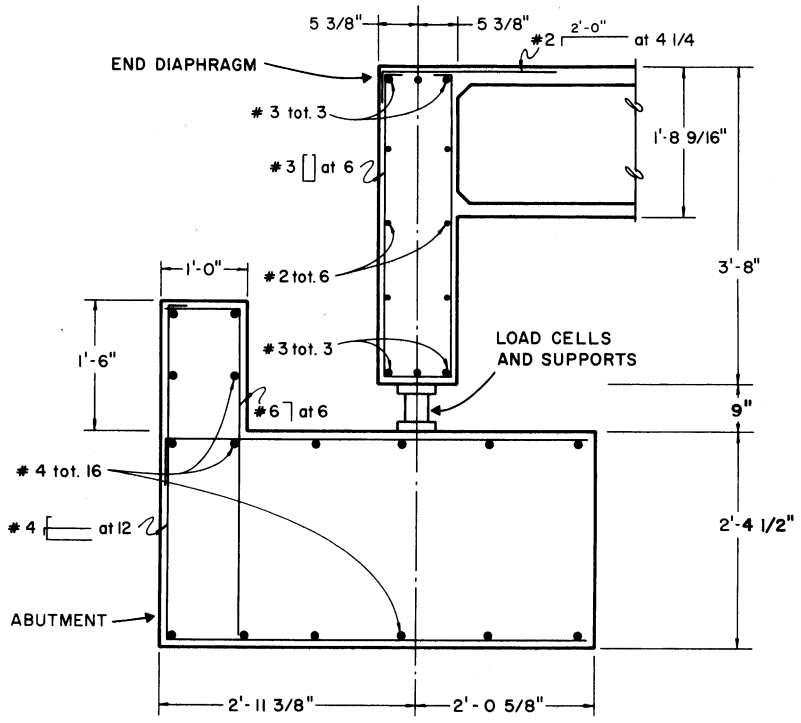

(a) TYPICAL END DIAPHRAGM AND ABUTMENT REINFORCEMENT

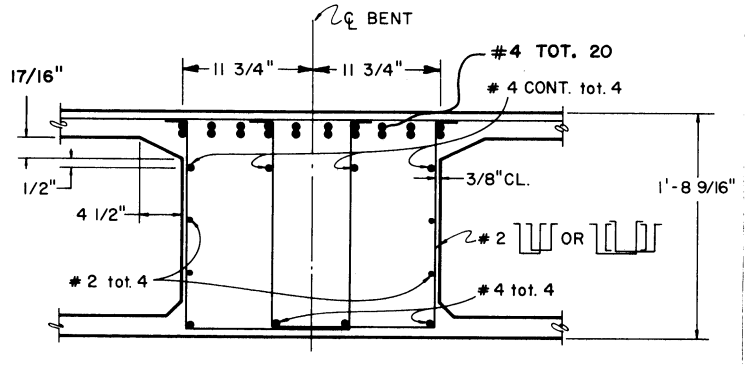

(b) CENTER BENT DIAPHRAGM REINFORCEMENT

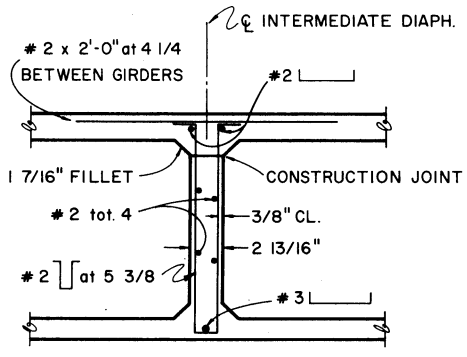

(c) REINFORCEMENT FOR DIAPHRAGM AT MIDSPAN SECTION X

FIG. 2.5 REINFORCEMENT FOR END, CENTER BENT AND MIDSPAN DIAPHRAGMS

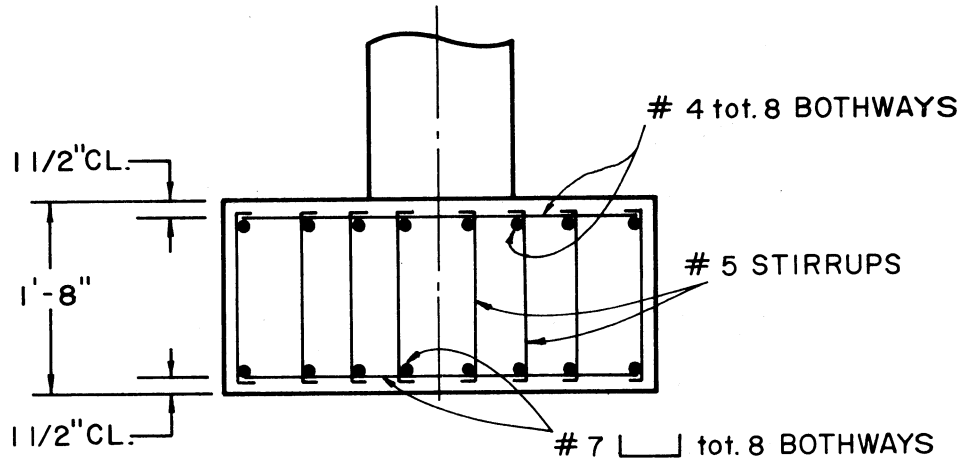

(a) ELEVATION OF FOOTING WITH REINFORCEMENT

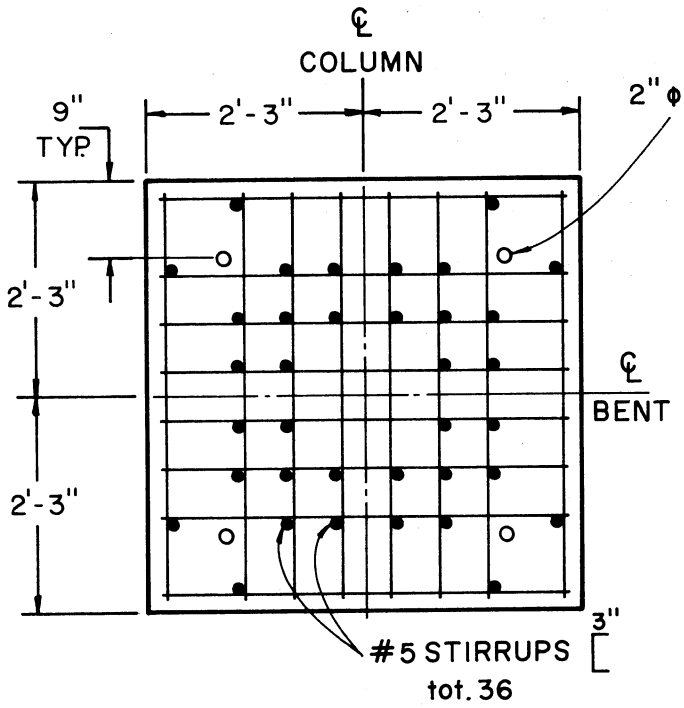

(b) PLAN OF FOOTING WITH REINFORCEMENT

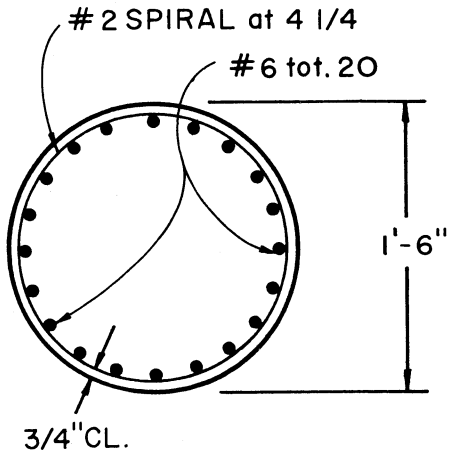

(c) SECTION OF COLUMN WITH REINFORCEMENT

FIG. 2.6 REINFORCEMENT FOR CENTER COLUMN AND FOOTING

3. INSTRUMENTATION

3.1 Basic Measurements

In a large scale model, such as the box girder bridge model, the number of measurements to be taken for a given load or support condition obviously have to be limited for reasons of expense and convenience. The fundamental measurements in any study of a structural model are loads, reactions, deflections and strains.

Reactions give a check on statical equilibrium, and their magnitudes indicate the percentage of the loads on the structure taken by each support. Deflections show the shape of the structure under load. As the determination of the load-deflection relationship for a structural system is of major importance, deflection readings are significant experimental data, describing the ranges of elastic, inelastic and ultimate response. Strains are a measure of the extent of deformation of the structure at a given location and are the starting point of all further calculations and comparisons of internal forces and moments.

In view of the large number of reaction, deflection and strain readings envisaged during the testing of the box girder model from the start of the experimental program to its destruction, it was decided at the very outset to record measurements electronically.

In addition to external loading, environmental factors play a part in affecting the behavior of a structure. Foremost among these factors as far as the box girder bridge model was concerned were temperature and humidity conditions. The box girder bridge model was built and tested in the main test bay of the Structural Engineering and Materials Laboratory [S.E.M.L.] where stable temperature and humidity conditions pre-

vail to minimize environmental effects. As a check, temperature was measured continuously throughout the construction and testing periods.

3.2 Choice of Locations to be Instrumented

Reactions were measured under each girder at each of the two abutments of the bridge model, and at four locations under the central footing. As this footing was to be anchored to the floor by means of prestressed steel rods, hollow load cells were also fitted above this footing to indicate the change of tensile force in each rod. The difference between the two load cell readings at each location represented the net reaction at that point.

Vertical deflections of the box girder bridge model along the length were measured at several locations by means of potentiometers. These locations included transverse sections X, QB, Z, QC and Y, Fig. 2.2. At each of these sections five potentiometers were placed, one under each girder, except at Z, where the central column under girder 3 allowed only four potentiometers.

Longitudinal strain measurement was confined to Sections A and B in the span with the diaphragm and to Sections C and D in the other span, Fig. 2.2. As has already been observed, Section A is in the region of maximum positive moment in Span I and Section D is in the region of maximum positive moment in Span II. Sections B and C are at distances of 3 ft., respectively, on each side of the bridge center support, and provide information on the negative moments at those locations. Measurements of strain at each gaged section consisted of measuring devices in the top and bottom slabs.

3.3 Choice of Instrumentation

The selection of reliable load cells of 50 kips and 200 kips capacity, Fig. 3.1, used for the measurement of support reactions and linear potentiometers, Fig. 3.2, of 6 in. travel for the measurement of vertical deflections at various sections of the bridge soffit did not present any special difficulties. A decision had to be reached, however, regarding the choice of instrumentation for the measurement of longitudinal and transverse reinforcement strains, and for the compressive strains in concrete.

On the basis of previous experience it was decided to use strain meters, Fig. 3.3, for the measurement of concrete compressive strains, and weldable waterproofed strain gages, Fig. 3.4, for the measurement of strains in the steel reinforcing bars. The strain meter and the weldable gage were known for their reliability in strain measurement, and also eliminated the uncertain effects of laboratory water-proofing methods on the final results.

In order to improve the reliability of the tensile strains measured from the reinforcing bars and to reduce the influence of possibly uncracked concrete in the immediate vicinity of the gage, a 1/4 in. thick strip of masonite was inserted in the concrete section near the outer surface in the same vertical plane as the strain gages at the reinforcing bars. By this artificial weakening of the section, a crack was automatically induced and the strain results more correctly represented the fundamental condition of a cracked section. The concrete cover of the tensile reinforcement at Sections A, B, C and D was artificially weakened in this manner. The gages on the reinforcing bars were also wrapped in cellophane to prevent bonding of the gages to the

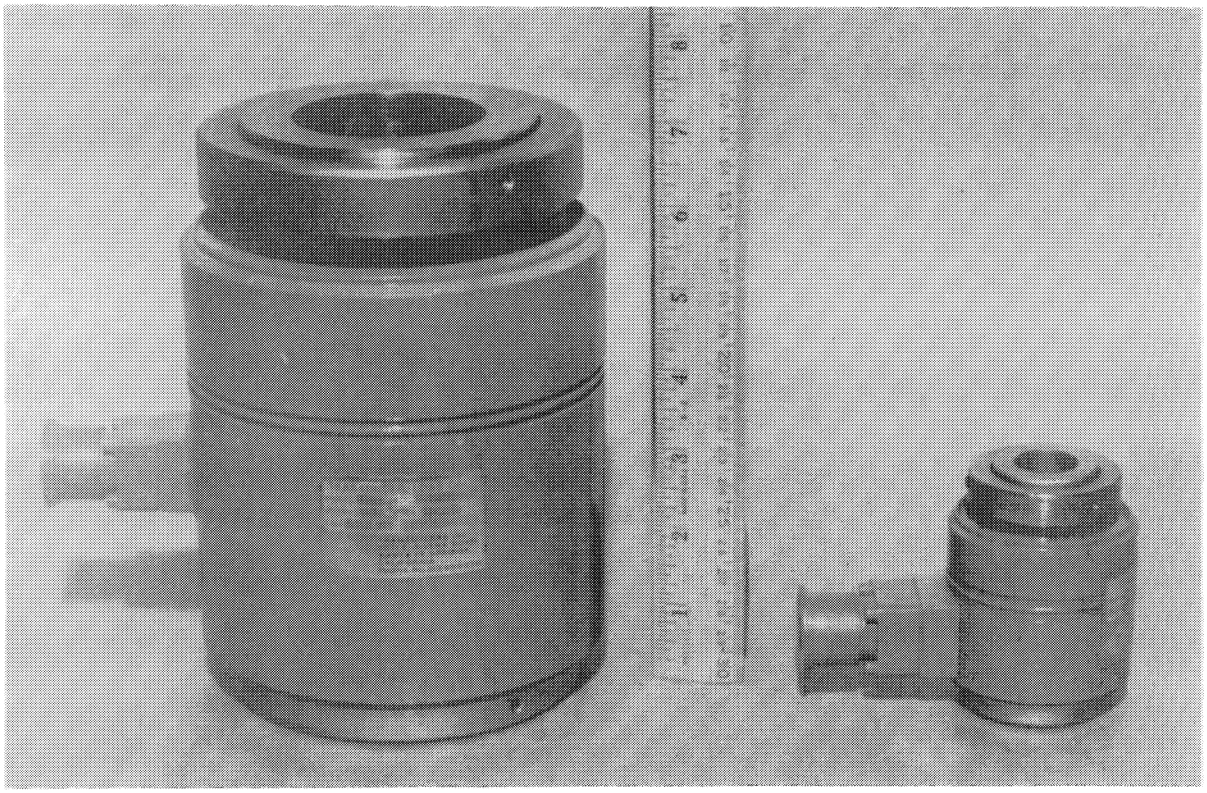

FIG. 3.1 200 KIP AND 50 KIP LOAD CELLS

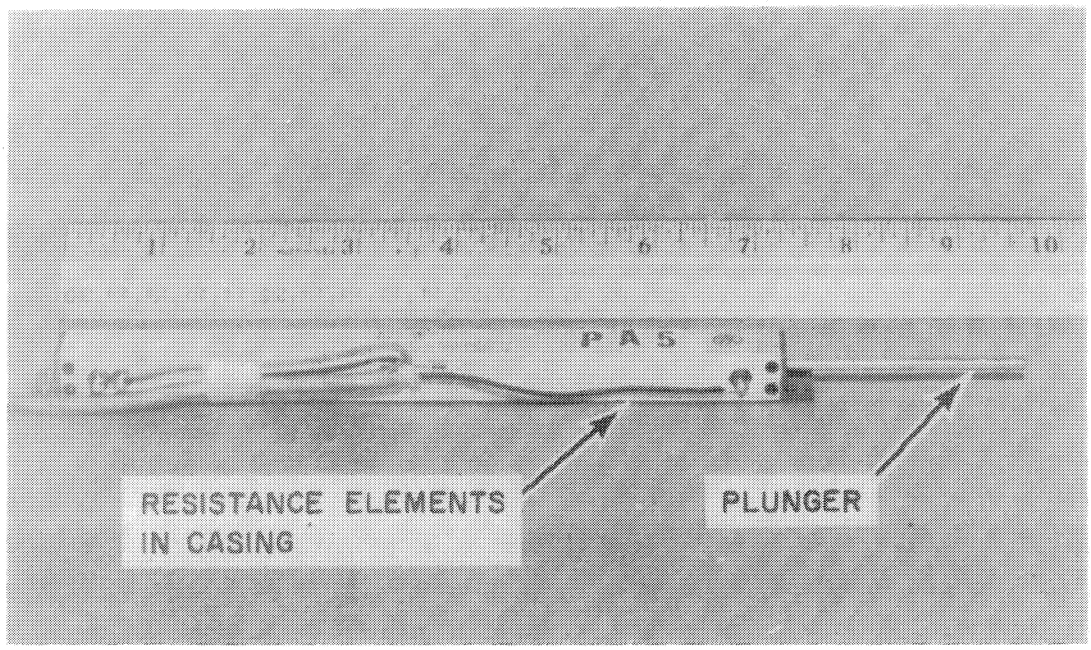

FIG. 3.2 RECTILINEAR POTENTIOMETER FOR DEFLECTION MEASUREMENTS

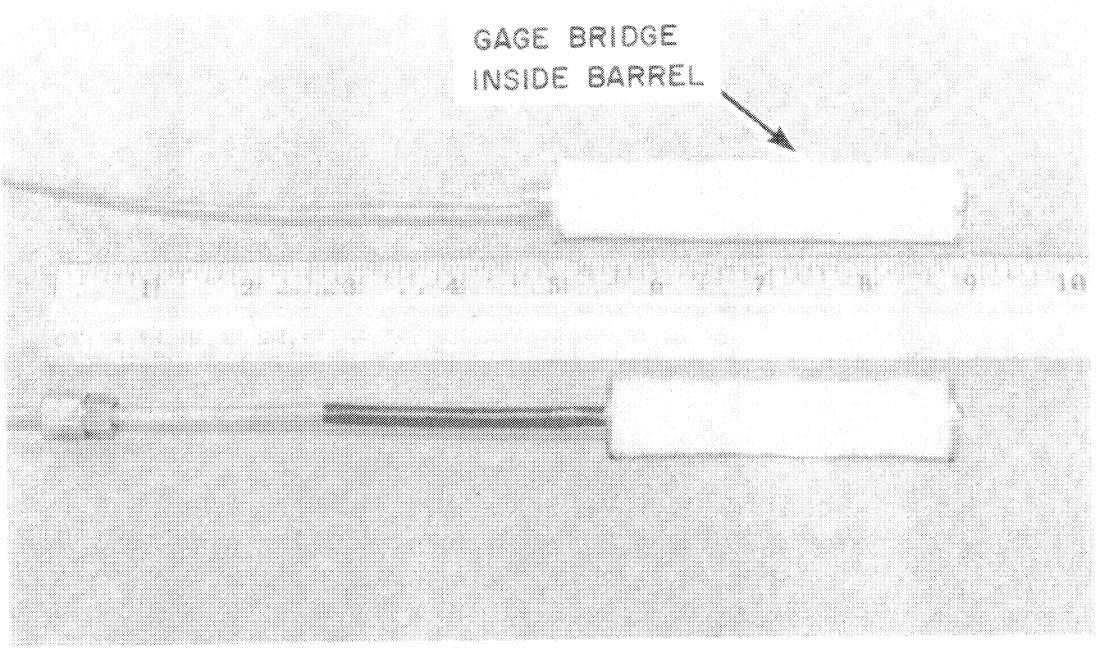

FIG. 3.3 CONCRETE STRAIN METERS

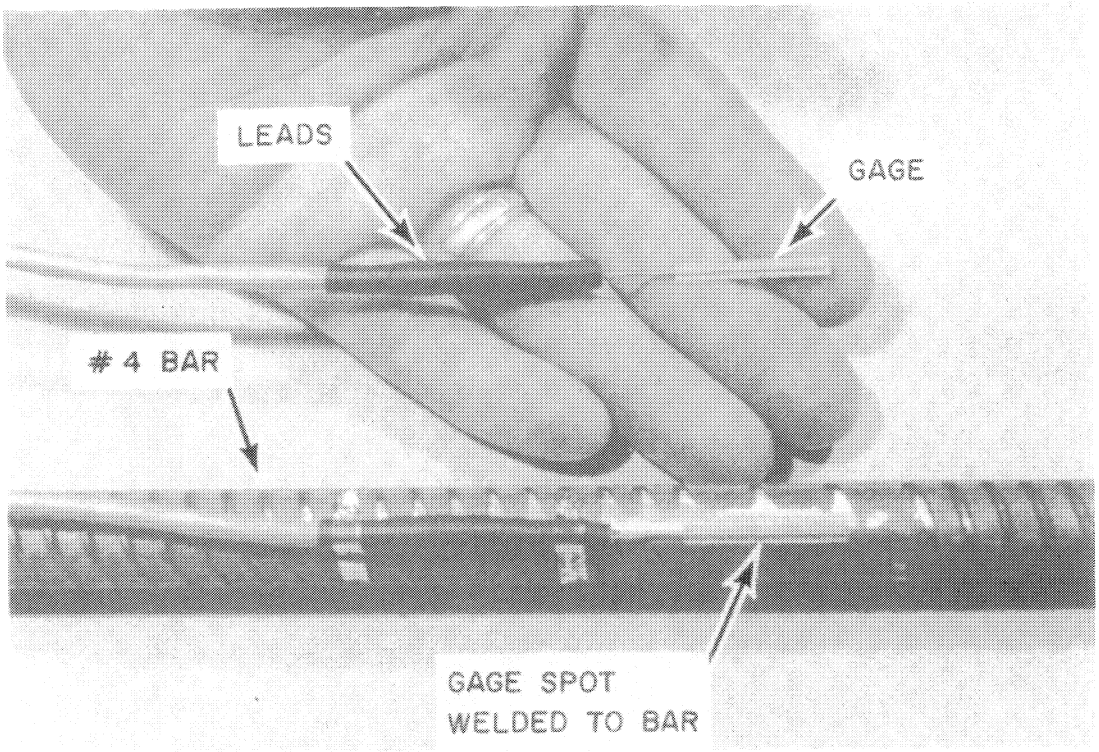

FIG. 3.4 WELDABLE STRAIN GAGE FOR STEEL REINFORCEMENT

to the concrete and to provide a realistic strain value in the region of each gage.

3.4 Description, Calibration and Installation of Instrumentation

After the selection of measuring devices and gages for the measurement of reactions, vertical deflections and strain, these devices had to be calibrated. A description of calibration and installation of each item of instrumentation is treated separately in the following sections.

3.4.1 Load Cells for Support Reactions

The box girder bridge model study required the use of 10 load cells of 50 kips capacity (five under each end diaphragm with one at each girder location) and 8 hollow load cells of 200 kips capacity at the top and bottom surfaces of the square footing of the central column support. Two load cells, each of 50 kips capacity also served in conjunction with the loading jacks to measure the magnitude of the applied loads at any stage. Commercially available load cells were used in all cases.

Each load cell, Fig. 3.1, incorporated eight strain gages wired so as to eliminate the effects of eccentric loading, and bending or torsion effects. The gages functioned as a four-arm resistance bridge and were temperature compensated. Other details relating to the load cells are given below:

Height	50 kips capacity, 3.12 in. 200 kips capacity, 7.12 in.
Diameter	50 kips capacity, 2.25 in. 200 kips capacity, 5.00 in.
Rated Output	2 + 0.50 millivolts/volt
Nonlinearity	$\pm$ 0.25%

Repeatability . . . . . ± 0.10%

Excitation Voltage . . . . . 10 volts D.C.

Least Reading . . . . . 50 kips capacity, 12.5 lbs.

Least Reading . . . . . 200 kips capacity, 50.0 lbs.

3.4.1.1 Calibration of Load Cells

All load cells were accompanied by individual calibration charts from the manufacturer giving millivolt/volt output for the full range of load capacity. These charts were checked using a 400 kip and 60 kip testing machine, and found to be accurate within the expected load range.

3.4.1.2 Installation of Load Cells

A photograph showing the typical installation of the 50 kips capacity load cells at one abutment comprises Fig. 3.5. Each cell was placed between two plates. The top plate was 1 in. thick and the lower plate was 2 in. thick. The lower plate rested on a rocker, which in turn was supported by a 2 in. base plate. To the base plate was bonded a 2/32 in. teflon pad that was free to slide against a similar teflon pad on a stationary steel plate hydrostoned to the abutment. This reaction assemblage allowed horizontal displacements of the load cell in both tangential and radial direction, and also sufficient freedom of rotation about the radial axis.

In order to simplify the installation procedure, the entire reaction assemblage was placed in position before the bridge model was cast. Wedges and stiff styrofoam were used to support the rocker and top plate in the proper position during construction.

The load cells of 200 kips capacity are shown in Fig. 3.6. These were hollow cells which had steel rods of 1 1/8 in. diameter prestressed

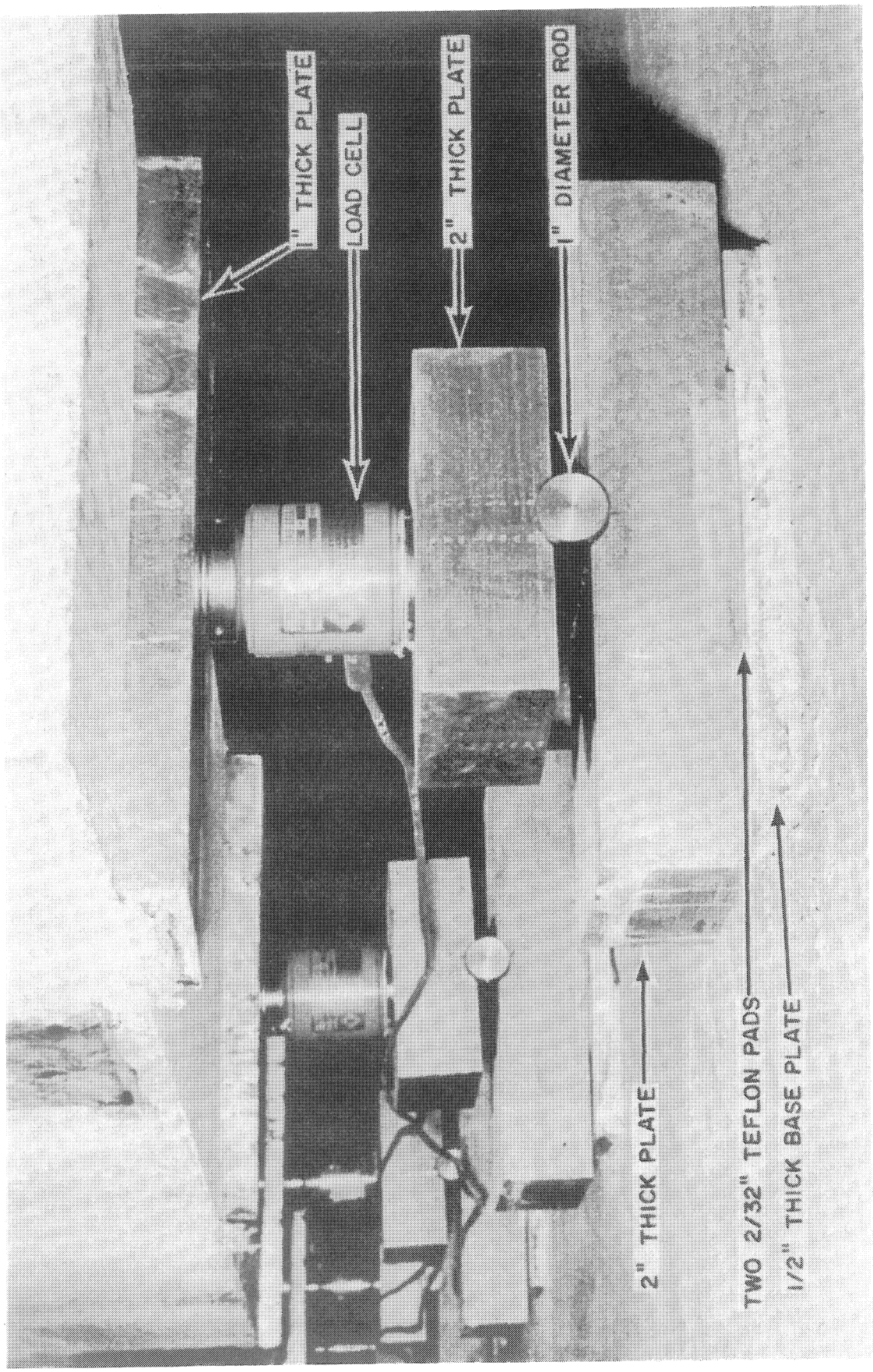

FIG. 3.5 LOAD CELLS OF 50 KIP CAPACITY UNDER EACH GIRDER AT ABUTMENT

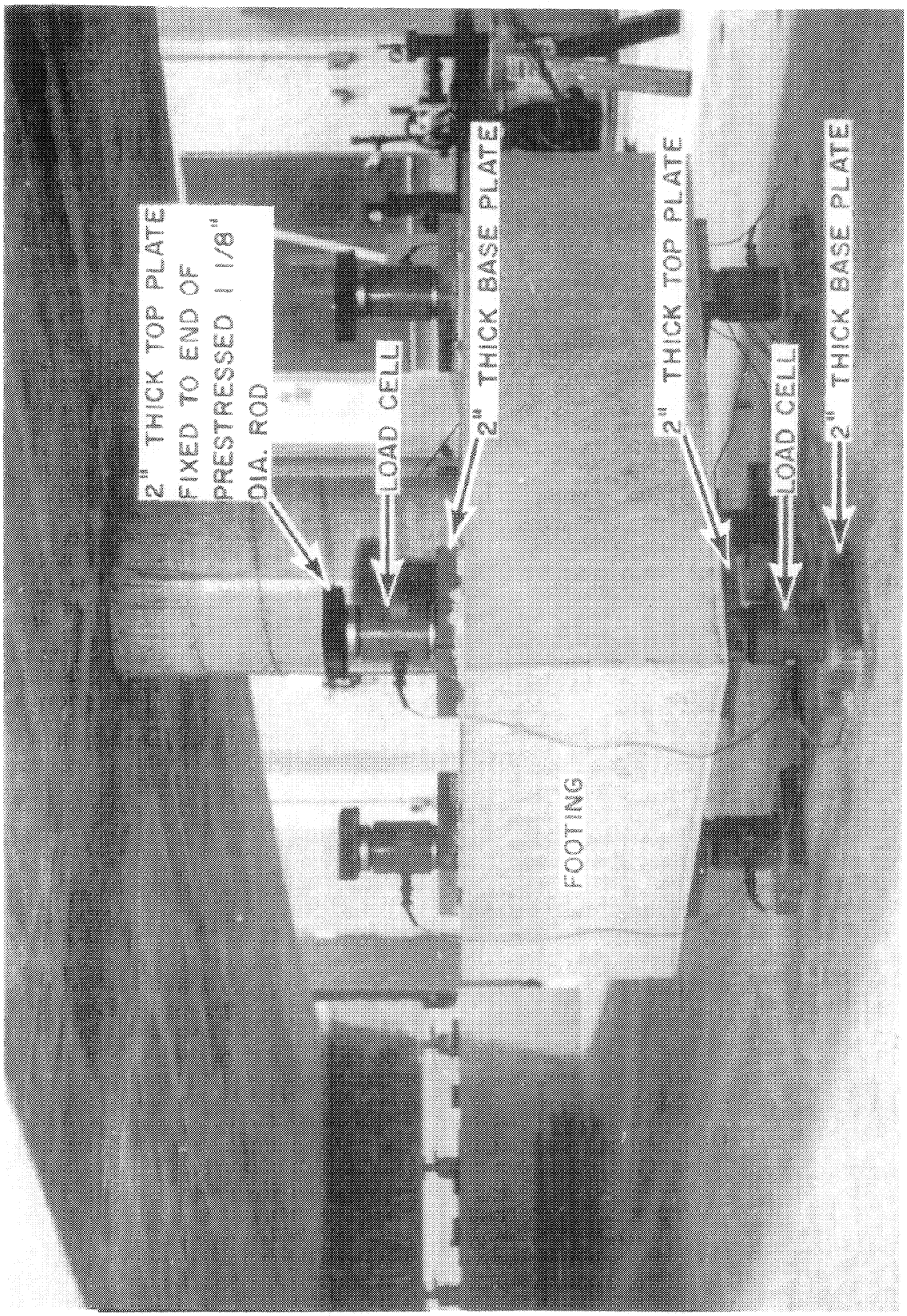

FIG. 3.6 LOAD CELLS OF 200 KIP CAPACITY AT CENTER COLUMN FOOTING

to a force of 80 kips passing through them and tying the square footing of the central column support to the floor of the laboratory. One load cell above the footing and the other between the footing and the laboratory floor allowed a measurement of the change of the reaction force at each rod location. The four bottom load cells were placed in the formwork before the footing was cast, such that no adjustments were necessary later. The top load cells were placed after the footing had hardened, and the steel rods were then prestressed to the prescribed load before the cellular part of the bridge model was cast.

3.4.2 Rectilinear Potentiometers for Deflection Measurements

A total of 24 rectilinear potentiometers was used for deflection measurements of points on the bottom surface of the box girder bridge model. The commercially available potentiometers, Fig. 3.2, consisted of cermet resistance elements in a compact rectangular casing with mounting brackets. Each potentiometer had a rod-like plunger, the mechanical movement of whose tip was converted into a millivolt/volt output. Details of the potentiometer are given below:

Travel	6.00 in.
Tolerance	$\pm$ 0.1%
Power Rating	8.0 watts
Initial Actuating Force . . .	1.00 lb.
Least Reading	0.006 in.

3.4.2.1 Calibration of Potentiometers

Each potentiometer was calibrated by mounting it alongside a scale and giving the plunger a series of movements of known magnitude. The output for each of these movements were given in terms

of inches by the Low Speed Scanner when an assumed calibration constant was given. It was found that all the potentiometer outputs were not only highly linear but also gave practically identical calibration factors in terms of millivolt/volt per inch of deflection.

3.4.2.2 Installation of Potentiometers

Each potentiometer was mounted on a wooden board fixed to a triangular stand fabricated from small structural angles as shown in Fig. 3.7. Five potentiometers, one below the centerline of each girder of the box girder bridge model at a transverse section formed a set that could, if necessary, be placed at any location beneath the bridge. Five such sets of potentiometers were made, enabling the deflections at different transverse sections of the bridge model to be made simultaneously. In order to take care of horizontal movement of the point of deflection measurement, laterally flexible but vertically rigid mounting rods of about 3 in. in length were used to connect the potentiometer plungers to the bottom surface of the bridge model. The top end of each mounting rod had a small circular disk that was glued to the bridge soffit with epoxy.

3.4.3 Concrete Strain Meter

This commercially available meter, Fig. 3.3, was a special, recently developed miniature version of a type of strain meter extensively used for the measurement of compressive strains in full scale concrete structures. It consisted of a cylindrical barrel with a flange at each end, and the relative movement of the flanges resulted in a strain output from the gage bridge inside the barrel. The barrel was wrapped in cloth so as to prevent bonding to the concrete. Two versions of the gage were used in the model. The data for gages used in the top flange are as follows:

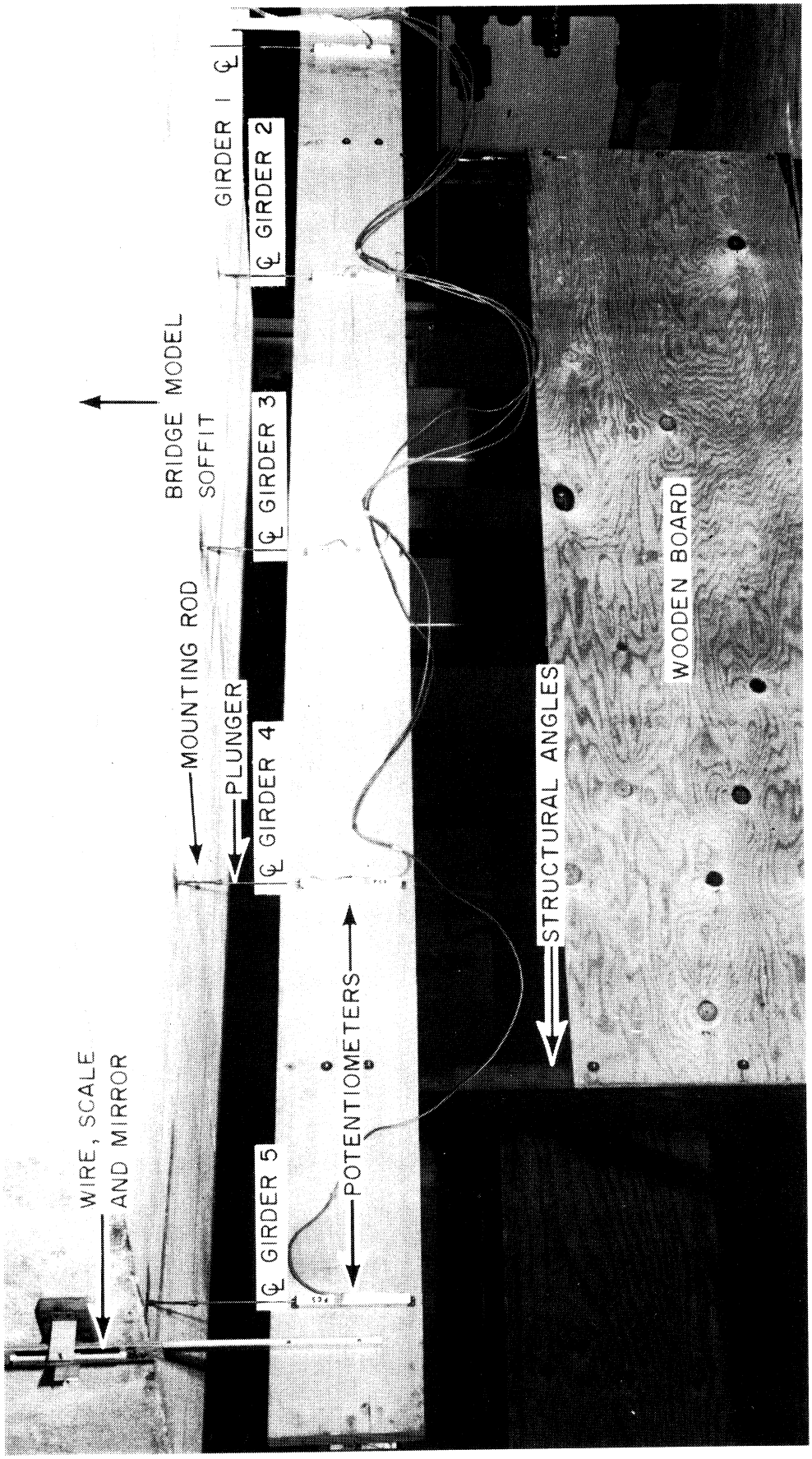

FIG. 3.7 ARRANGEMENT OF POTENTIOMETERS AT A TRAVERSE SECTION

Gage length	4.06 in.
Body diameter	0.63 in.
Flange diameter	0.88 in.
Weight	0.19 lb.
Range in Tension/Compression	3900 με
Least reading	6 με

The gage used for the bottom flange was similar, but had the following dimensions:

Gage length	3.1 in.
Body diameter	0.50 in.
Flange diameter	0.75 in.

3.4.3.1 Calibration of Concrete Strain Meters

The calibration constant of each concrete strain meter as obtained from the manufacturer was corrected for temperature and lead resistance. Meters were then tested in a standard calibration jig in which they were subjected to carefully controlled deflection increments of 0.002 in. The output was given as millivolt/volt on a digital voltmeter, from which the calibration constants in terms of microstrain/millivolt/volt were determined. The results of the tests agreed quite well with the calibration constants given by the manufacturer.

3.4.3.2 Installation of Concrete Strain Meters

The strain meter needs to be placed in concrete in the direction in which strains are to be measured. Care must also be taken to ensure that its orientation and position do not change after it has been covered with concrete, especially when the concrete in its vicinity is being vibrated.

Each meter barrel was therefore attached by means of thin steel wire to neighboring reinforcement bars to ensure the flanges freedom of movement. A close-up can be seen in Fig.3.8. After installation, the resistance of each strain meter was checked on a DC ohmmeter.

3.4.4 Weldable Waterproofed Strain Gage

The commercially available gage consisted of a hermetically sealed and mechanically protected nickel-chrome strain filament housed in a small stainless steel cylindrical shell, Fig. 3.4. The shell had two flanges allowing spot welding of the gage to a metal surface. The gage is designed to perform under severe conditions of moisture and shock, the filament being inherently shielded in the cylindrical shell by highly compacted magnesium oxide insulating powder. Information for the gage is given below:

Length of Gage	1 3/32 in.
Width of each Flange	1/16 in.
Diameter of Cylindrical Shell	0.03 in.
Strain Gage Resistance	120 $\pm$ 3.5 ohms
Rated Strain Level	$\pm$ 6000 μ in./in.
Gage Factor	1.8
Least Reading	5 μ in./in.

The gage is temperature compensated over the range $0^{o}F$ - $180^{o}F$, and its fatigue life exceeds a million cycles.

3.4.4.1 Calibration of Weldable Waterproofed Gages

These gages had been previously used extensively [9,10,11] for strain measurement in reinforcement bars, and had been found to be reliable and accurate. No calibration tests were therefore made for these gages,

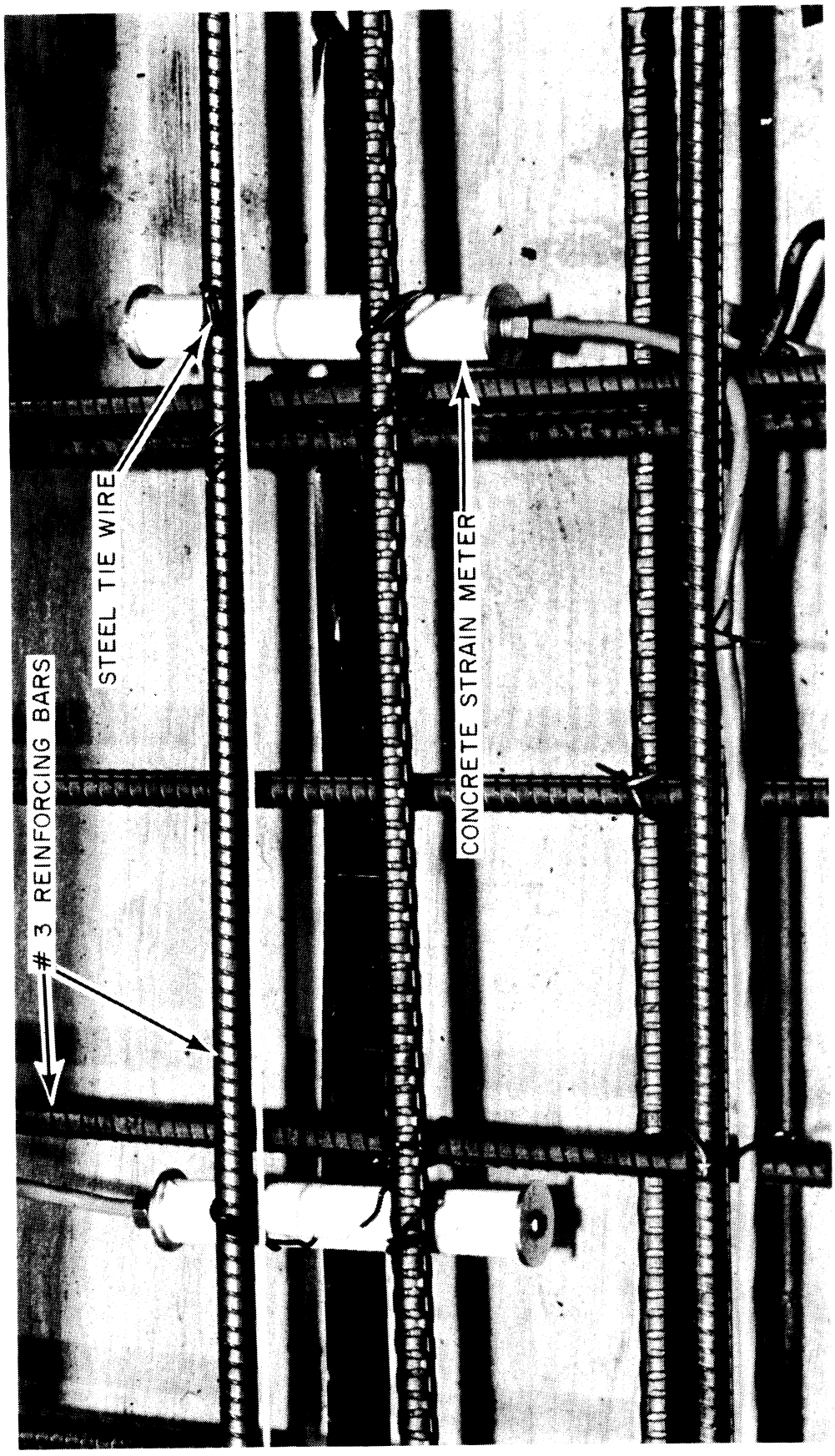

FIG. 3.8 TYPICAL INSTALLATION OF A CONCRETE STRAIN METER

and the manufacturer's calibration constants were used throughout.

3.4.4.2 Installation of Weldable Waterproofed Strain Gages

The installation of a weldable waterproofed gage turned out to be a much faster and less difficult operation than the mounting and waterproofing of a conventional strain gage.

At each gaged location, a reinforcing bar had two gages welded on diametrically opposite areas on the bar surface to obviate bending effects and to provide accurate measurement of axial strain of the bar. The bar surface at these areas was prepared by grinding off the bar lugs and subsequently polishing the areas with an emery wheel. Degreasing was done by cleaning the areas where the gages were to be welded with cotton swabs dipped in acetone.

The welding of a gage to the reinforcing bar was accomplished by allowing a low voltage current to pass through the point of welding. In order to prevent overheating (or local fusion) the power source had to be of the capacitor-discharge type. A special welding unit was used for this purpose, and a supply of 10 - 15 watt-seconds was found to be adequate. The unit had a hand probe with a pointed welding tip which fired only when a force of 2 1/2 lbs. was applied to it. Fig. 3.9 shows a series of reinforcing bars in place with two weldable gages located diametrically opposite to each other on two of the bars. This area was wrapped with cellophane tissue after welding to prevent bonding of the gage to the concrete.

3.5 Deflection Measurements using Scales and Wire

It was not possible to install potentiometers for the measurement of the box girder bridge model deflections prior to the removal of shoring and formwork for the taking of dead load readings in view of the

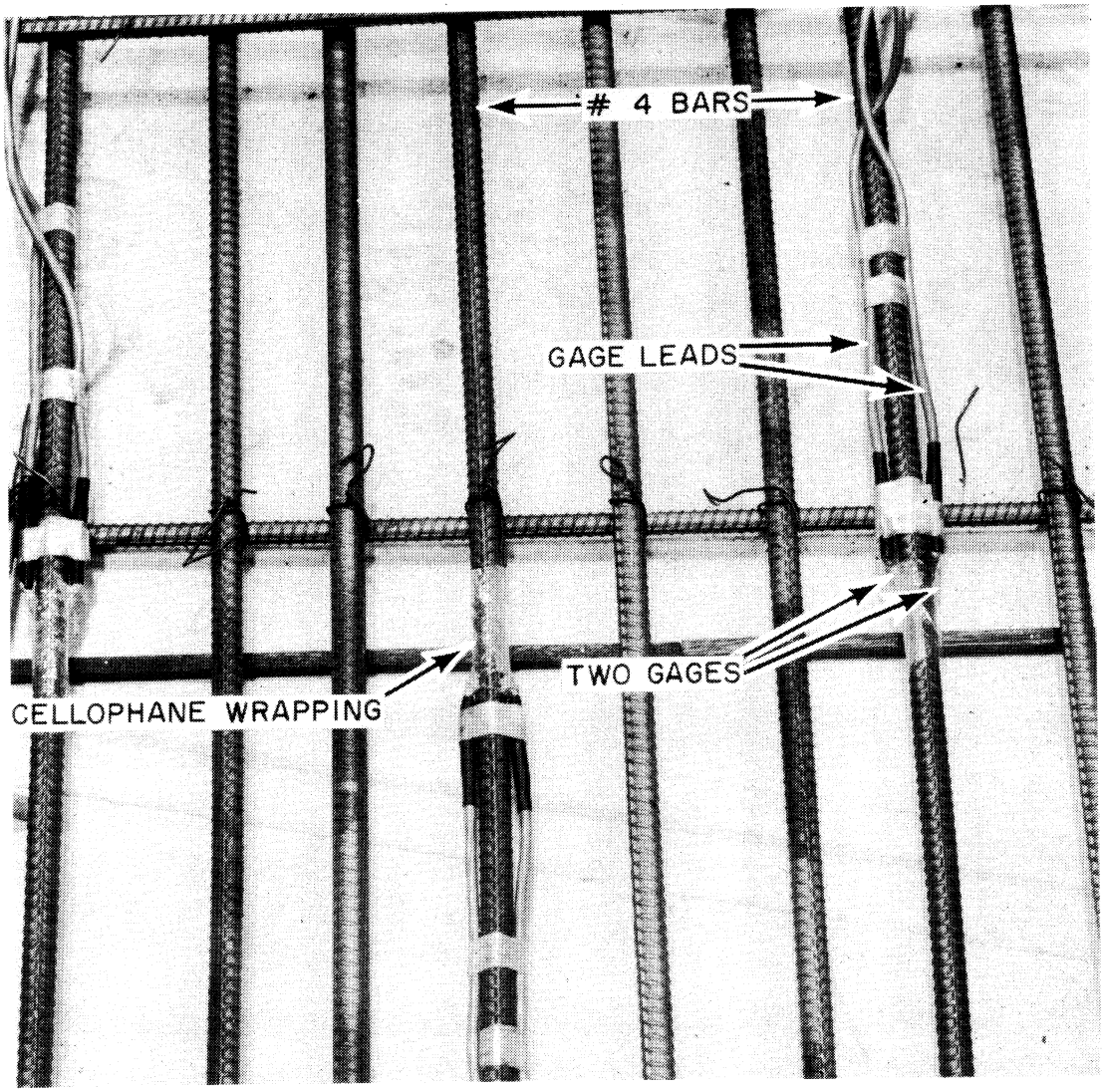

FIG. 3.9 TYPICAL INSTALLATION OF WELDABLE WATERPROOFED STRAIN GAGE ON STEEL REINFORCEMENT

damage that might occur during the stripping of formwork. Level readings were therefore taken before and after the removal of the forms, using a high precision level and scales graduated to 0.01 in. A total of 10 scales were mounted to the two cantilever edges of the top flange at sections X, QB, Z, QC and Y.

After the dead load phase of the testing was completed the scales were used for a visual control of the deflection of two girders, numbers 1 and 5. The scales were mounted on an aluminum angle and attached to the same wooden board that carried the potentiometers, Fig. 3.7. Ten targets, consisting of a piano wire stretched between two angles in front of a mirror were mounted on the webs of girders 1 and 5 at sections X, QB, Z, QC and Y. The targets moved with the bridge as it deflected, allowing the displacements to be read on the fixed scales. By aligning the piano wire and its image in the mirror the effect of parrallax was eliminated. A typical detail of the wire and scale arrangement at a section of the box girder bridge model is shown in Fig. 3.10.

Initial and final readings of the level of the wires relative to the scales at each station resulted in the obtaining of the overall deflection profile of the bridge model, and provided a useful check on the bridge model deflection magnitudes at any stage.

3.6 Data Acquisition and Recording System

All readings for the box girder bridge model experimental program except for the dead load [Phase 0] were obtained by means of a data acquisition and recording system called the S.E.S.M. Low Speed Scanner. The scanner comprised a portable computer of 8 k storage, a digital voltmeter unit, a teletype and four terminal boxes, Fig. 3.11. The lead wires from each gage or measuring device were mounted to the terminals of the

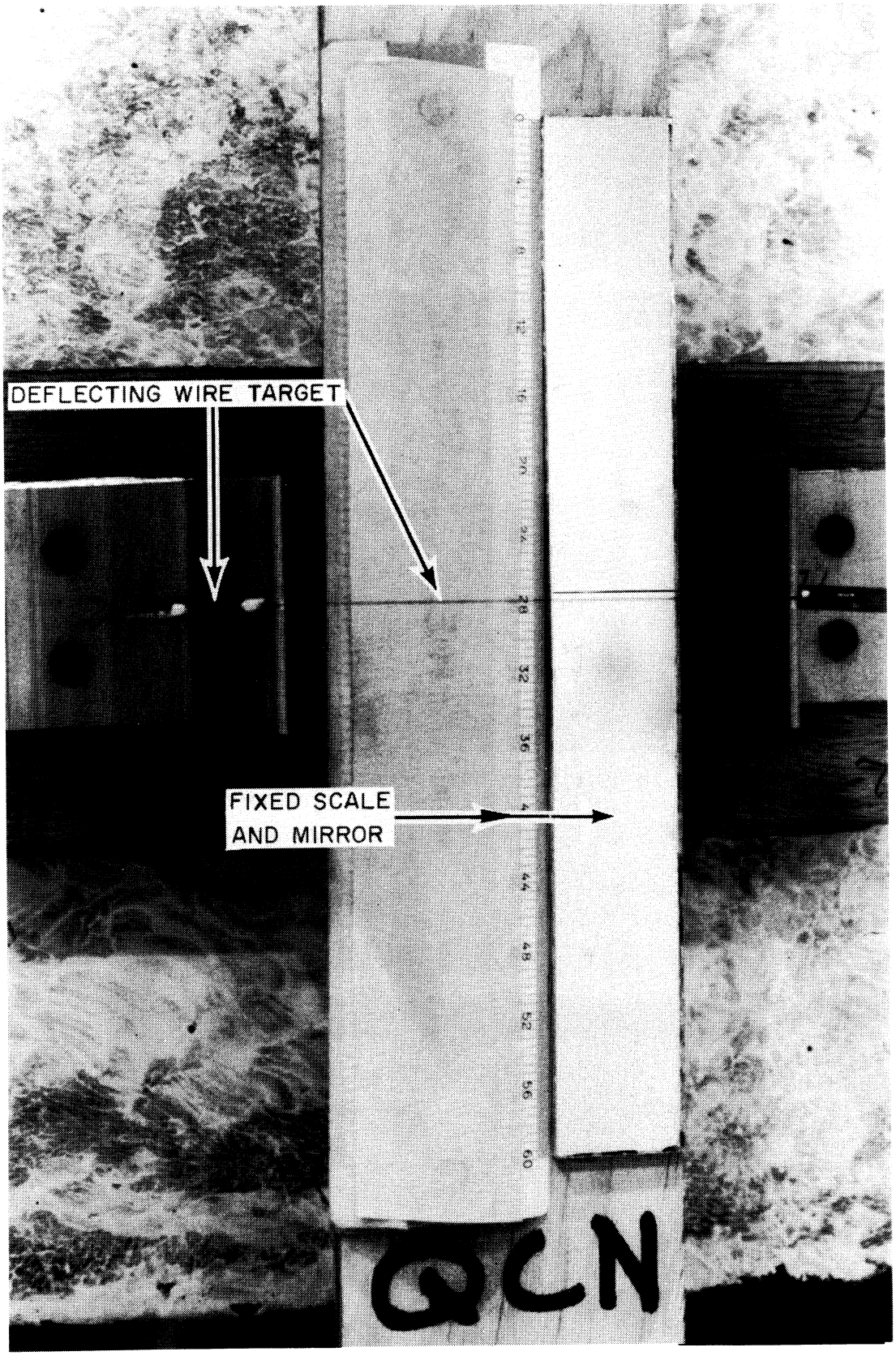

FIG. 3.10 WIRE, SCALE AND MIRROR ASSEMBLY FOR MEASURING BRIDGE DEFLECTIONS

four boxes. Each box provided 64 channels of electronic measurement in 8 rows and 8 columns. The total number of channels used during the testing of the box girder bridge model was 192. Box 1 contained the channels for the weldable gages, Box 2, the weldable gages and the linear potentiometers, Box 3 contained the channels for the majority of the concrete meters and Box 4 contained the channels for the remaining concrete meters and the load cells. This arrangement was used because different items of instrumentation needed different voltages, and also for convenience in recording and spot-checks.

Dummy resistors were provided in each box to balance the gage circuits. In addition, one channel in each terminal box was hooked to a separate standard resistor such that the "drift" in the terminal box could be checked.

The computer was programmed to convert gage readings to direct values of strain in micro inch/inch, deflection in inches, and reaction or load in kips. The calibration factors for each device were fed into the computer to make those conversions.

The basic routine for the calculation and output was as follows. After the bridge was loaded at any stage, the computer scanned each gage or meter five times and averaged the readings. The output, in which each reading was the difference from a datum established before each session of loading, was obtained by means of the teletype on punched paper tape and was also simultaneously printed on paper. As a simple check on the stability of the equipment, the first four readings recorded the variation of the standard resistors from datum readings taken for each session of testing. The next two readings gave the values of the loads on the bridge as registered by the load cells of the loading jacks. All these readings were carefully scrutinized at each loading and unloading step.

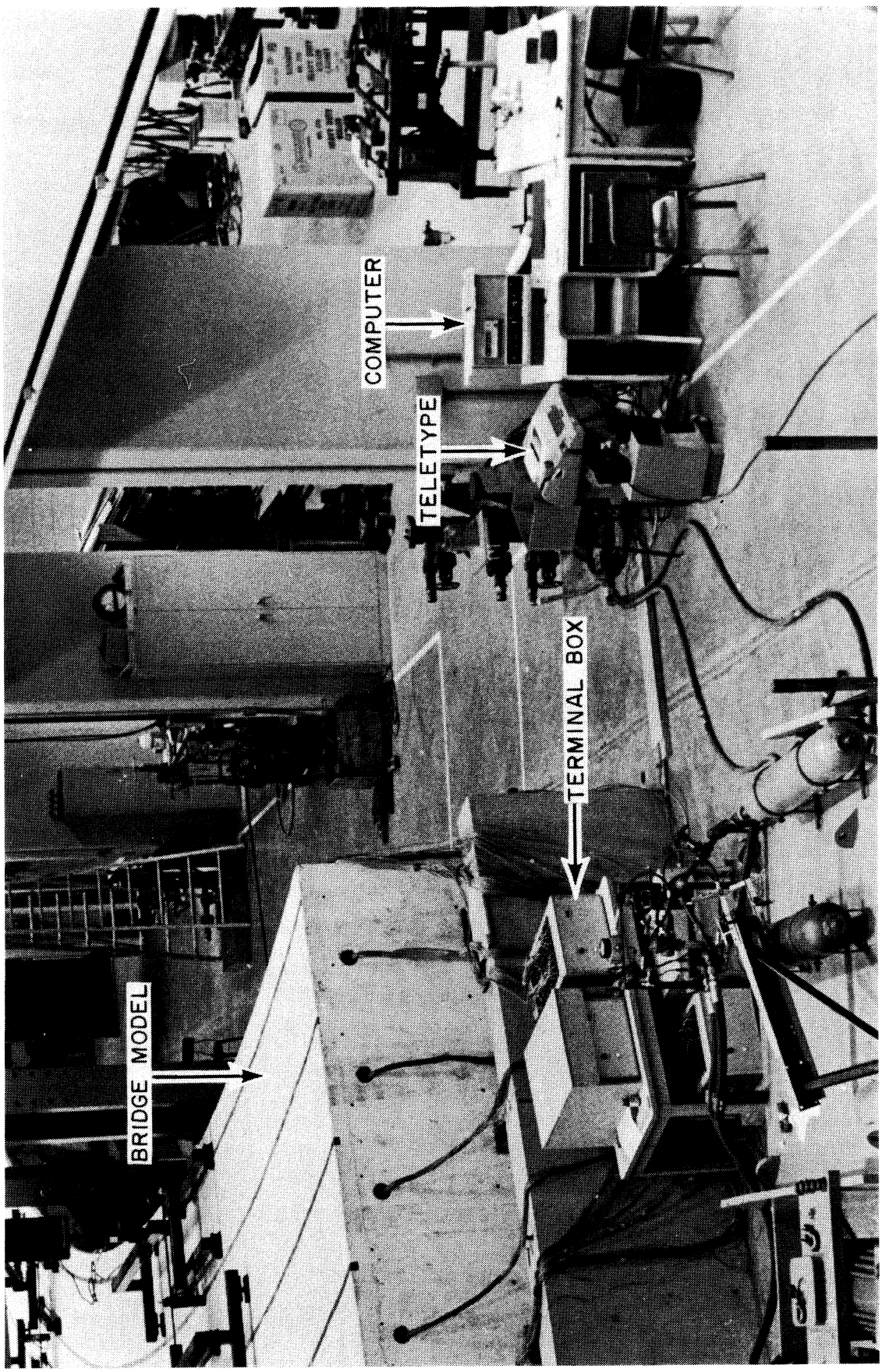

FIG. 3.11 DATA ACQUISITION SYSTEM

Fig. 3.11 shows the portable computer with the digital voltmeter unit, teletype and terminal boxes.

3.7 Instrumentation Identification Code

The origin of coordinates for the box girder bridge model, transverse sections and longitudinal sections have already been defined and can be seen in Figs. 2.2 and 2.3.

The various types of measuring devices were specified as follows:

W: Weldable waterproofed strain gage

K: Concrete Strain Meter

P: Linear Potentiometer

R: Load Cell Reaction

J: Applied Jack Load

With the above information, all measuring devices were fully identified by means of a code giving each type, the longitudinal section of location, the transverse section of location and the number of devices at that location.

The location of all internal concrete strain meters, K, and weldable strains gages, W, attached to the steel reinforcement are shown for positive moment Sections A and D and for negative moment Sections B and C, in Fig. 3.12. Note that all of these were placed in either the top or bottom slab and that measurements of strain were obtained at the end, quarter and midpoints in each transverse bay at all sections.

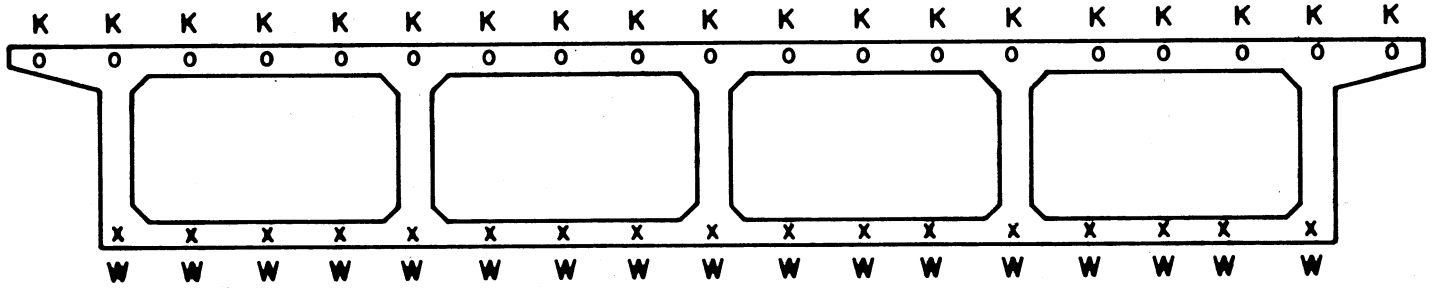

(a) SECTION A AND D

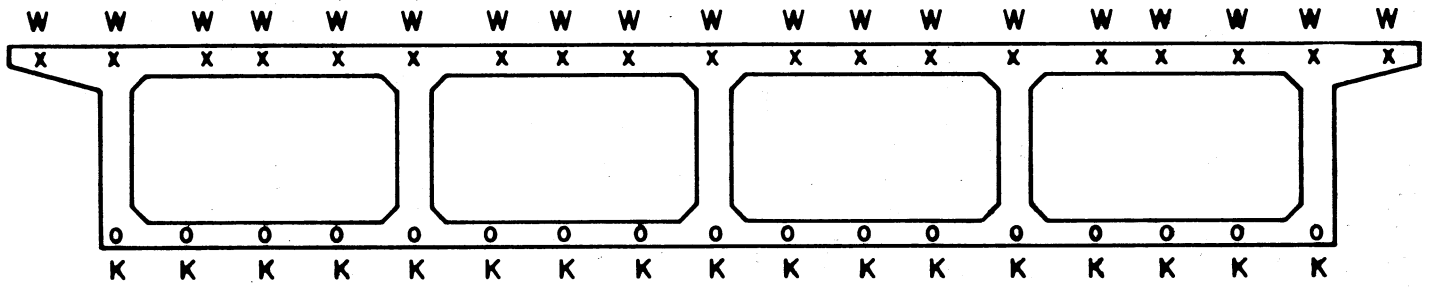

(b) SECTION B AND C

K-CONCRETE STRAIN METER
W-STEEL REINFORCEMENT WELDABLE GAGE

FIG. 3.12 LOCATIONS OF INTERNAL CONCRETE STRAIN METERS AND STEEL REINFORCEMENT WELDABLE GAGES

4. CONSTRUCTION OF BOX GIRDER BRIDGE MODEL

4.1 General Remarks

The size and complexity of the box girder bridge model, and the importance of completing the job in a minimum amount of time, dictated that the construction of the box girder bridge model be put out for bidding. As a result, the box girder bridge model was built under contract. The structural design of the bridge model was done by the California Division of Highways in an identical manner to that of the prototype. Strict specifications, dealing in detail with the design of the concrete mix, with formwork requirements and with the stringent tolerances in construction dimensions necessitated by the scaled down model used, were set by the investigators in consultation with engineers from the California Division of Highways. Reinforcement was cut, bent and placed by the contractor under supervision of the project staff. All instrumentation was purchased, calibrated and installed in place by the project staff. The box girder bridge model was located on the tie-down test floor of the Structural Engineering Materials Laboratory. The model covered the south-east quadrant of the laboratory test floor.

4.2 Chronological Record of Bridge Model Construction

Significant dates, all in 1972, dealing with the construction of the box girder bridge model are given below:

March 22: End abutments cast.

March 24: Center column and footing cast.

March 27: Work started on shoring and formwork for bottom slab.

April 17 - June 26: Building Trades Unions on Campus on strike. No work done on the model.

June 29:	Bottom slab, girder webs and diaphragms of bridge model cast.
July 11-13:	Inner forms for girder webs removed.
July 19-20:	Sand and steel billets placed inside the cells of the model.
August 8:	Top slab of bridge model cast.
September 12:	Soffit forms for top slab dropped.
October 5:	Removal of shoring and bottom form. Readings for dead load taken.

4.3 Details of Construction of Box Girder Bridge Model

A broad sheet of polyethylene was spread out to protect the surface of the test floor during construction of the box girder bridge model. The formwork of the abutments rested on thick asphalt-impregnated paper so as to prevent bonding of the concrete to the test floor.

All forms were made of 3/4 in. thick Douglas fir plywood of first class quality, with a Duraply exterior. The formwork was constructed so as to hold displacements under load to a minimum. The supporting scaffolding had wedges that enabled adjustment of the height of the supports which were spaced at close intervals to allow effective shoring of the bridge along its length. All cross sectional measurements of the structure and supports agreed with those in the design drawings to a tolerance of 1/8 in. The alignment of the forms in the horizontal plane was checked using two piano wires, one on each side of the bridge, from which offsets were measured. The maximum deviation in the alignment between design drawings and the model as constructed was 1/4 in.

The concrete used in the box girder bridge model was supplied

by a local company to the mix specifications set by the project staff, with the maximum size of aggregate being fixed at 3/8 in. Detailed information on the mix quantities is given in Chapter 6.

4.3.1 Casting of Abutments and Center Column

After the forms for the two end abutments and the center column with footing were completed and the steel reinforcement placed in position, the abutments, footing and column were cast. In order to better evaluate the properties of the concrete mix specified for the bridge itself, it was decided to use the same mix for the abutment casting as well, although a larger size of aggregate could have been used. The center column was provided with dowel bars to enable a strong connection with the center diaphragm to be formed.

Each end abutment was divided into two similar parts by plywood sheets so as to obtain manageable blocks of concrete at the end of the test program to be used as supports in other experiments.

4.3.2 Casting of Bottom Slab, Girder Webs and Diaphragms

Figs. 4.1 to 4.6 show the sequence of construction up to the casting of the bottom slab, girder webs and diaphragms. The sequence of construction was similar to that used on prototype structures in California.

In Fig. 4.1 the bottom slab forms have been completed. The layout of the steel reinforcement is clearly depicted in Fig. 4.2. Specially fabricated inner cell forms were then placed in position, Figs. 4.3 and 4.4. The forming was completed by placing transverse supporting members across the width of the bridge at regular intervals, Fig. 4.5. These members, in addition to blocking, were used to support

the inner cell forms and also provided supports for longitudinal planking, Fig. 4.6, which was used as a platform during the casting operation.

Three truck loads of concrete were used for the casting of the bottom slab, girder webs and diaphragms. Concrete from truck 1 was placed in the forms from section W to section QB; truck 2 from section QB over the center bent diaphragm to section QC; and truck 3 from section QC to section E. This casting sequence was chosen in order to insure uniform concrete properties throughout the respective longitudinal tension and compression zones in the bottom slab. The concrete was delivered to the laboratory by transit mix trucks and was transferred from these trucks by a concrete pump truck through a large rubber hose for direct placement into the earlier wetted forms, Fig. 4.6. The girder webs were filled first, the concrete being vibrated with a small, flexible shaft immersion vibrator of frequency 10,000 vibrations per minute till it emerged from the base of the girder forms into the region of the bottom slab. Further concrete was added till the girders were full. Concrete was then deposited to cover the bottom slab reinforcement. No vibration was permitted in the vicinity of the gaged sections. Concrete covering the instrumentation in the bottom slab was placed and compacted by hand. Lead wires from the gaged bars were carefully coiled and tucked away behind wooden covers nailed to the outside of the girder web forms.

The concrete was worked into corners and around reinforcement and screeded to obtain a uniform thickness. Subsequently the bottom slab was finished with floats and trowels to obtain a smooth surface. Excess concrete in the neighborhood of the forms was swept away and the exposed reinforcing bars protruding from the top of the girder webs

were wire-brushed to clear away dried concrete.

The bottom slab and girder webs were then covered with wet burlap over which sheets of polyethylene were spread to prevent moisture loss. Water was sprinkled on the burlap daily. At the end of 12 days, the inner cell forms were removed. Fig. 4.7 shows the cells of the bridge with the center bent and span I diaphragms after removal of the inner forms.

4.3.3 Placing of Steel Billets in the Bridge Model Cells

To allow for the placement of steel billets within the cells, the 50, 75 and 100 ft. long lead wires of the gages and strain meters located at sections A, B and C, and D, respectively were first uncoiled. Within each cell, these wires were bundled together and strapped with a tie-gun. Each braid of wire was made to pass through holes which were provided in the diaphragms for this purpose, Fig. 4.7. During its passage to the west end of the bridge model, each braid of wire was laid alongside a girder and attached to snap tie rods that protruded from the girders at intervals along the length.

This allowed the cells to remain free for the placing of the steel billets and also prevented the lead wires from damage through shearing when the formwork for the top slab was subsequently pushed down and made to fall on top of the steel billets.

In order to simulate prototype behavior, rented steel billets of approximate dimensions 9 in. x 9 in. x 65 in. were placed in the cells in the form of a uniformly distributed load over the length and width of the bridge model. Six pairs of steel billets per cell per span were placed end to end giving a total of 96 billets for the box girder bridge

model. To provide for better distribution of the weight of each billet, each cell had been earlier provided with a layer of sand of about 1 in. thickness. Fig. 4.8 shows the bridge model cells with the billets in place. The total weight of the steel billets and sand was 116.3 kips, which compared favorably with the required extra load value calculated as 116 kips.

As a final operation, each gage was checked for leakage using a mega-ohmmeter, and damaged lead wires were replaced.

4.3.4 Casting of Top Slab

One of the problems associated with the casting of the top slab in the box girder bridge model was to ensure that the formwork holding the top slab in place did not adhere to the bottom surface of the slab and provide unwanted added stiffness or longitudinal restraint. The prefabricated top slab soffit forms were made in approximately 9 ft. long sections, and consisted of 3/4 in. plywood sheets with 2 by 4 in. strong backs. Thin steel rods suspended from overhead cross beams carried the soffit forms, Fig. 4.9. Tackwelded washers on the rods on top of the plywood allowed the forms to be forced down, making the forms fall freely down into the cells of the bridge model.

After the two layers of reinforcement for the 2-1/4 in. thick top slab were placed in position and the gages and strain meters checked, Fig. 4.9, the top slab was cast in the same manner as the bottom slab and girders. Two truck loads of concrete were used for the top slab; one for each of the two spans.

The concrete after being pumped from the transit mix truck to the top slab was leveled and vibrated, care being taken to stay

clear of the lead wires and instrumentation. The concrete was jiggered, screeded and troweled to obtain a uniform height and the surface was then finished with a troweling machine.

The top slab was cured for 14 days in the same manner as the bottom slab and girder webs by being covered with wet burlap and sheets of polythene. Water was sprinkled on the burlap daily during this period.

4.4 Removal of Formwork

The formwork on the sides of the box girder bridge model was removed 3 weeks after the top slab was cast, and the formwork for the shoring under the end diaphragms was removed after 4 weeks. The rods with washers holding the soffit forms for the top slab were forced down 5 weeks after the slab was cast. The exposed surfaces of the bridge were then cleaned and whitewashed, and centerlines of the girders and transverse sections were marked by means of masking tape, Fig. 4.10.

The shoring for the bottom slab was finally lowered by removing the wedges for the studs, and the formwork was removed. This took place on October 5, 1972, approximately 8 weeks after casting the top slab or 14 weeks after casting the bottom slab, girder webs and diaphragms. After all dead load readings were taken and the crack pattern was recorded, the bottom of the bridge was whitewashed for further crack observation.

Several views of the completed bridge model showing its clear curving lines are shown in Figs. 4.11 and 4.12.

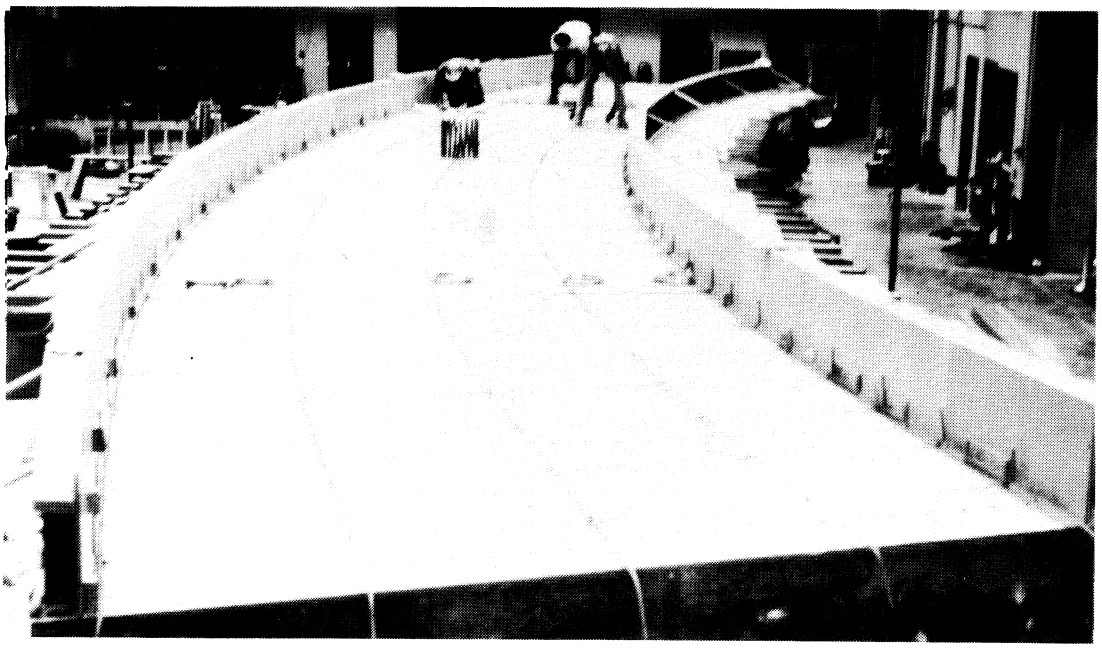

FIG. 4.1 BOTTOM SLAB FORMS IN PLACE

FIG. 4.2 STEEL REINFORCEMENT FOR BOTTOM SLAB AND GIRDER WEBS AND DIAPHRAGMS

FIG. 4.3 INNER CELL FORM PLACEMENT PARTIALLY COMPLETED

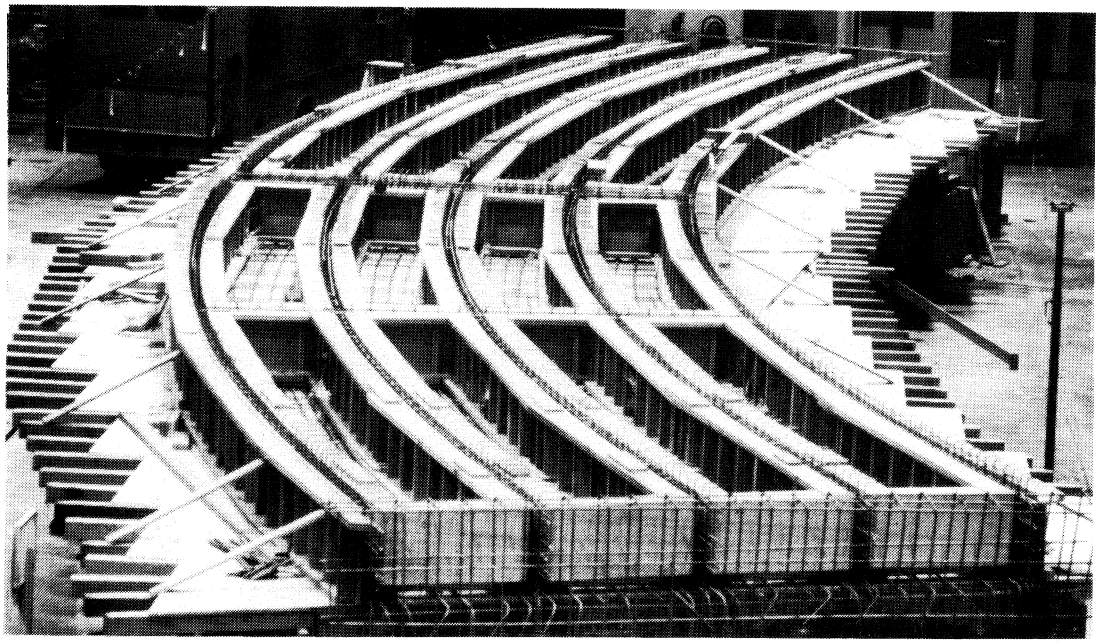

FIG. 4.4 INNER CELL FORM PLACEMENT ALL COMPLETED

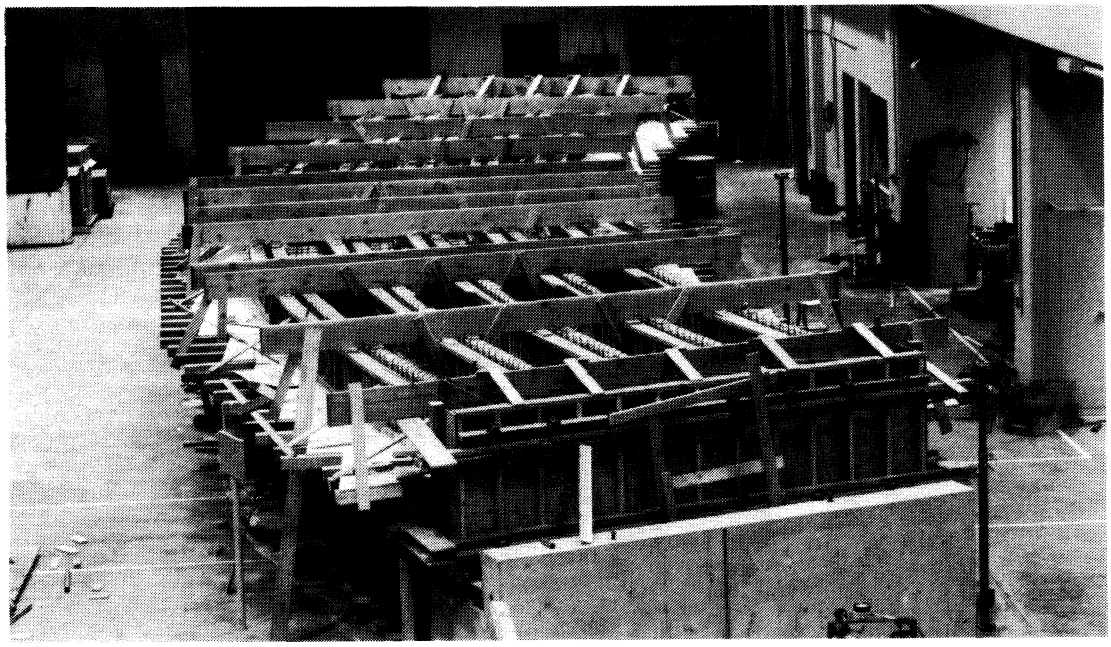

FIG. 4.5 FORMS FOR BOTTOM SLAB, GIRDER WEBS AND DIAPHRAGMS READY FOR CASTING OF CONCRETE

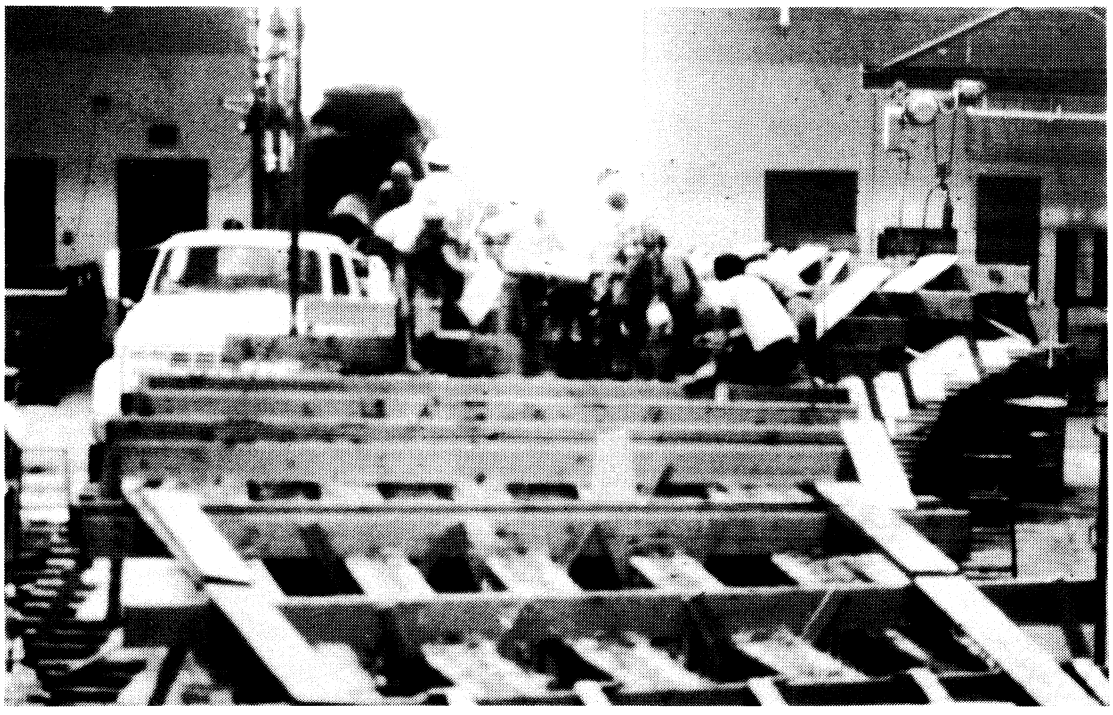

FIG. 4.6 CASTING OPERATION SHOWING CONCRETE TRANSIT MIX TRUCK AND PUMP TRUCK

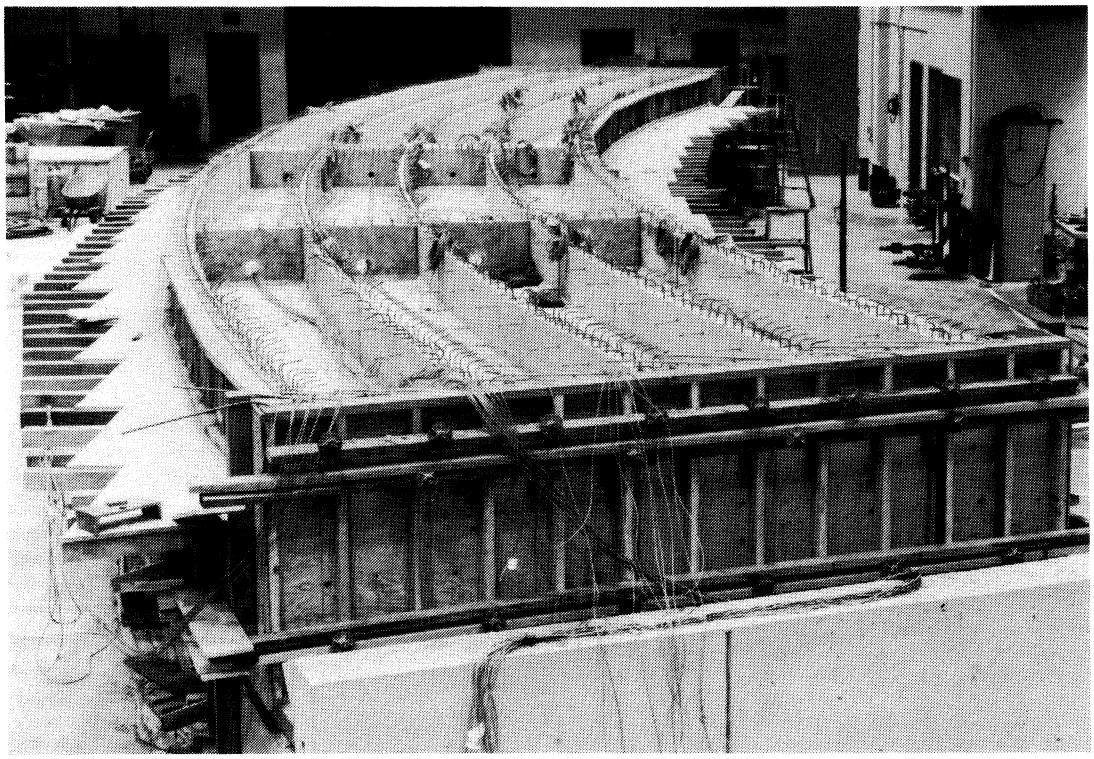

FIG. 4.7 BRIDGE MODEL AFTER REMOVAL OF INNER FORMS

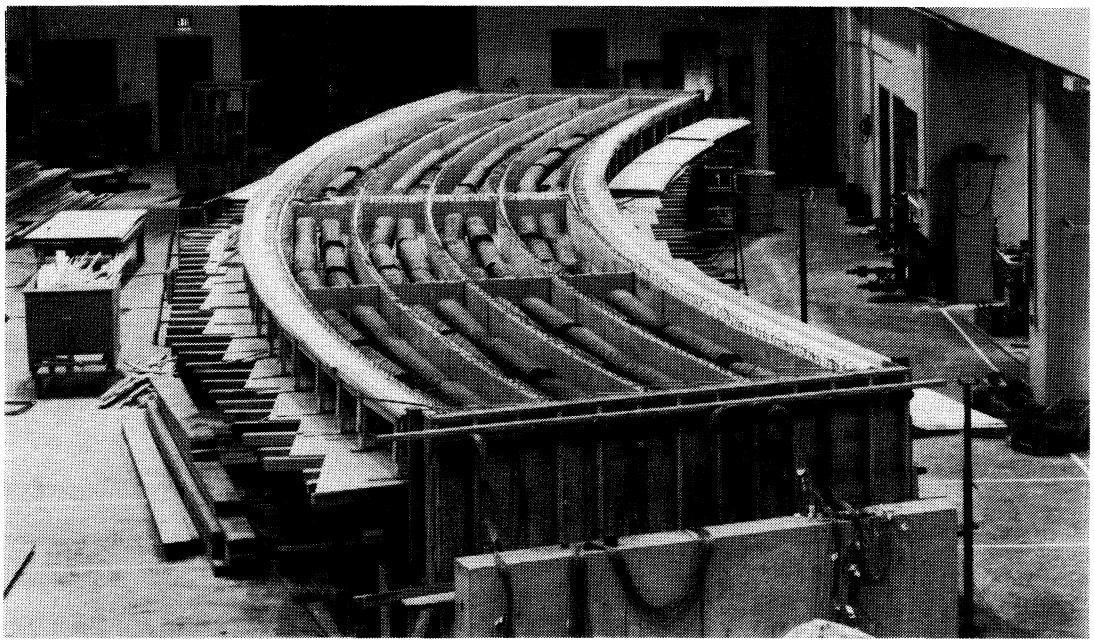

FIG. 4.8 STEEL BILLETS IN PLACE WITHIN CELLS OF MODEL

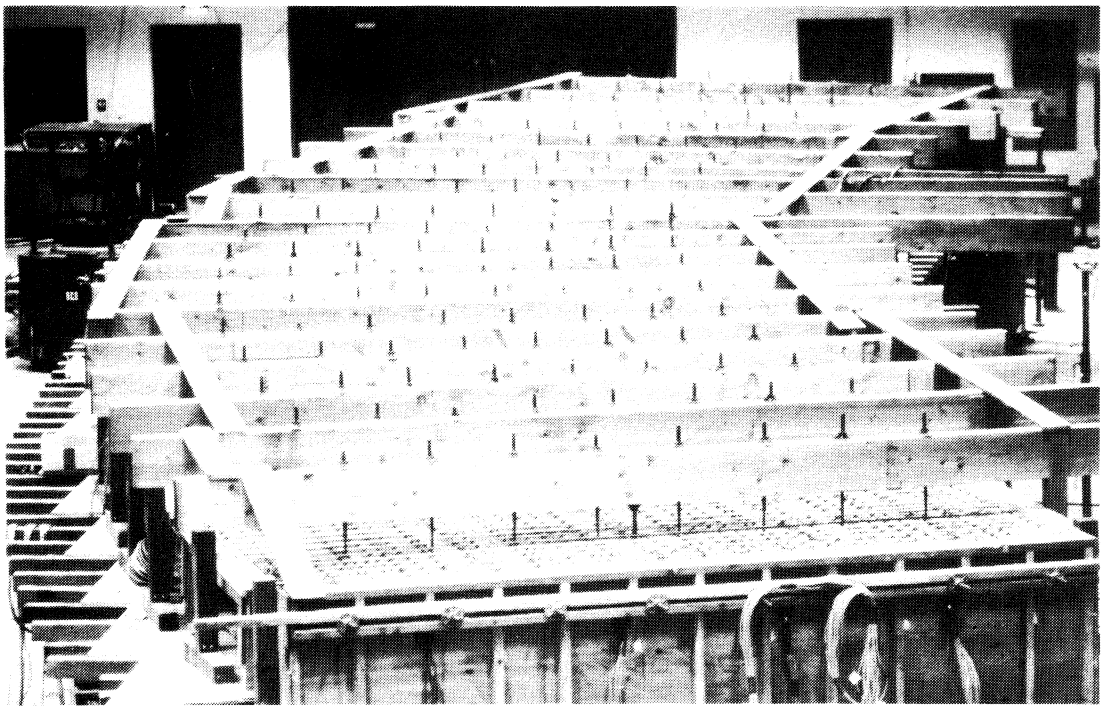

FIG. 4.9 STEEL REINFORCEMENT AND FORMS FOR TOP SLAB READY FOR CASTING OF CONCRETE

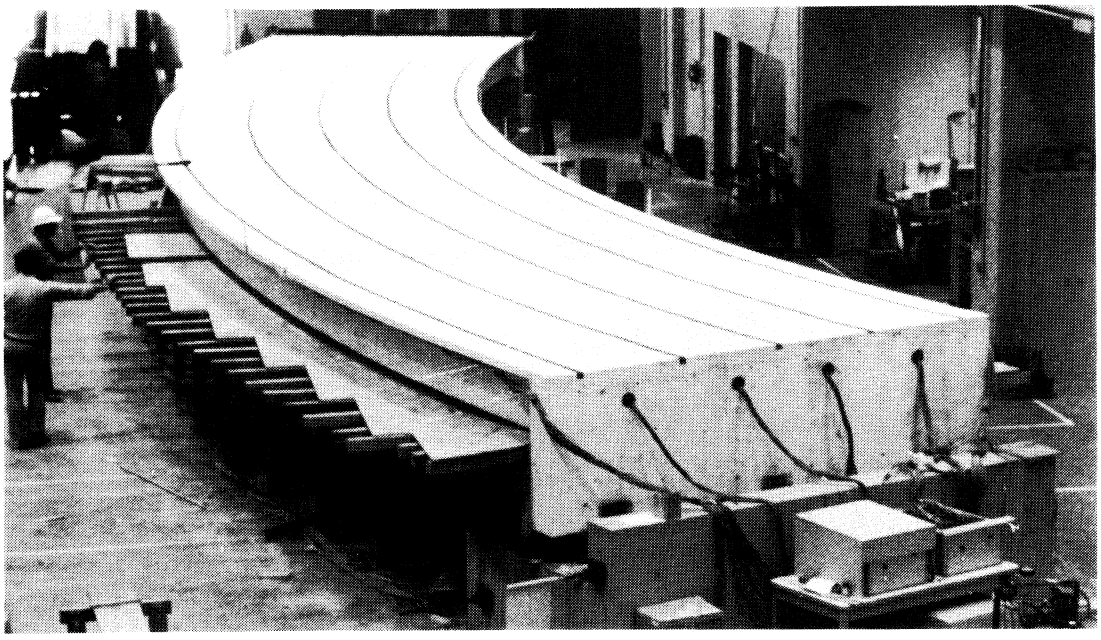

FIG. 4.10 BRIDGE MODEL AFTER STRIPPING OF ALL FORMS EXCEPT FOR BOTTOM SLAB SHORING

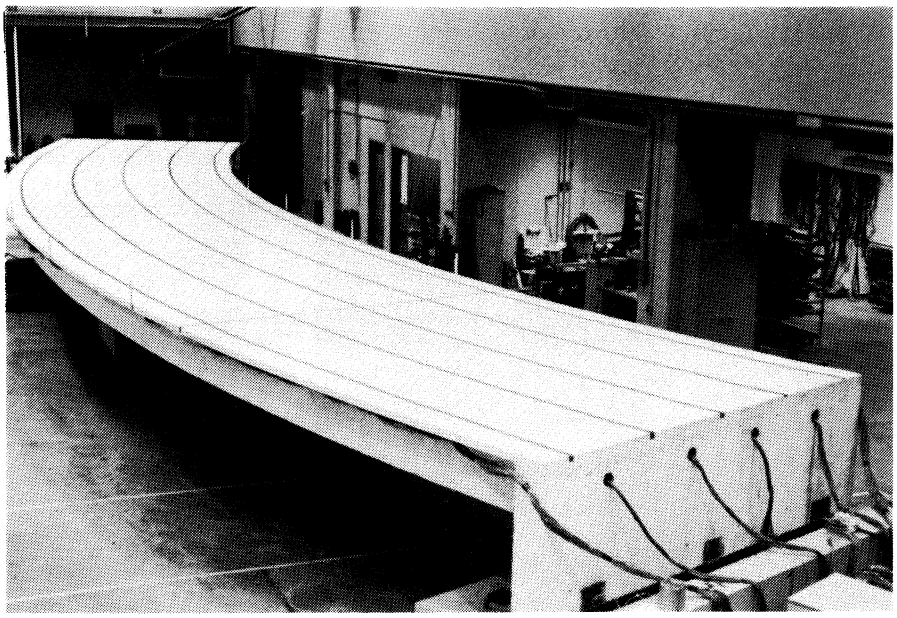

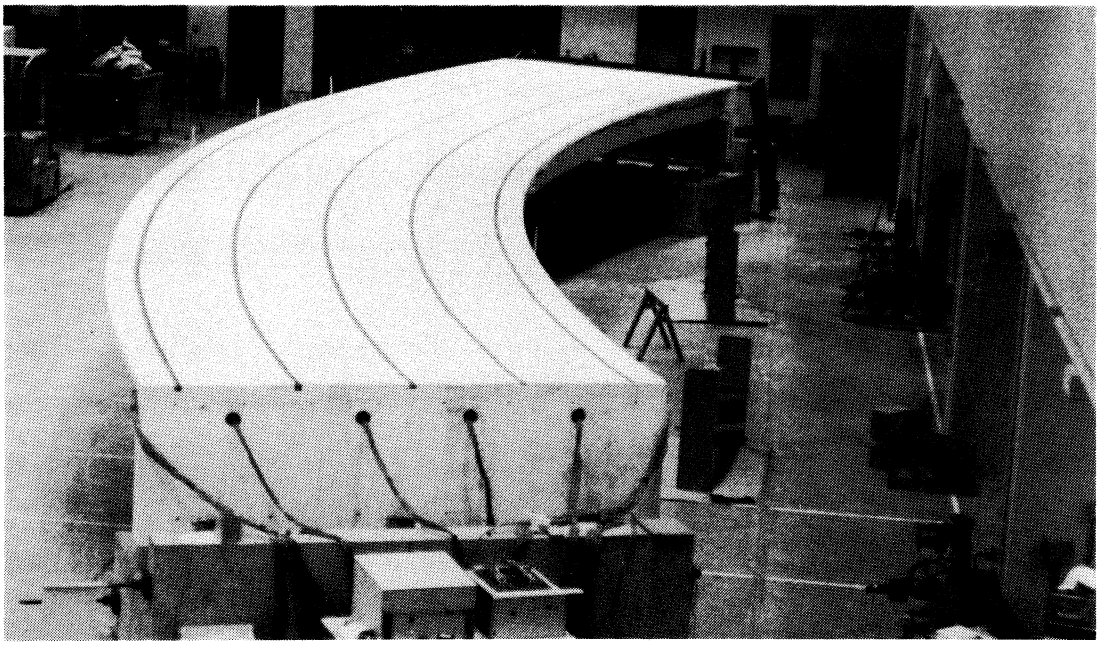

FIG. 4.11 VIEWS OF COMPLETED BRIDGE MODEL

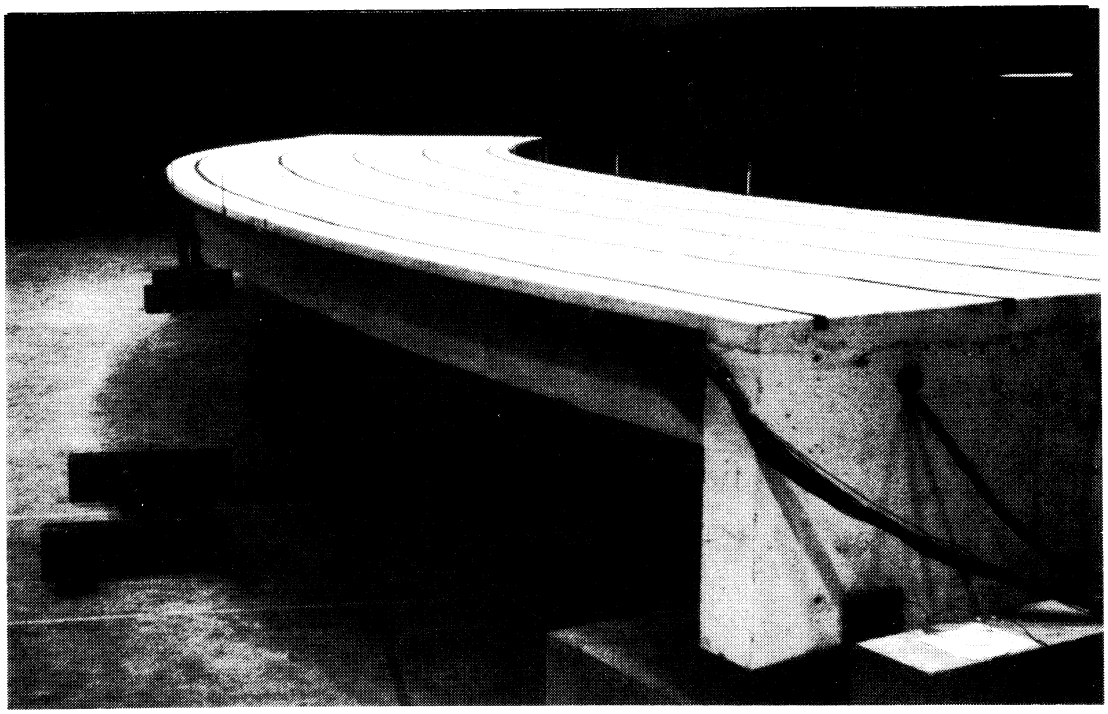

FIG. 4.12 VIEWS OF COMPLETED BRIDGE MODEL

5. EXPERIMENTAL PROGRAM

5.1 General Remarks

The experimental program was planned to accommodate a wide variety of loading conditions at various stress levels. The main object of the test program was to obtain information on load distribution in reinforced concrete box girder bridges under conditions of working loads. Working loads would result in total stresses of 24 ksi in the tensile steel at the sections of loading. Bearing in mind, however, that the tensile stresses in the tensile reinforcement at these sections due to the self weight and extra dead load of the bridge model alone was about 12 ksi, it was decided to consider two levels of working loads -- those producing total stresses in the steel of 24 ksi, and those resulting in total tensile steel stresses of 30 ksi at the sections of loading. The advantage of the latter stress level was that 50% higher values of live load stresses and strains could be registered for a total increase in the bridge model stresses of only 6 ksi.

The experimental program was divided into two parts as described below:

Part 1 - Dead load and Working load

Part 2 - Overload and loading to failure

In terms of the actual experimental data, it was convenient to divide the experimental program into seven phases, from the dead load condition [Phase 0] through the 24, 30, 40, 50 and 60 ksi stress levels [Phases I to V] to the failure condition [Phase VI].

The box girder bridge model had a loading frame at each mid-span enabling live loads to be applied at each of the five girders by

means of jacks singly and in various combinations, Fig. 5.1. Each phase of the experimental program for live loads comprised firstly the application of equal loads on each girder at both midspans to produce the same nominal steel stress at sections of maximum positive and negative moment. These loads were termed "conditioning loads". Subsequently after the removal of the conditioning loads, point loads were applied in several combinations. The conditioning loads were chosen to produce total steel stresses of 24, 30, 40, 50 and 60 ksi at the sections of maximum positive and negative moment, and to represent the successive deterioration of the box girder bridge model due to the effects of overload. The point loads however were chosen in all cases to produce stresses where applied of the order of the working stresses, i.e. 24 and 30 ksi total stresses in the tensile reinforcement.

The loading phase involving the application of the conditioning loads to produce the 30 ksi steel stress was chosen as the most representative from the point of view of assessing actual box girder bridge behavior for design purposes. The single and combined point loads after the conditioning loads in this phase were applied to the box girder bridge model for three different types of support condition: simply supported ends, center bent restrained against transverse rotation thus preventing torsional rotation of the bridge at that section, and bottom of end abutments restrained against longitudinal movement.

In addition to the point loads, scaled down truck and heavy construction vehicle loads and a moving load were applied to the bridge in this loading phase.

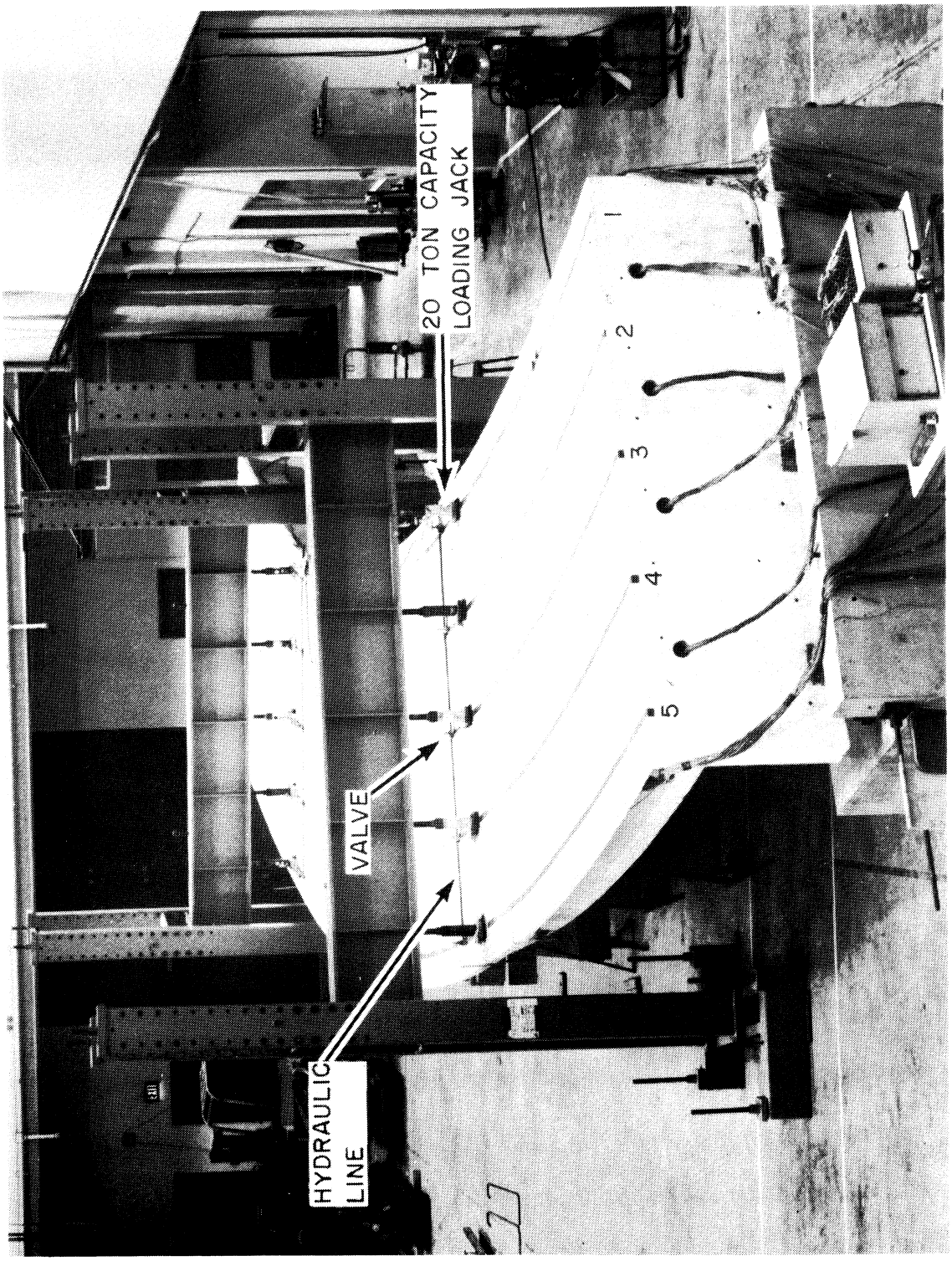

FIG. 5.1 MIDSPAN LOADING FRAMES WITH TEN 20 TON JACKS IN POSITION

For the application of live loads to the bridge in each span as envisaged by the experimental program, two identical loading frames were designed by the project staff and fabricated in the Structural Engineering Materials Laboratory. Scaled down AASHO trucks, heavy construction vehicles and accessories for loading, changes in support conditions, etc., had also to be fabricated and assembled.

It was decided to apply live loads to the box girder bridge model only at the midspan sections X and Y in view of the following considerations:

(a) Application at midspan of the conditioning loads - a preliminary to each live loading phase - resulted in nominally identical stresses in the reinforcing steel in the maximum positive moment region in the spans and in the maximum negative moment region on either side of the center bent diaphragm. As a result, an approximate uniformity of total positive and negative stresses in the reinforcing steel at the critical sections was obtained.

(b) As Span I had a transverse diaphragm at Section X, whereas Span II did not have a transverse diaphragm, the true effects of the diaphragm on load distribution could be assessed more readily when loads were applied at midspan than when applied elsewhere.

(c) It was desirable, in order to eliminate local irregularities, concentrations of stress and possible damage to the gages and strain meters, to have the location of the instrumented sections in the spans, i.e. Sections A and D, at a short distance from the sections of loading.

5.2 Description of Loading Frames

Each of the two identical loading frames, Fig. 5.1, positioned above a midspan consisted of a W24 x 145 beam 18 ft. long, transversely spanning the section at a height above the model deck sufficient to allow for the placing of loading jacks, load cells, bearing plates and pads, and scaled down trucks as required. Each end of the W24 x 145 beam was held by a 2 ft. 5 in. long W10 x 77 beam which had two end plates of dimensions 18 in. x 12 in. x 1/2 in. welded to it. These end plates had four pairs of holes at 4-3/4 in. vertical intervals, which allowed the wide flange beam arrangement to be bolted by means of 7/8 in. diameter high strength steel bolts to two vertical columns of structural tubing of 12 in. x 6 in. x 1/2 in. section at 3 ft. centers on each side of the bridge model.

The 24 in. deep wide flange steel beam was stiffened by means of 1/2 in. thick stiffeners, located in pairs at the ends and at five intermediate locations above the centerline of each girder of the box girder model. The bottom flange of the beam had five steel rings tack-welded to it at the stiffener locations to allow for proper positioning of the loading jacks above the girder webs.

The vertical 12 in. x 6 in. x 1/2 in. columns of structural tubing each contained a 1-1/8 in. diameter high strength steel pre-stressing rod which allowed the frame assembly to be fastened to a base plate assembly which in turn was anchored to the test floor of the laboratory. The tie-down floor had holes for anchorage purposes at 3 ft. intervals in two perpendicular directions.

5.3 Loading Arrangement for Box Girder Bridge Model

For point loads in various combinations to be applied at the centerlines of the girders at midspan, the following method was devised for convenience of loading:

Ten identical loading jacks, each of capacity 20 tons were placed, one over each girder centerline, at both midspans of the box girder bridge model, Fig. 5.1. The jacks rested on 5 in. x 5 in. x 1 in. steel plates which had neoprene bearing pads of the same dimensions under them for uniform application of load.

The five jacks at each midspan section were connected by means of hoses fitted with valves to a common manifold. Each of the two manifolds was connected by means of high pressure hoses to an air pressure hydraulic pump system. Load cells were used to check that each jack delivered an equal load when all valves were open. Calibrations for jack load versus pump pressure were made earlier, and confirmation of the load value in each case was obtained from load cells.

The use of ten identical jacks eliminated the need for moving the loading jacks into position, and all that was necessary was the opening or closing of the valves as the loading required.

For the loading of scaled down trucks and construction vehicles, the manifold system remained essentially the same but its height above the bridge model top deck had to be adjusted. The 24 in. deep cross beams of the loading frames had to be raised for the loading of the trucks and had to be removed for the application of the moving load.

5.3.1 Modifications for Changes in Support Conditions

Most of the experimental program was carried out for the bridge model with simply supported end abutments and the central column support with its footing prestressed to the tie-down test floor.

In loading phase II, after the application of conditioning loads to produce stresses in the steel reinforcement of 30 ksi at the sections of maximum positive and negative moment, the effect of altering the support conditions on the load distribution properties of the box girder bridge model was studied. The application of point loads at the girder centerlines was repeated for the case of torsional restraint at the center bent and separately for the case of longitudinal restraint at the two end diaphragms.

The torsional restraint at the center bent was accomplished by using similar concrete pedestals and screwjacks under girders 1 and 5 at section Z, i.e. the bridge centerline. Pressure meters between the concrete pedestals and the screwjacks gave readings of the load being taken by the torsional restraint. The torsional restraint, as applied above, modeled a box girder bridge with a three-pedestal center bent. Fig. 5.2 gives a picture of the screw jacks assembly under girder 5 at the center bent.

The longitudinal restraint at the end diaphragms was accomplished by using three screwjacks and pressure meters at each end abutment. The restraint was applied at girders 1, 3 and 5, where 1/2 in. thick steel plates had been cast into the end abutments for this purpose. The horizontal restraint introduced at the bottom of the end diaphragms modeled a box girder bridge with the end diaphragms cast

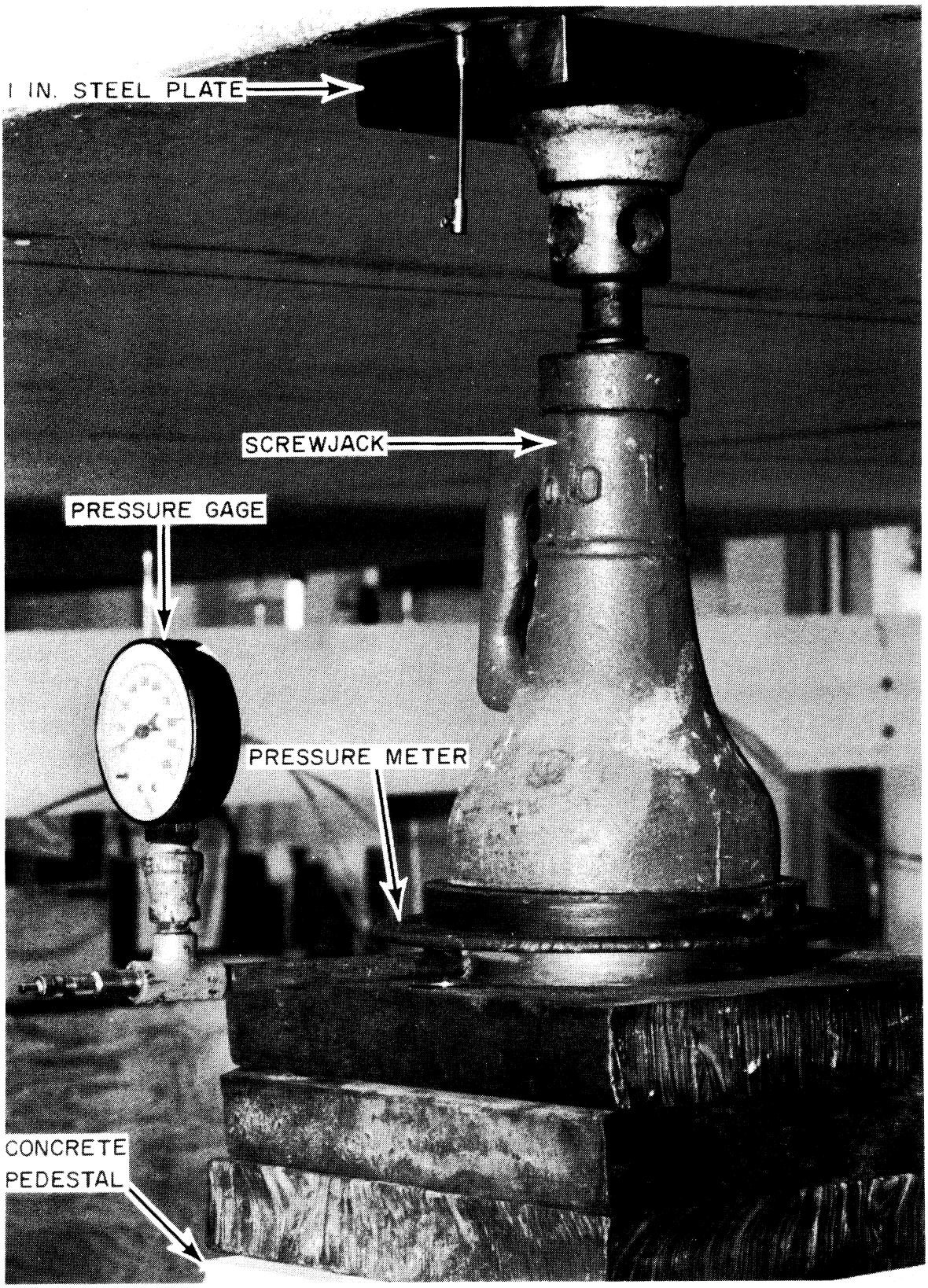

FIG. 5.2 SCREW JACK ASSEMBLY UNDER GIRDER 5 AT THE CENTER BENT FOR TORSIONAL RESTRAINT

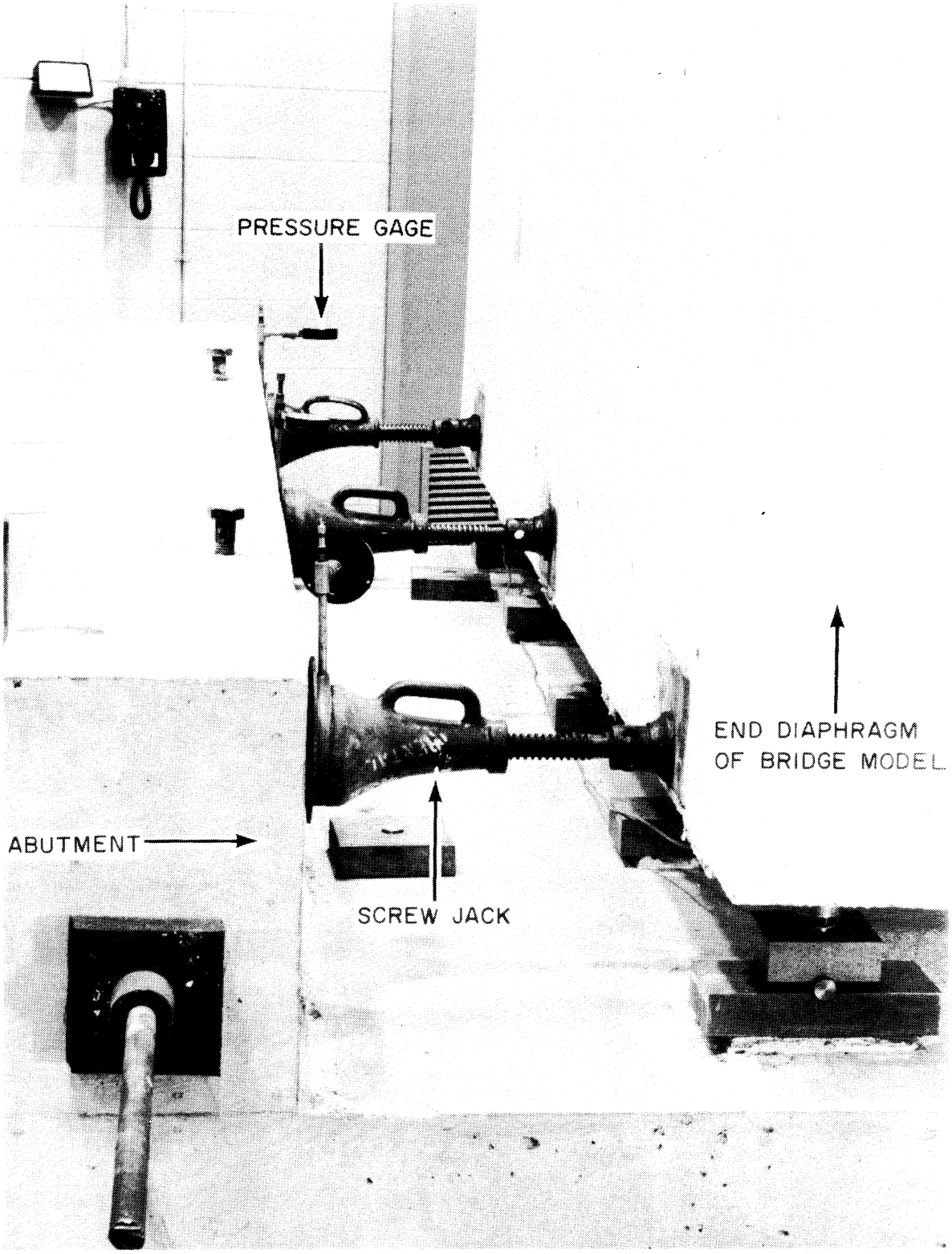

FIG. 5.3 END SUPPORT CONDITION FOR LONGITUDINAL RESTRAINT

directly on immovable vertical piles. Fig. 5.3 gives a picture of the longitudinal restraint.

5.4 Description of Scaled-down Trucks and Construction Vehicles

Schematic representations of prototype dimensions and wheel loads for the AASHO standard HS 20-44 truck (total load = 72 kips) and the proposed overload construction vehicle Class II (total load = 330 kips) are shown in Figs. 5.4 and 5.5. For the AASHO truck, the variable dimension was taken as 14 ft. to produce maximum stress.

As suggested by the California State Division of Highways, the wheelprint prototype area for the AASHO truck was a rectangle of 20 in. transverse by 10 in. longitudinal dimensions. For the overload construction vehicle, the procedure was to divide the wheel reaction by the tire pressure to obtain a gross wheelprint area. An elliptical wheelprint of major to minor axis ratio of 1.25 was then calculated, the major axis being in the direction of movement of the vehicle.

These calculations give a major axis of 40 in. and a minor axis of 32 in. for a 65 kip wheel load, using the manufacturer's suggested tire pressure of 65 psi.

The drawings for the scaled-down AASHO truck model (total load = 9 kips) and the overload construction vehicle model (total load = 41.25 kips) are shown in Figs. 5.6 and 5.7. All linear dimensions of the prototypes were reduced by the scale factor 1: 2.82 and all loads in the ratio 1:8 as necessitated by similitude conditions. For convenience, the elliptical wheelprints of the construction vehicle were replaced by rectangular areas of about the same magnitude. 1 in. thick neoprene pads were used at the six contact areas in the case of each

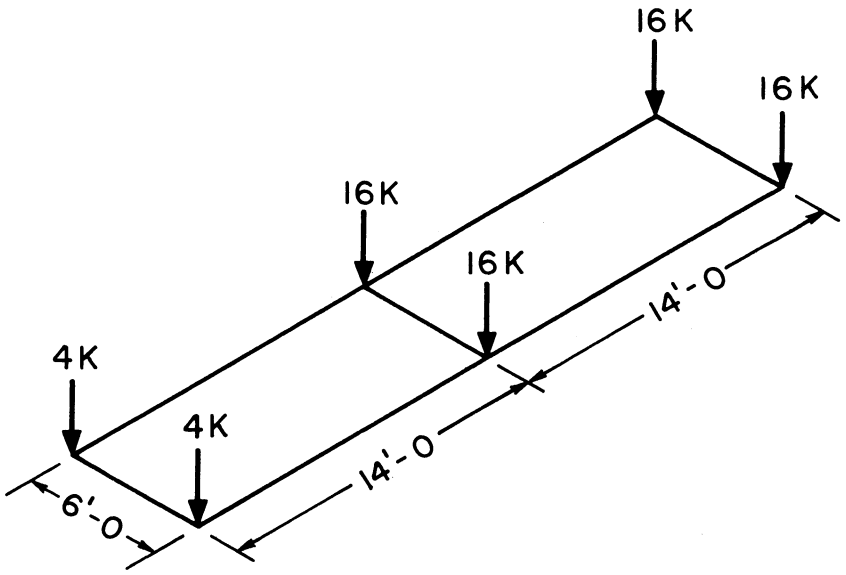

FIG. 5.4 WHEEL LOADS AND DIMENSIONS OF AASHO HS 20–44 TRUCK

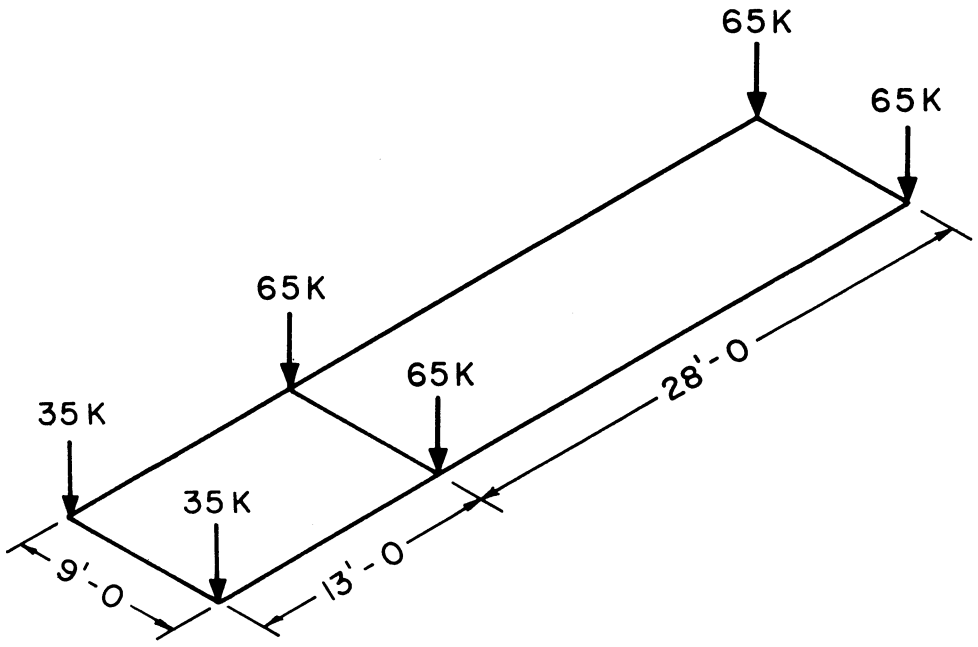

FIG. 5.5 WHEEL LOADS AND DIMENSIONS OF OVERLOAD CONSTRUCTION VEHICLE

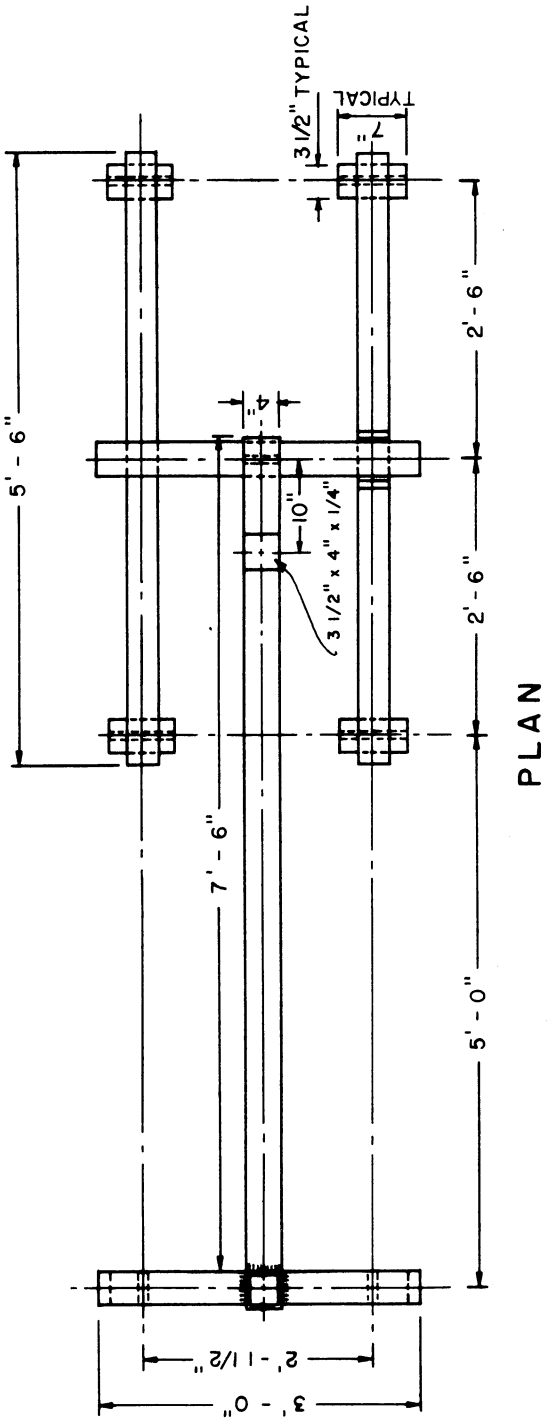

PLAN

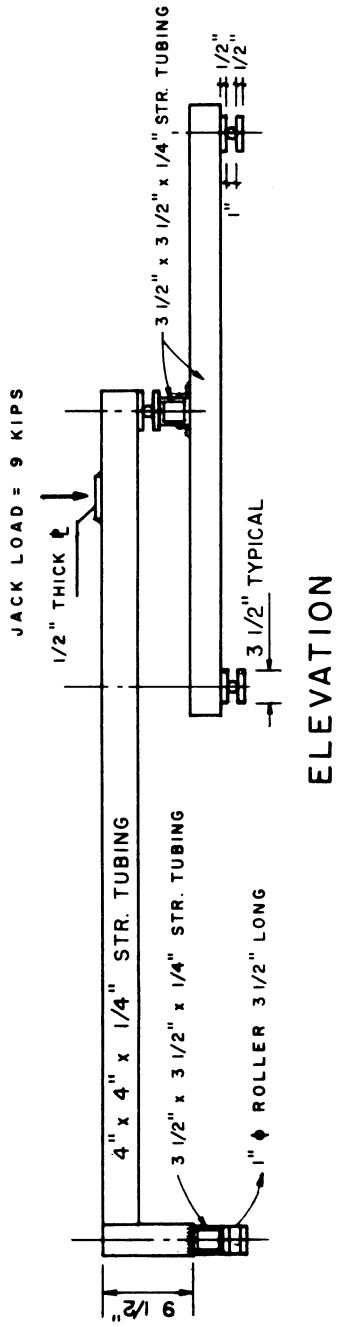

ELEVATION

FIG. 5.6 LOADS AND DIMENSIONS OF AASHO HS 20-44 TRUCK MODEL

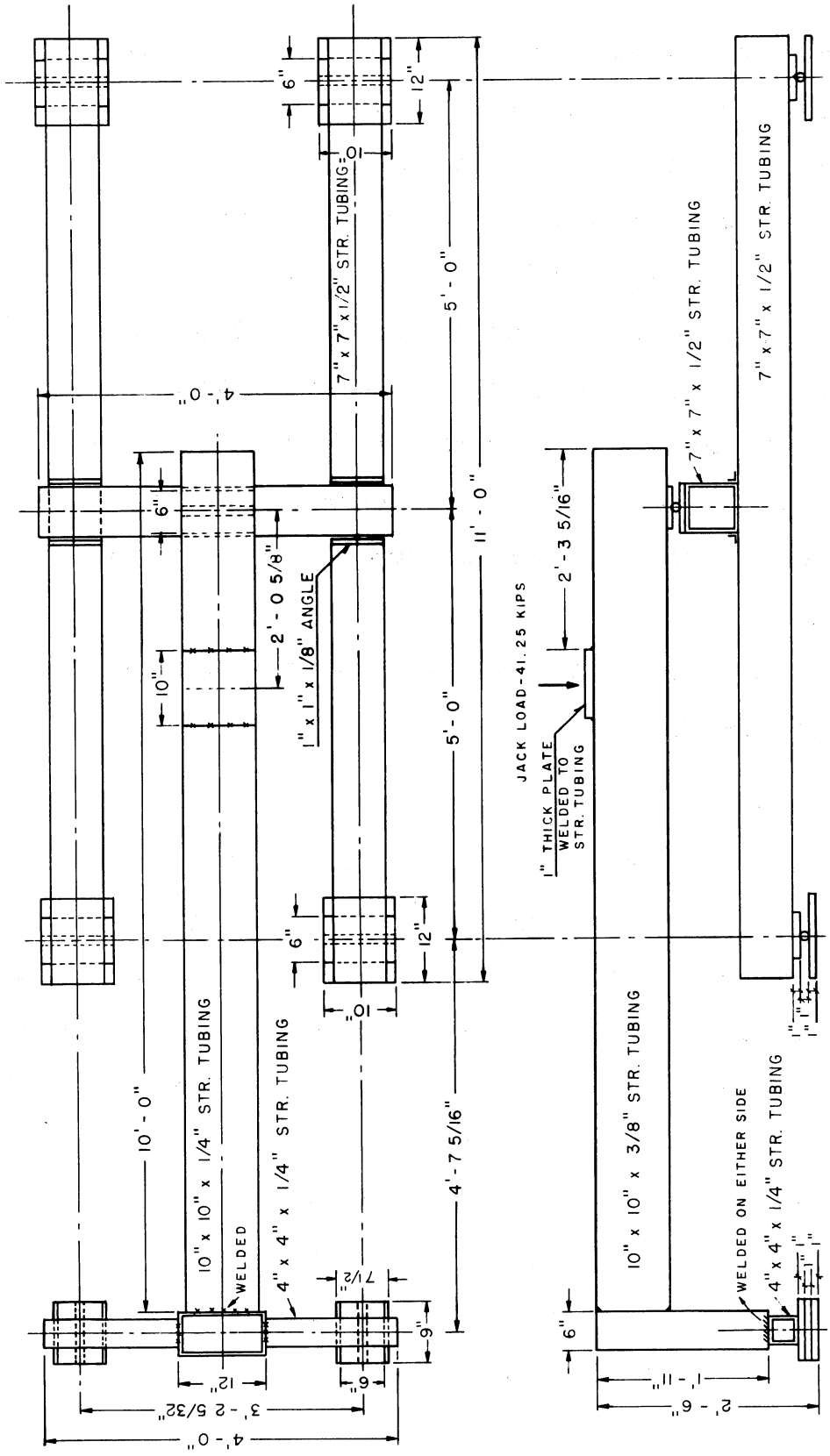

FIG. 5.7 LOADS AND DIMENSIONS OF OVERLOAD CONSTRUCTION VEHICLE MODEL

truck or vehicle.

Six AASHO trucks and two construction vehicles were fabricated in the Structural Engineering Materials Laboratory shop. A system of statically determinate beams was adopted in each case, the resultant of the wheel loads being applied at one point by means of a loading jack. On the bridge model deck, a truck or a construction vehicle was always placed such that the point of loading was directly above the midspan Section X or Y irrespective of the orientation of the truck. The trucks and construction vehicles thus essentially consisted of static loads. The number of trucks on the bridge deck and the orientation of the trucks were changed as will be shown in the loading schedule.

Fig. 5.8 shows a photograph with a three lane truck loading on the bridge model deck.

5.5 Description of Moving Load

A fork lift with two concrete blocks on the fork as shown in Fig. 5.9 was used as a moving load of about 10 kips. It had a spring-like pointer poised immediately above one of the longitudinal masking tapes showing the centerline of a girder. By keeping the pointer in position the driver of the fork lift was able to follow a path parallel to the longitudinal axis of the bridge.

The dimensions and wheel loads for the fork lift are given in Fig. 5.10. Three passes were made from Sections W to E and readings in each case were taken at 11 different transverse sections, in order to obtain an approximately continuous record. Details are given in the loading schedule.

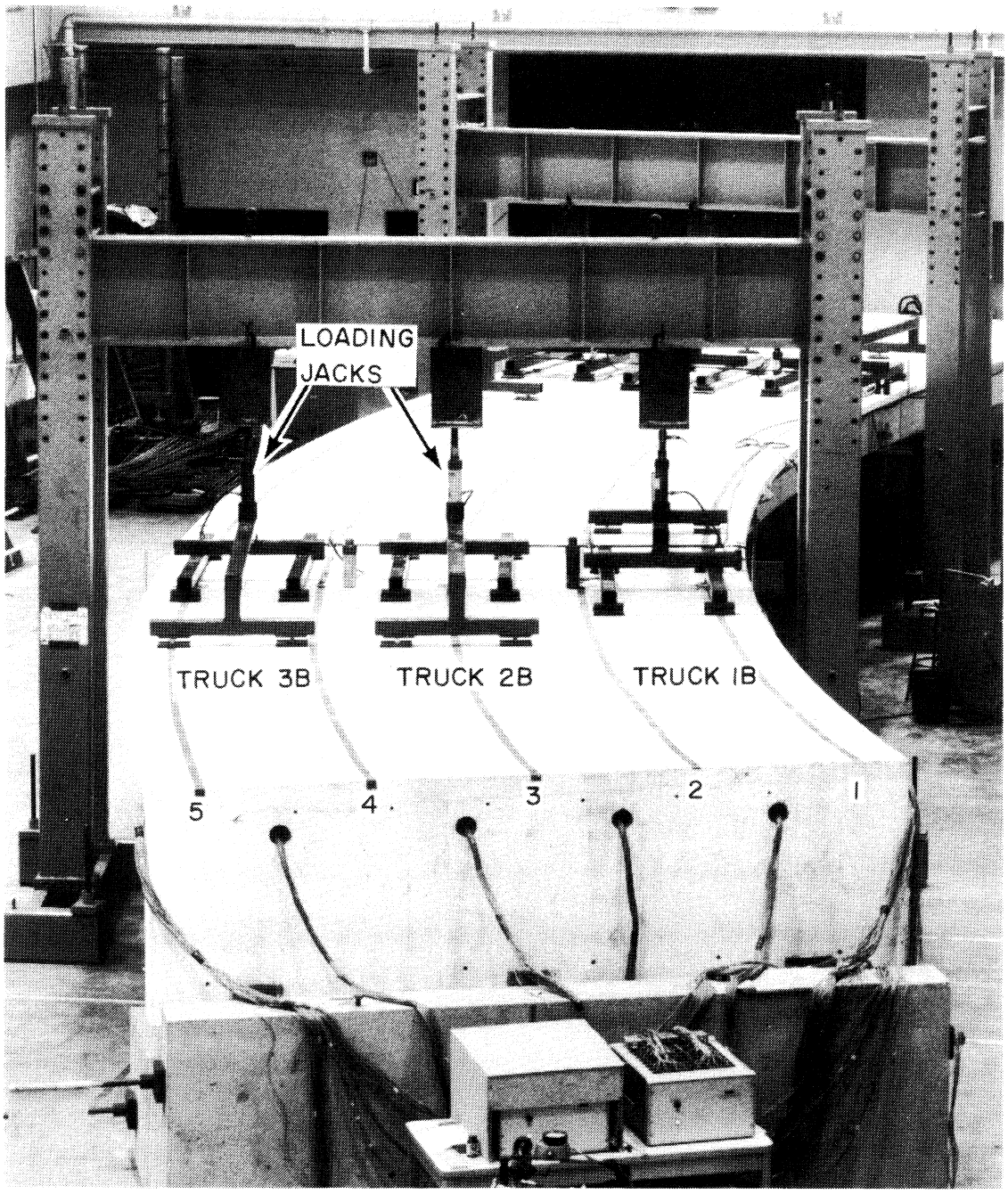

FIG. 5.8 THREE LANE AASHO TRUCK LOADING ON BRIDGE MODEL DECK

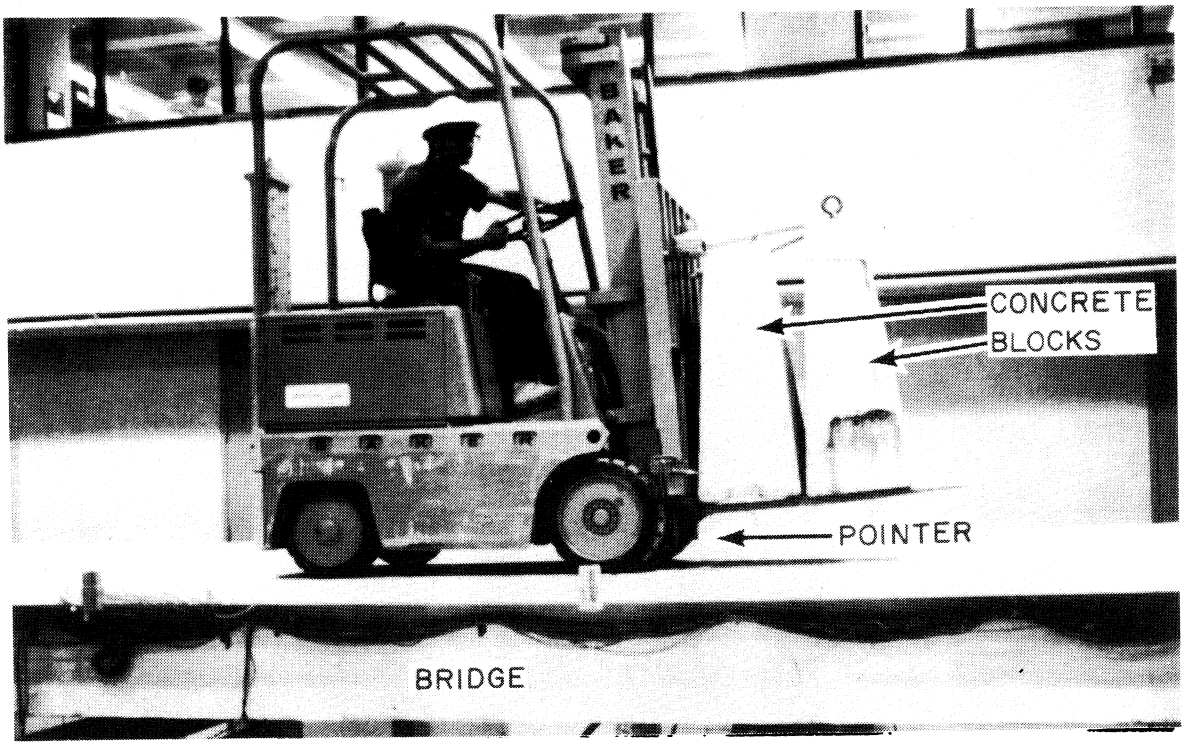

FIG. 5.9 FORK LIFT USED AS MOVING LOAD

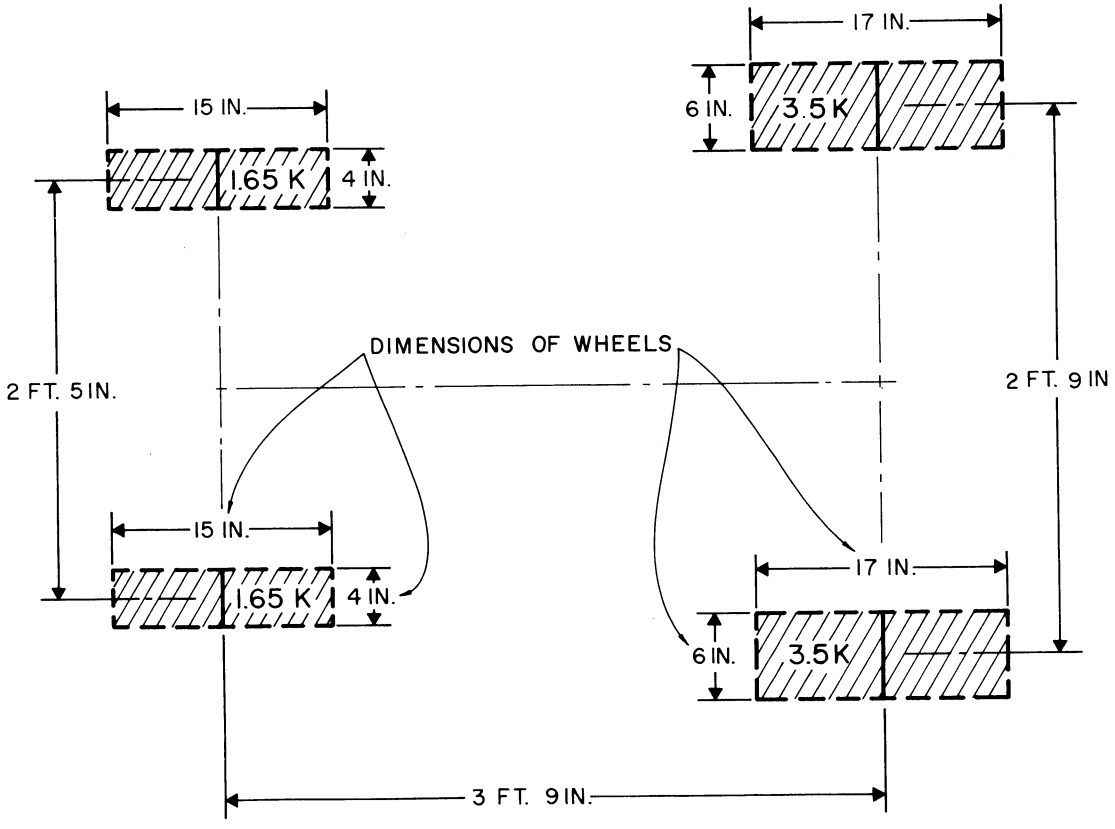

FIG. 5.10 DIMENSIONS AND WHEEL LOADS OF FORK LIFT

5.6 Loading Schedule for Box Girder Bridge Model

The design stress for the tensile steel reinforcement at locations of maximum moment in a reinforced concrete box girder bridge is 24 ksi when the steel used has a yield stress of 60 ksi.

It is found in actual practice that within a short time of use the stresses in various locations of a bridge approach the working stresses for which they have been designed. In fact, during construction, bridges are often subjected to heavy loads like those produced by construction vehicles which may create stresses in excess of the working level. For the determination of the live load characteristics of the box girder bridge model, it was decided that any combination of live loads that in conjunction with the self weight and extra weight for prototype simulation produced stresses within the bridge of less than 24 ksi was of little interest. The schedule of loading for the box girder bridge model was therefore based on the evaluation of box girder bridge behavior at the stress levels of 24 and 30 ksi in the tensile reinforcement at the section of loading. In addition, the bridge was loaded to higher levels of stress and finally to failure. The complete schedule is described below.

5.6.1 Loading Schedule - Part 1

The emphasis of the loading schedule was on Part 1 which dealt with the dead load and the working load condition of the box girder bridge model. Part 1 consisted of three phases, phases 0, I and II.

5.6.1.1 Phase 0 (Dead Load Phase)

Measurements were made for the dead load condition, i.e. self weight of box girder bridge model plus the extra weight of steel billets for prototype simulation. The end diaphragms were simply supported

for this phase, which consisted of two steps - zero readings before the final removal of the shoring and formwork and readings immediately after the removal of the shoring and formwork. The nominal stress in the tensile reinforcing steel due to the dead load alone was 11.5 ksi at midspan Sections X and Y and 8.9 ksi at instrumented Sections B and C.

5.6.1.2 Phase I (24 ksi Conditioning Load Phase)

Point loads of equal magnitude 7.7 kips were applied at both midspan Sections X and Y of the box girder bridge model, one over each girder making a total of ten loads, to create a nominal total stress of 24 ksi in the tensile reinforcing steel at Sections X and Y and a nominal total stress of 15.5 ksi in the tensile reinforcing steel at Section B and C. After removal of these conditioning loads, a standard point load of magnitude 12.7 kips, sufficient to create a nominal total tensile steel stress of 24 ksi in a girder when placed directly over it alone, was applied at various locations of the bridge model deck as shown in Fig. 5.11. For Phase I a total of 10 basic load combinations were used, shown in Fig. 5.11a, necessitating a total of 27 loading and unloading steps. The loads for the positions 1Y (indicating the position on the bridge deck at the intersection of girder 1 with transverse Section Y), and 5Y were applied in four increments, each a quarter of the total value, and then lowered to zero. Loads for the other positions consisted of two steps, from zero to total value and back to zero.

5.6.1.3 Phase II (30 ksi Conditioning Load Phase)

Point loads of equal magnitude 11.4 kips were applied at both midspan Sections X and Y of the box girder bridge model, one over each girder making a total of ten loads. These created a nominal total stress

of 30 ksi in the tensile reinforcing steel at Sections X and Y and a nominal total stress of 18.7 ksi in the tensile reinforcing steel at Sections B and C. After removal of these conditioning loads, a standard point load of magnitude 19.3 kips, sufficient to create a nominal total tensile steel stress of 30 ksi in a girder when placed directly over it alone, was applied at the various locations of the bridge model deck in the 19 combinations shown in Figs. 5.11a and b. In addition, the 10 basic load cases shown in Fig. 5.11a were repeated for the same value of load, i.e. 19.3 kips with the center bent of the bridge model restrained against torsion, and separately for the case with the end diaphragms of the bridge model restrained against longitudinal movement.

Next, two truck loadings consisting of four and six trucks respectively were applied to the bridge model deck in 11 and 3 combinations respectively, as shown in Figs. 5.12 and 5.13.

The next loading in this phase was the construction vehicle loading, in 8 combinations as shown in Fig. 5.14. Lastly, the fork lift shown in Fig. 5.9 was used as a moving load to make three passes from Section W to Section E with a total of 11 readings per pass. The location of the fork lift on the bridge model deck for each pass is shown in Fig. 5.15 and the 11 positions for which readings of the moving load were taken are given in Fig. 5.16.

5.6.2 Loading Schedule - Part 2

Part 2 of the loading schedule for the box girder bridge model dealt with stresses beyond the working load condition, and with the final loading to failure. The phases in Part 2 were phases III, IV, V and VI.

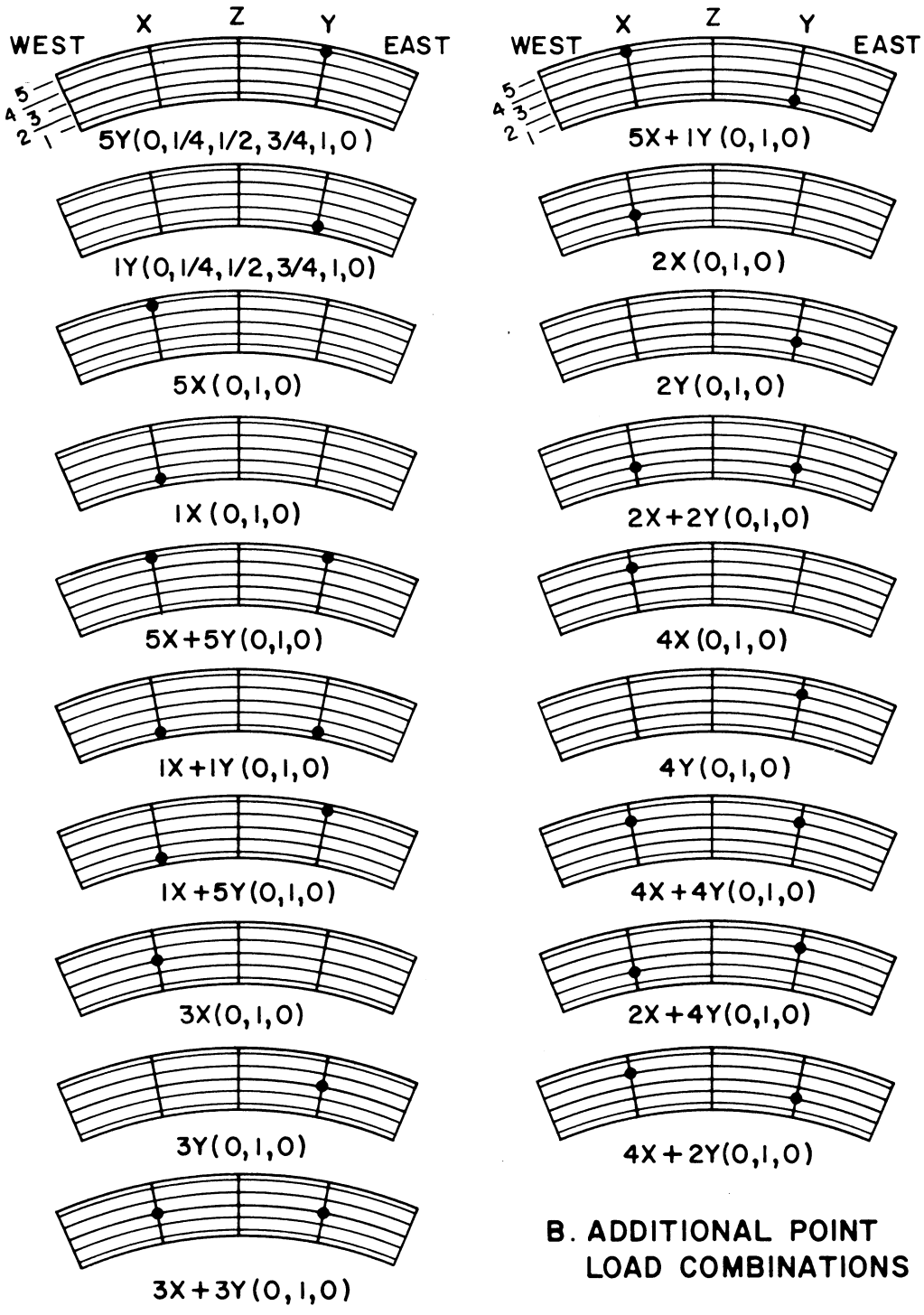

A. BASIC POINT LOAD COMBINATIONS

B. ADDITIONAL POINT LOAD COMBINATIONS

(NOT TO SCALE)

FIG. 5.11 BASIC AND ADDITIONAL POINT LOAD COMBINATIONS APPLIED AFTER CONDITIONING LOADS

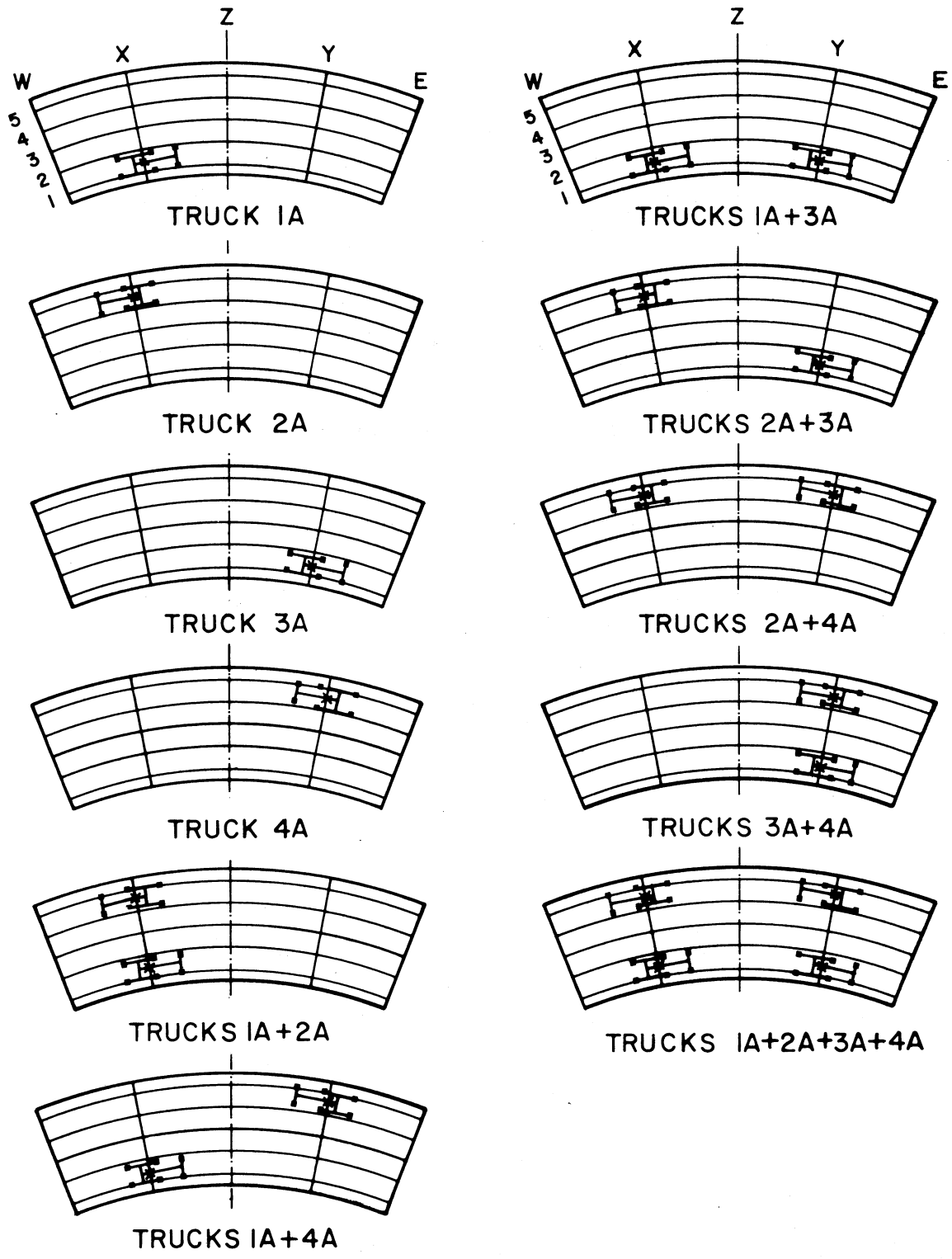

ONE WHEEL-LINE OF EACH TRUCK PLACED ON AN EXTERIOR GIRDER (NOT TO SCALE)

FIG. 5.12 TWO LANE AASHO TRUCK LOADINGS – 11 COMBINATIONS

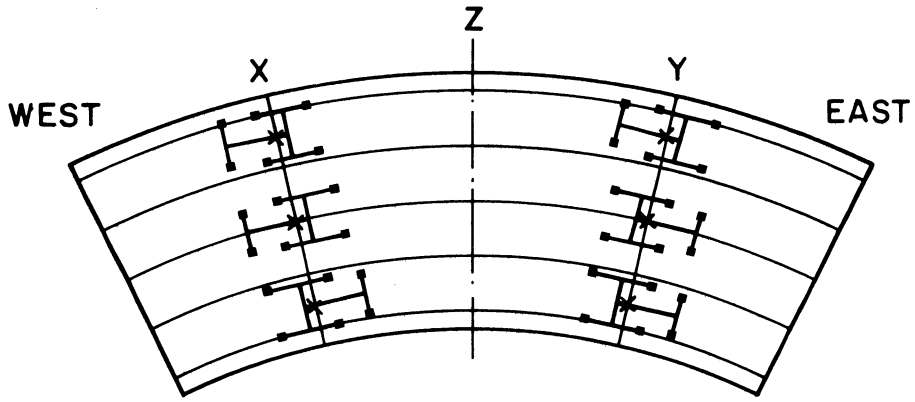

TRUCKS 1B+2B+3B+4B+5B+6B

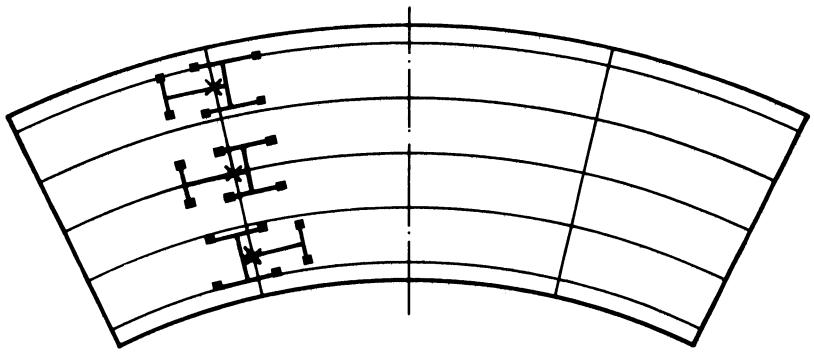

TRUCKS 1B+2B+3B

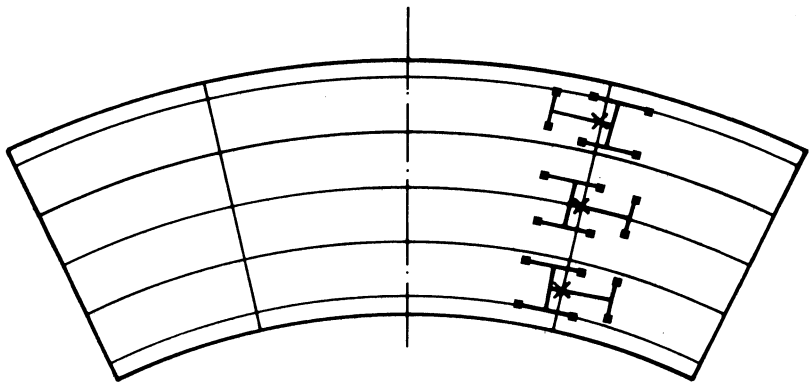

TRUCKS 4B+5B+6B

ONE WHEEL-LINE OF EACH TRUCK PLACED ON AN EXTERIOR GIRDER (NOT TO SCALE)

FIG. 5.13 THREE LANE AASHO TRUCK LOADINGS – 3 COMBINATIONS

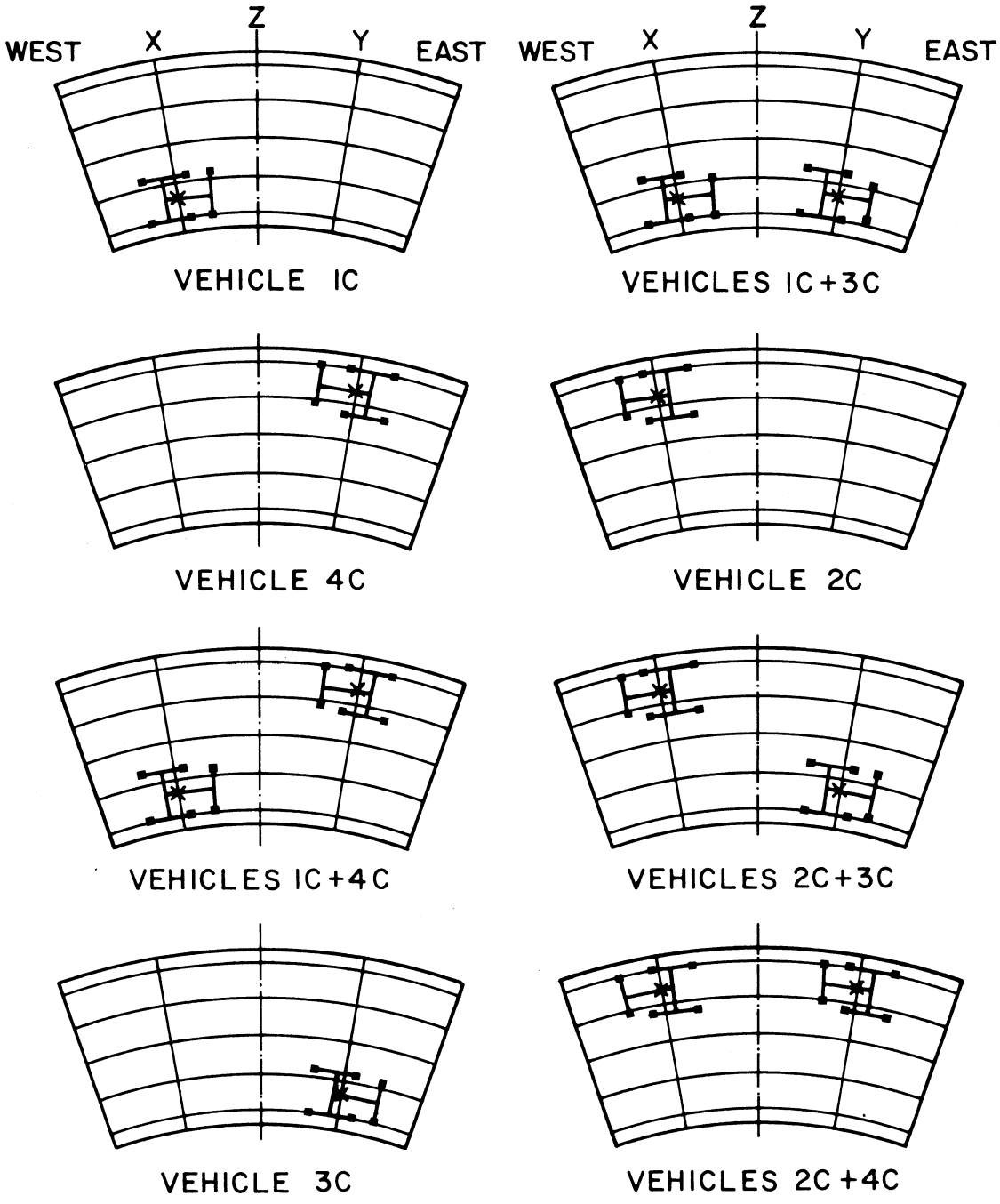

ONE WHEEL-LINE OF EACH VEHICLE PLACED ON AN EXTERIOR GIRDER (NOT TO SCALE)

FIG. 5.14 CONSTRUCTION VEHICLE LOADINGS – 8 COMBINATIONS

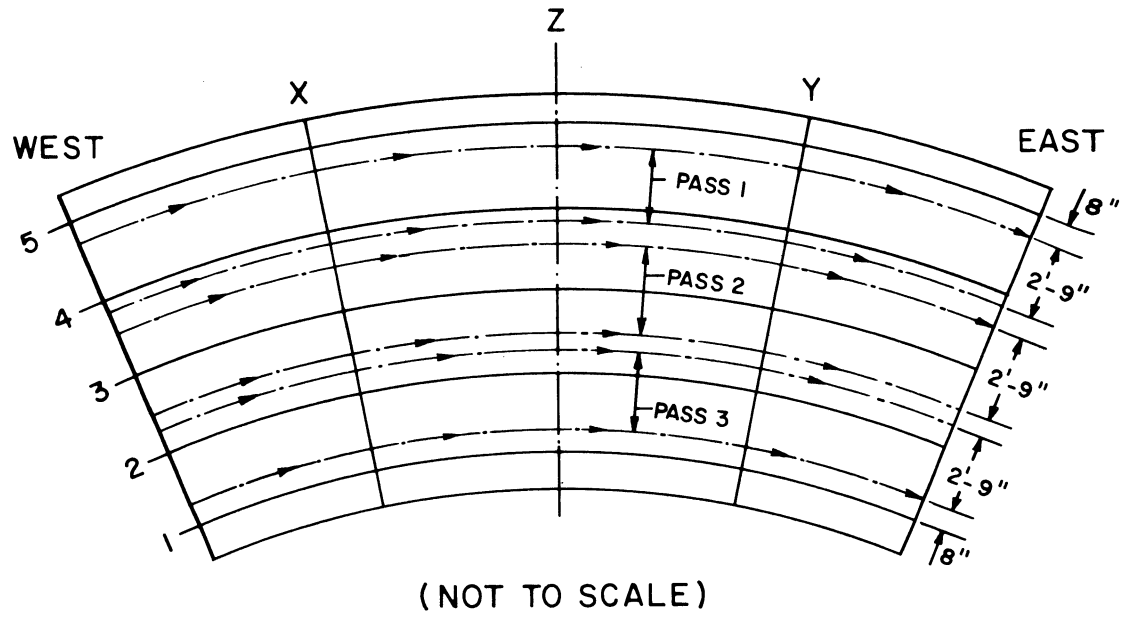

FIG. 5.15 PLAN SHOWING PATHS OF FORK LIFT FRONT WHEELS

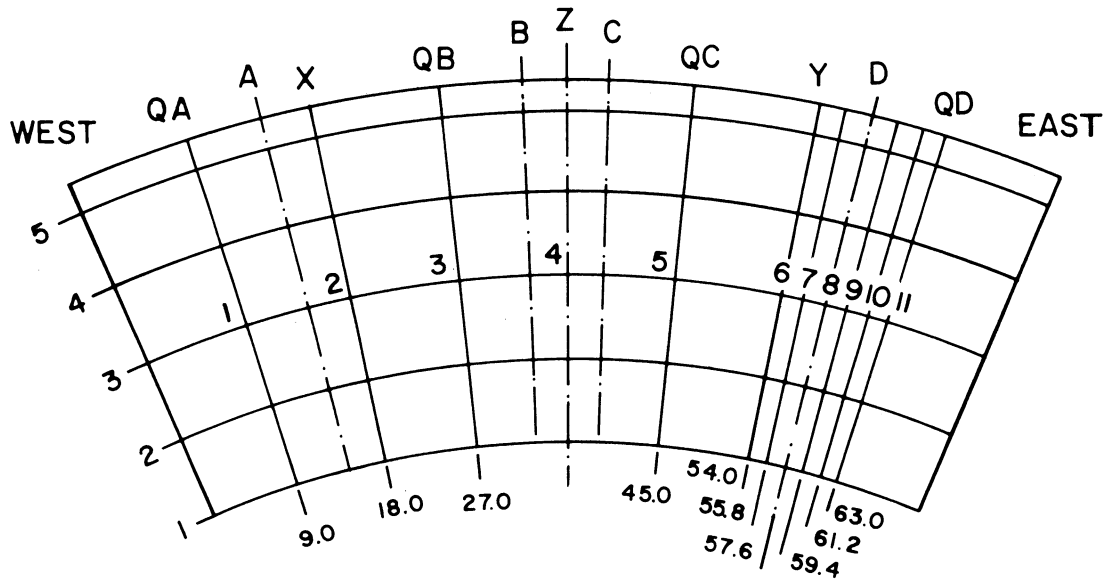

NOTE: ALL DISTANCES MEASURED ALONG BRIDGE CENTERLINE

FIG. 5.16 PLAN SHOWING 11 LOCATIONS OF FORK LIFT FRONT WHEELS AT WHICH SCANNER READINGS WERE TAKEN FOR EACH PASS

5.6.2.1 Phases III, IV and V (40, 50 and 60 ksi Conditioning Phases)

In each of these phases, point loads of equal magnitude were applied at both midspan Sections X and Y of the box girder bridge model, one over each girder making a total of ten loads, to create nominal total stresses of 40, 50 and 60 ksi respectively in the tensile reinforcing steel at Sections X and Y and nominal total stresses of 23.9, 29.2 and 34.5 ksi in the tensile reinforcing steel at Sections B and C. After removal of these conditioning loads the same standard point load of magnitude 19.3 kips as used in Phase II and sufficient to create a nominal total tensile stress of 30 ksi in a girder when placed directly over it, was applied at the various locations of the bridge model deck in the 10 basic load combinations shown in Fig. 5.11a.

5.6.2.2 Phase VI (Loading to Failure)

The final loading to failure required a larger load than could be delivered by the five 20 ton jacks in each span shown in Fig. 5.1. Only six 100 ton jacks were available, so for the final loading to failure it was decided to use three rams of 100 ton capacity each over girders 2, 3 and 4 at the midspan Sections X and Y, as shown in Fig. 5.17. The box girder bridge model was loaded to failure in several stages.

5.7 Summary of Loading Schedule

Table 5.1 shows the loading schedule in summary form from the dead load phase and working load condition (Part 1) to the overload and failure phases (Part 2). As certain loadings were carried out in several increments and others in two steps, the 135 loading combinations altogether necessitated a total of 450 sets of scanner readings for their

TABLE 5.1 LOADING SCHEDULE FOR BOX GIRDER BRIDGE MODEL

		PART 1			PART 2			
LOAD PHASE		0	I	II	III	IV	V	VI
Conditioning load per girder at midspan Sections X, Y (kips)		0 Dead Load	7.7	11.4	17.5	23.7	29.8	Loading to FAILURE
Nominal steel tensile stress due to self weight, extra dead load and conditioning loads (ksi)	Midspan Sections X, Y	11.5	24.0	30.0	40.0	50.0	60.0	
	Instrumented Sections A, D	12.9	22.9	27.7	35.7	43.7	51.7	
	Instrumented Sections B, C	8.9	15.5	18.7	23.9	29.2	34.5	
	Sections at edge of center bent diaphragm	12.6	21.1	25.3	32.1	38.9	45.8	
Standard single load applied on a girder at Sections X, Y after removal of conditioning loads (kips)		0	12.7	19.3	19.3	19.3	19.3	
Total steel tensile stress produced in a girder at Sections X, Y due to a single load (ksi)		0	24	30	30	30	30	
LOAD COMBINATIONS	Simple supports	1	10	19	10	10	10	
	Torsional Restraint			10				
	Longitudinal restraint			10				
	Two lane truck loading			11				
	Three lane truck loading			3				
	Construction vehicle loading			8				
	Moving load (fork lift)			33				
	TOTAL	1	10	94	10	10	10	135

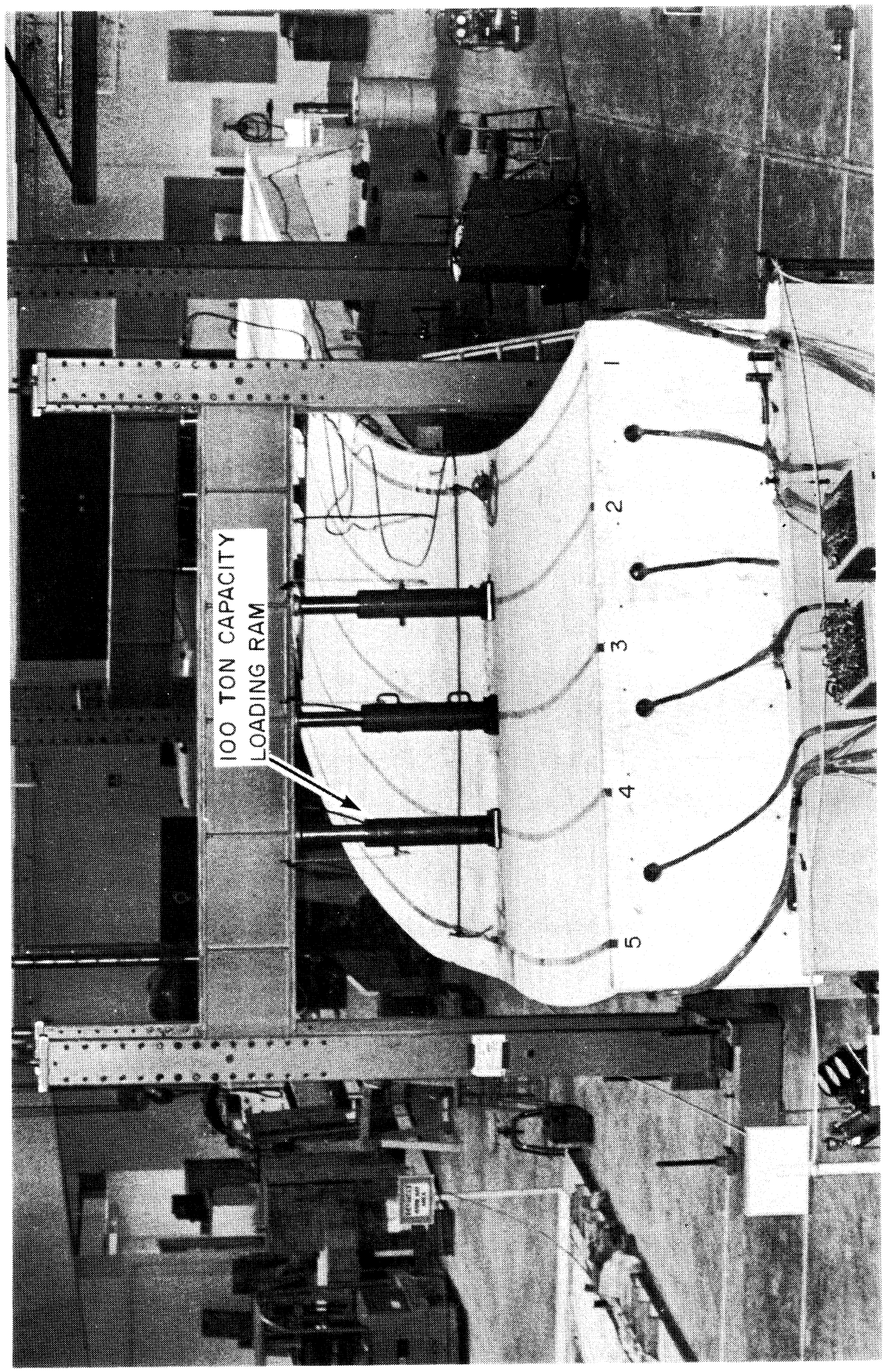

FIG. 5.17 LOADING ARRANGEMENT FOR FINAL LOADING TO FAILURE WITH SIX 100 TON JACKS.

evaluation.

5.8 Chronological Record of Experimental Program

The schedule for testing program was as follows (all dates in 1972 and 1973).

Part 1

October 5:	Phase 0 - removal of shoring and dead load readings.
October 27:	Phase I - 24 ksi conditioning load
October 30:	Phase I - point loads
October 31:	Phase II - 30 ksi conditioning load
November 1-2:	Phase II - point loads
November 7-9:	Phase II - point loads with longitudinal restraint
November 13-14:	Phase II - point loads with torsional restraint
November 17-20:	Phase II - AASHO truck loadings
November 22-27:	Phase II - construction vehicle loadings
November 29:	Phase II - moving load (fork lift)

Part 2

December 21:	Phase III - 40 ksi conditioning load
December 27:	Phase III - point loads
December 28:	Phase IV - 50 ksi conditioning load
January 2-3:	Phase IV - point loads
January 11-12:	Phase V - 60 ksi conditioning load
January 18-19:	Phase V - point loads
February 1-2:	Phase VI - loading to failure.

6. MATERIAL PROPERTIES AND TEST ENVIRONMENT

6.1 Concrete Mix

The mix for the concrete used in the box girder bridge model was designed by the project staff to give an f'_c = 3000 psi at 28 days. Ready mix was supplied by a local dealer. The batch quantities for one cubic yard of concrete with saturated-surface-dry aggregates were as follows:

Sierra Brand Type II Modified Dark Cement . .	564 lbs.
Tidewater Blend Sand	352 lbs.
Livermore Top Sand	1243 lbs.
Livermore #10 x 1/4 in. Pea Gravel	1323 lbs.
Potable Water (42 Gallons]	350 lbs.
Total	3832 lbs.

The allowable slump specified for this concrete mix was 6 inches.

6.2 Placement of Concrete and Slump Tests.

Details of concrete placement have already been described in Chapter 4. The concrete for the bottom slab, girder webs and diaphrams came in three truckloads. The concrete for the top slab came in two truckloads. The location of concrete placement is shown in Fig. 6.1.

Truck 1 had concrete with a slump of 3 3/4 in. at arrival. After the end diaphragm was cast an additional 2.5 gallons of water per cubic yard of concrete was added. Truck 2 had a concrete with a slump of 4 in. at arrival which was brought up to 7 1/2 in. by adding 2.5 gallons of water per cubic yard of concrete before placement. Similarly a total

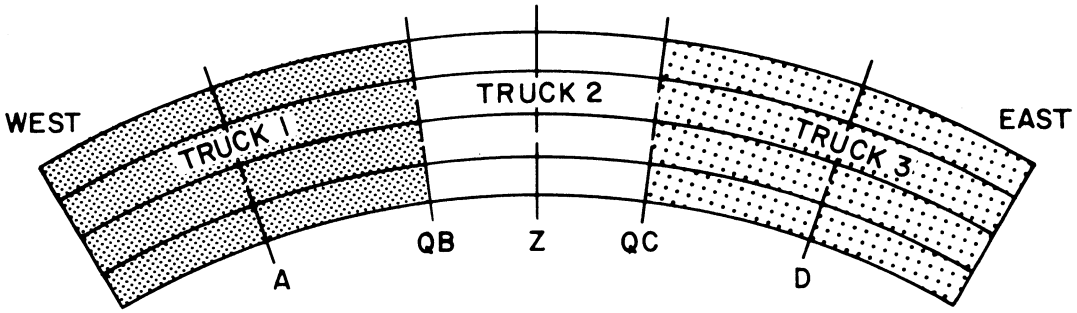

A. LOCATION OF CONCRETE PLACEMENT IN BOTTOM SLAB AND GIRDER WEBS

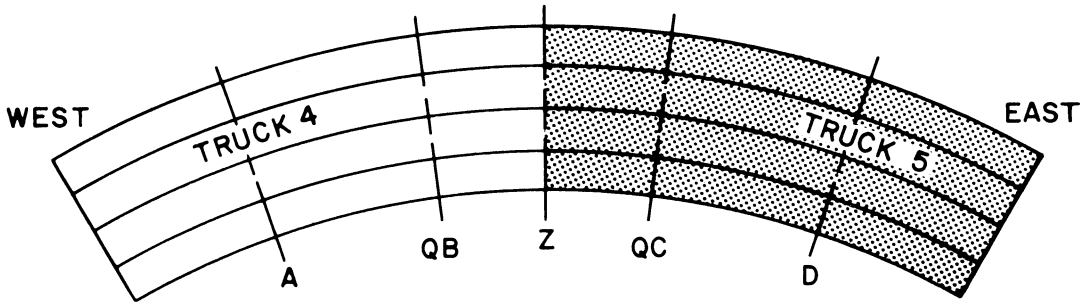

B. LOCATION OF CONCRETE PLACEMENT IN TOP SLAB

FIG. 6.1 PLAN SHOWING LOCATION OF CONCRETE PLACEMENT BY TRUCK NUMBER

of 2 gallons of water per cubic yard of concrete was added to Truck 3 in order to maintain the slump at 4 1/2 in. throughout placement. No added water was necessary for the placement of the concrete in the top slab, Trucks 4 and 5.

6.3 Control Tests on Concrete Cylinders

For the evaluation of the concrete compressive strength f'_c and the elastic modulus E_c of concrete, and the variations of these quantities with age, 72 concrete cylinders of 6 in. diameter and 12 in. height were cast, and subsequently tested over the duration of the experimental test program. The control specimens were cured in the same manner as the box girder bridge model. The control test cylinders are summarized in Table 6.1.

TABLE 6.1 SUMMARY OF CONCRETE CONTROL TESTS

Location of Concrete in Box Girder Bridge Model	Top Slab		Bottom Slab and Girder Webs		
	Section W to Z	Section Z to E	Section W to QB	Section QB to QC	Section QC to E
Number of cylinders tested for compressive strength f'_c	18	18	12	18	6
Number of cylinders for which elastic modulus E_c was measured	18	18	12	18	6

Graphs showing the increase in cylinder compressive strengths with age for concrete from the top and bottom slabs are shown in Figs. 6.2 and 6.3. The variation of the concrete elastic modulus with age is

plotted in Figs. 6.4 and 6.5. Data points on these graphs represent the average of three concrete cylinder tests. These graphs also show the schedule of testing of the box girder bridge model with pertinent dates.

An electronic X-Y Recorder was utilized in obtaining the concrete elastic modulus. Each concrete cylinder was loaded to approximately 0.4 f'_c and then unloaded. This loading cycle was repeated a total of four times for each cylinder and a load-strain curve was recorded for each of the cycles. The first load cycle allowed seating of the compressometer. The three subsequent load-strain records were used to obtain the concrete elastic modulus by averaging the slopes of the three records between zero and approximately 0.5 f'_c. The curves were essentially linear in this range.

The measured values of the compressive strength of the concrete f'_c and the elastic modulus of concrete E_c as obtained from the control tests on each cylinder are given in Tables 6.2 and 6.3. A typical stress-strain curve for concrete is given in Fig. 6.6.

For the reduction of experimental data, average values of the concrete elastic modulus at each of the instrumented sections were taken from the above graphs. At instrumented Sections A and D, the reading for the elastic modulus E_c of the top slab was necessary for the computation of the compressive force in the top slab, and the reading for the elastic modulus E_c of the concrete in the bottom slab and girder webs was necessary for the computation of the compressive force in the upper part of the girders. At instrumented Sections B and C, however, only the values of the concrete elastic modulus E_c in the bottom slab and girder webs were required for the determination of the slab and web compressive forces. In order to take into account the changes in the properties of

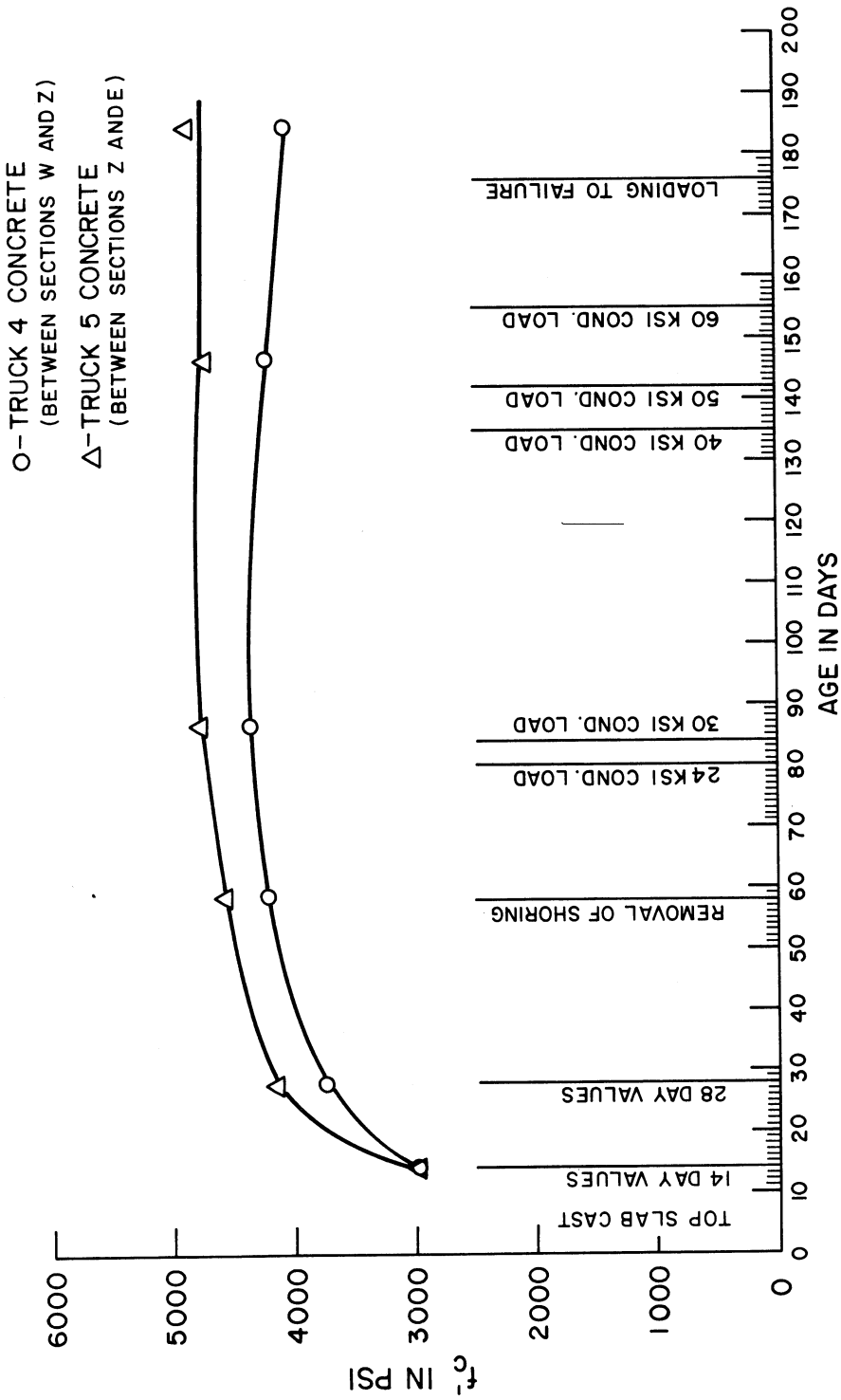

FIG. 6.2 RESULTS OF COMPRESSIVE STRENGTH TESTS ON TOP SLAB CONCRETE CYLINDERS

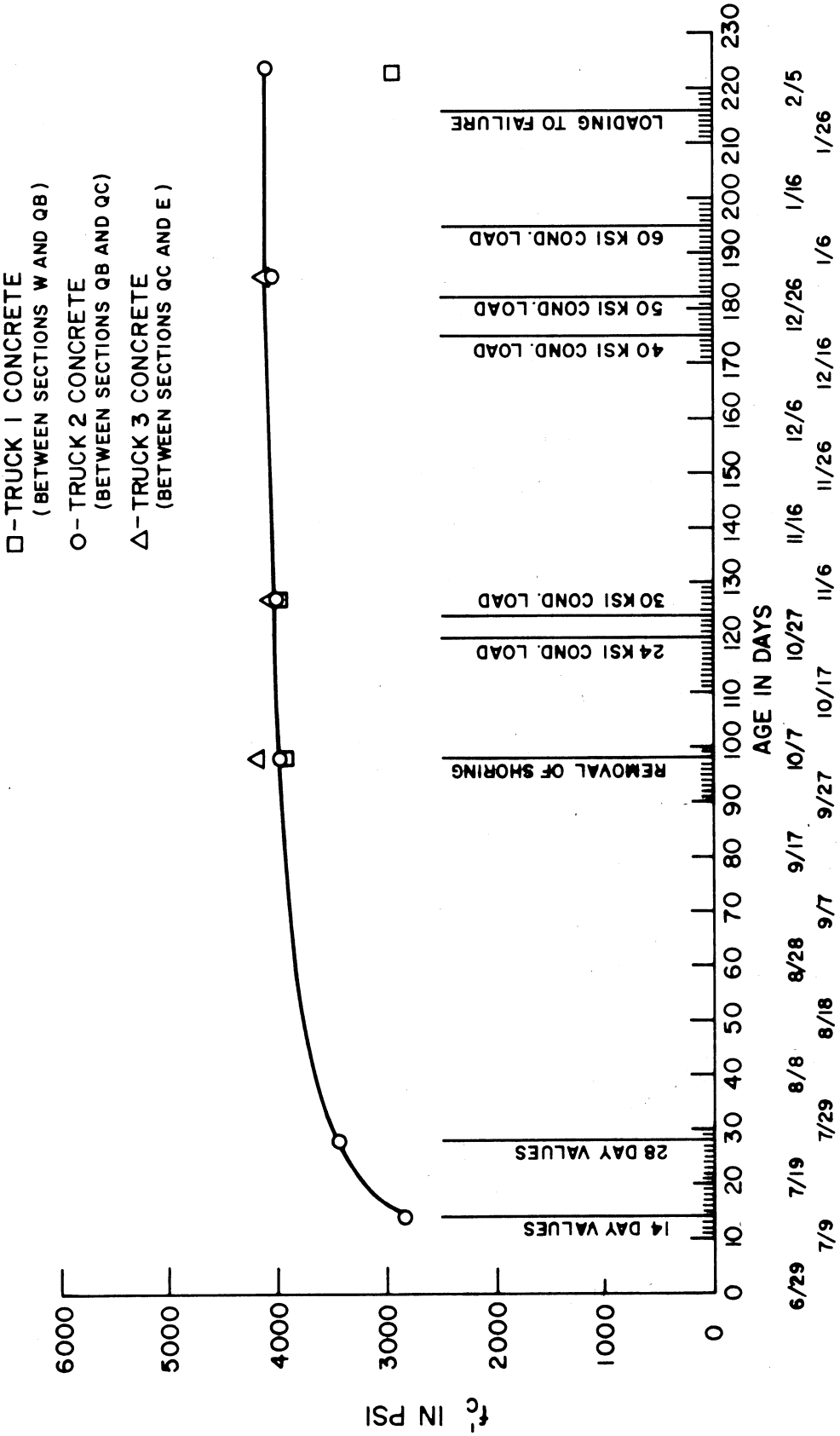

FIG. 6.3 RESULTS OF COMPRESSIVE STRENGTH TESTS ON BOTTOM SLAB CONCRETE CYLINDERS.

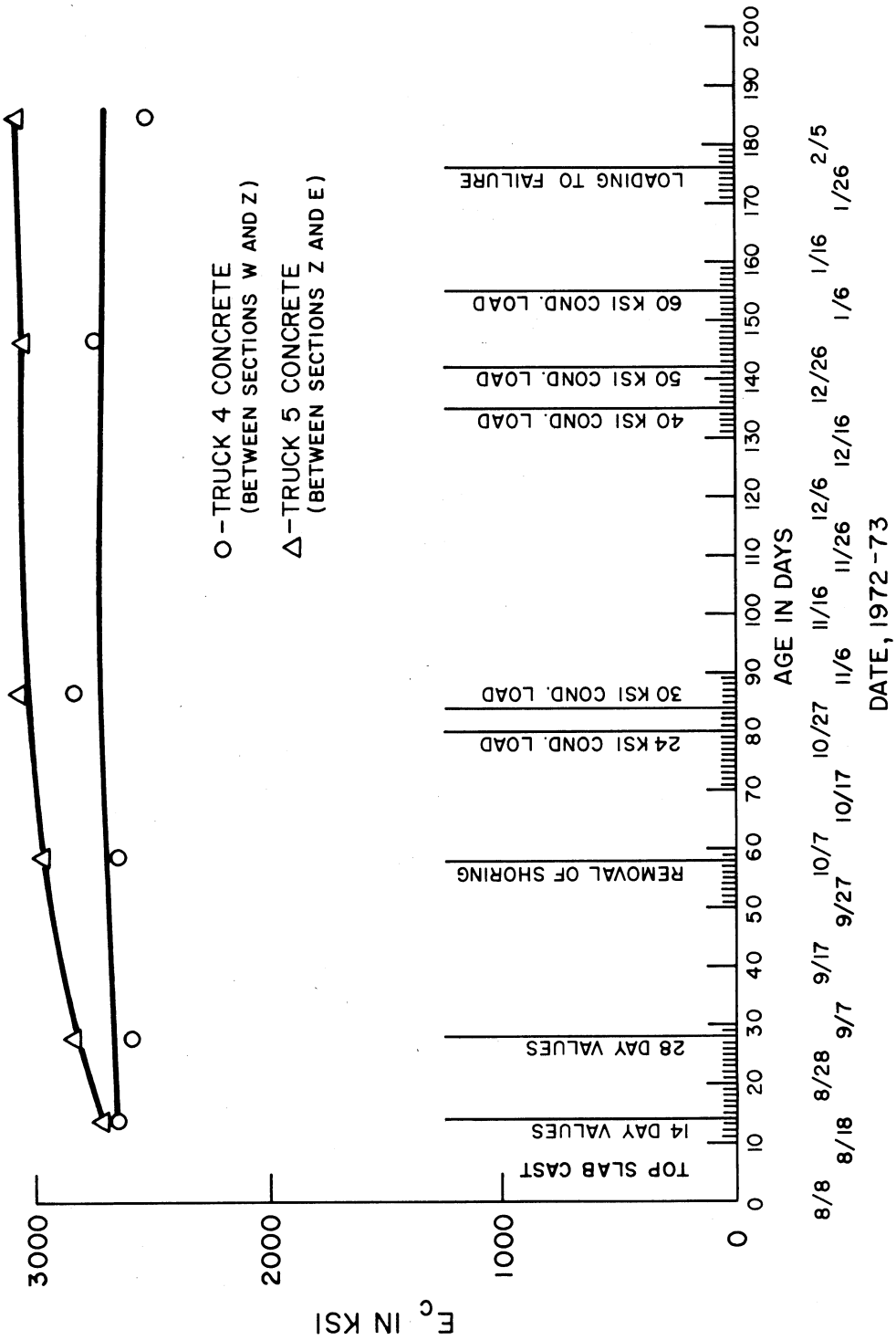

FIG. 6.4 VARIATION OF TOP SLAB CONCRETE ELASTIC MODULUS WITH AGE

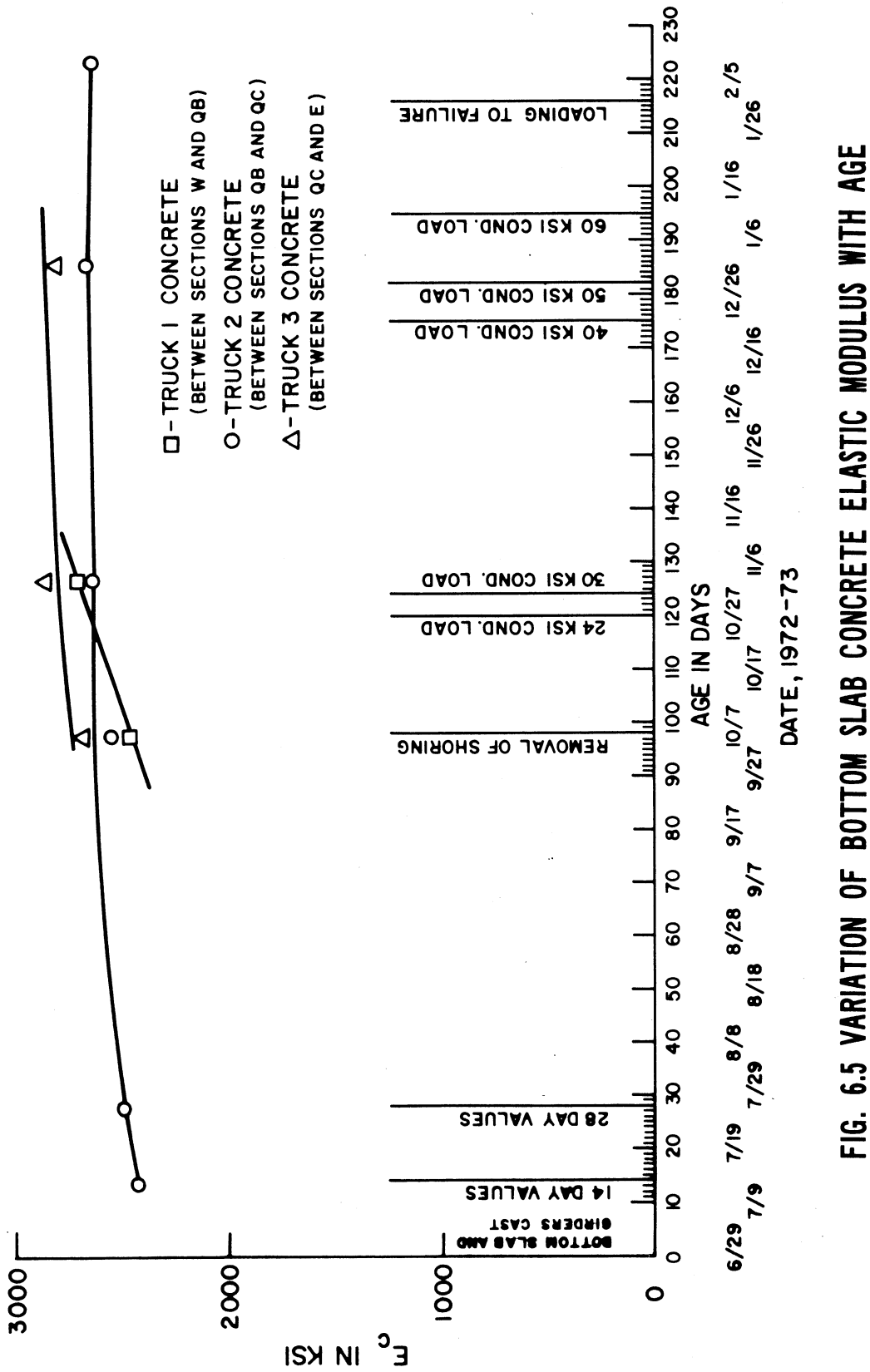

FIG. 6.5 VARIATION OF BOTTOM SLAB CONCRETE ELASTIC MODULUS WITH AGE

concrete with age, it was decided to use three sets of the concrete elastic modulus values for the purposes of reduction of experimental data.

The first set of concrete elastic modulus values consisted of average values for the top slab, bottom slab and girder webs for a time period from the beginning of the dead load phase through the 24 ksi loading phase. This set of concrete elastic modulus values was used for the data reduction for dead load, Phase 0, and for Phase I where conditioning loads caused maximum nominal tensile stresses of 24 ksi in the steel.

The second set of concrete elastic modulus values consisted of average values over the time period spanning Phases II and III of the test program, during which conditioning loads of 30 ksi and 40 ksi were applied. The third set of concrete elastic modulus values consisted of average values over the remaining test period until failure of the concrete box girder bridge model.

These average values for the concrete elastic modulus used in the reduction of experimental data are given in Table 6.4.

TABLE 6.2 RESULTS OF COMPRESSIVE STRENGTH TESTS ON CONCRETE CYLINDERS

Age of Concrete at Test (Days)	Value of Compressive Strength f'_c in psi				
	Top Slab		Bottom Slab and Girder Webs		
	Section W to Z	Section Z to E	Section W to QB	Section QB to QC	Section QC to E
14	2980 2920 2900	3010 2940 2980		2820 2825 2840	
28	3520 3810 3880	4240 4030 4140		3510 3440 3500	
59	4170 4330 4100	4610 4470 4620			
87	4330 4340 4330	4800 4720 4730			
98			4160 4230 4183	3860 4080 3980	4000 3880 3910
127			4230 4040 3780	3960 4020 4010	4020 3950 4020
147	4310 4180 4100	4780 4830 4470			
185	3900 4070 4120	4610 4860 5030			
186			4280 4180 3840	4130 3970 3980	
223			2880 2920 2920		
224				4030 4260 4010	

TABLE 6.3 RESULTS OF MODULUS OF ELASTICITY TESTS ON CONCRETE CYLINDERS

Age of Concrete at Test (Days)	Values of Concrete Modulus E_c in ksi				
	Top Slab		Bottom Slab and Girder Webs		
	Section W to Z	Section Z to E	Section W to QB	Section QB to QC	Section QC to E
14	2620 2660 2640	2720 2700 2720		2390 2440 2440	
28	2580 2600 2580	2880 2790 2860		2520 2480 2480	
59	2560 2660 2690	2980 2950 2970			
87	2800 2880 2560	3020 3080 3100			
98			2640 2610 2830	2480 2580 2590	2510 2470 2440
127			2950 2895 2780	2640 2640 2680	2750 2720 2690
147	2810 2750 2710	3020 3120 3040			
185	2420 2630 2540	3090 3100 3070			
186			2860 2820 2770	2700 2620 2680	
223			1940 1880 4160		
224				2680 2700 2550	

TABLE 6.4 VALUES OF CONCRETE ELASTIC MODULUS E_c IN KSI AT INSTRUMENTED SECTIONS USED IN REDUCTION OF EXPERIMENTAL DATA

Instrumented Section	Location	Average Values of Concrete Modulus E_c in ksi		
		Phases 0, I: After Dead Load, 24 ksi Tensile Stress	Phases II, III: 30 ksi Tensile Stress to 40 ksi Stress	Phases IV, V, VI: 50 ksi Stress to Failure
A	Top slab	2650	2700	2750
	Bottom slab and girder webs	2550	2650	2650
B	Top slab	2650	2700	2750
	Bottom slab and girder webs	2550	2650	2650
C	Top slab	3000	3050	3050
	Bottom slab and girder webs	2550	2650	2650
D	Top slab	3000	3050	3050
	Bottom slab and girder webs	2550	2650	2650

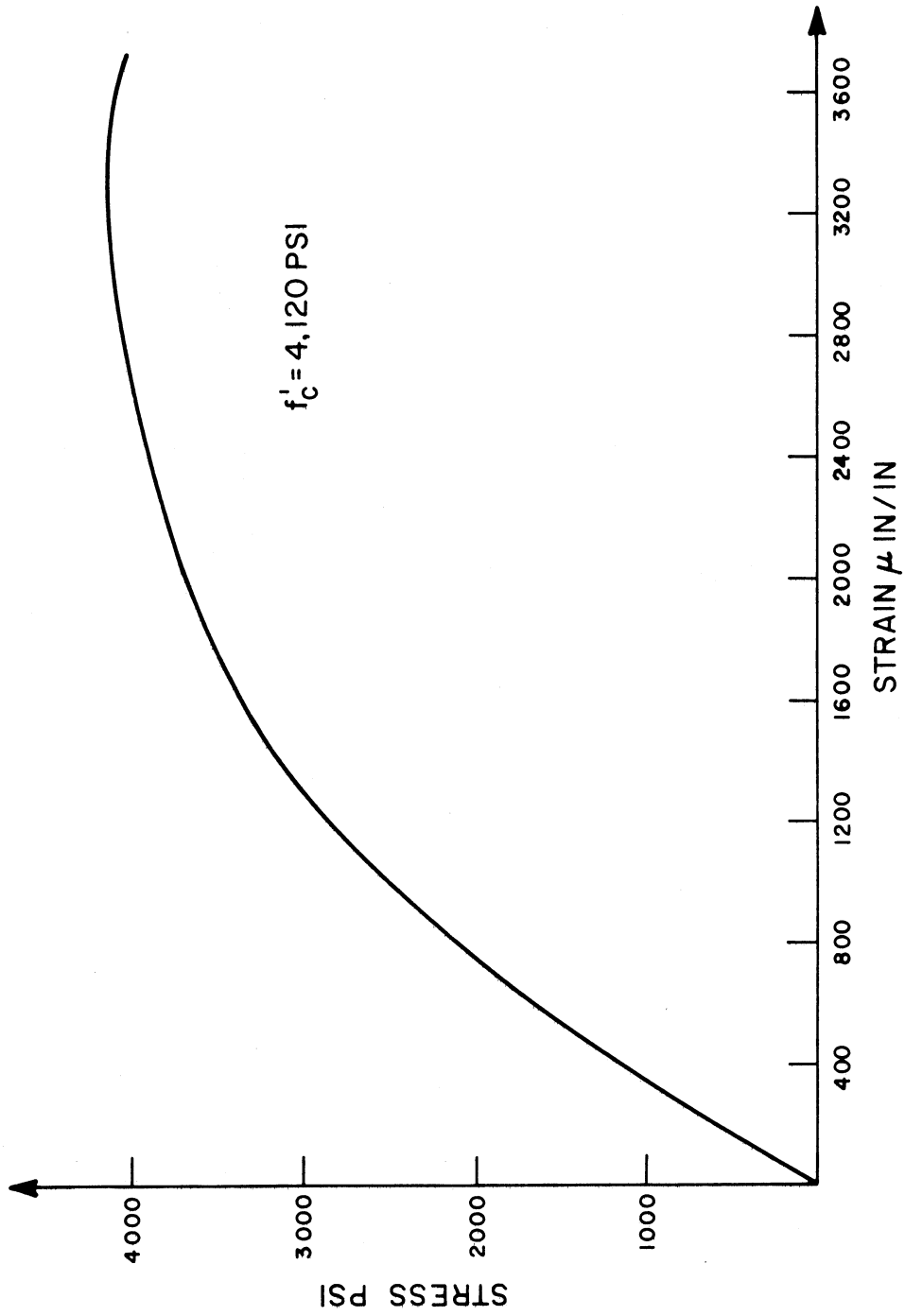

FIG. 6.6 TYPICAL STRESS-STRAIN CURVE FOR CONCRETE CYLINDER

6.4 Tests on Control Beams for the Measurement of Concrete Tensile Strength

Modulus of rupture tests were carried out for the determination of concrete tensile strength on 12 control beams after Phase II (30 ksi) of the experimental program. Each beam was 5 in. wide, 6 in. deep and 18 in. long, and was subjected to third-point loading in a testing machine. The results of the tensile strength tests are given in Table 6.5.

TABLE 6.5 MODULUS OF RUPTURE TESTS ON CONCRETE BEAMS

Age of Concrete at Test (Days)	Values of Tensile Strength f_t in psi			
	Top slab		Bottom slab	
	Section W to Z	Section Z to E	Section W to QB	Section QB to E
90	680 655 695	585 640 600		
130			810 555 715	525 695 720

6.5 Steel Reinforcement Tests

All instrumented reinforcement for the box girder bridge model was instrumented and placed by the project staff. The main longitudinal reinforcement in the top and bottom slabs consisted of No. 4 deformed bars. Additional longitudinal reinforcement in the slabs and the girder webs and transverse reinforcement in the slabs consisted of No. 3 deformed bars. The stirrup reinforcement in the girder webs was composed of No. 2 deformed bar in zones of high shear near the center bent, and the remainder of the stirrups were made of

1/4 in. diameter undeformed bars. The nominal yield strengths of the reinforcement were as follows: 1/4 in., 45 ksi; No. 2, 40 ksi; No. 3 and No. 4 bars, 60 ksi.

A total of thirty-seven tensile control tests were performed on nominal 24 in. long samples from the steel reinforcement used in the concrete box girder bridge model. These thirty-seven samples consisted of: twelve deformed No. 4 bars; fifteen deformed No. 3 bars; five deformed No. 2 bars; and five 1/4 in. diameter plain bars.

All of the deformed test specimens had a parallel lug pattern, and identification marks on the No. 3 and No. 4 bars indicated they were produced by Judson Steel Corporation, Grade 60, New Billet Type Steel. The No. 2 deformed and 1/4 in. diameter plain bars were grade 40 and had no identification symbols.

Prior to testing, all specimens had an 8.00 in. gage length punched on them. The testing apparatus used was an electronic X-Y Plotter, 4 in. gage length extensometer, 60 kip hydraulic testing machine, dividers and a scale with 0.01 in. graduations.

The testing procedure established permanent plots of the force-strain curve in the linear elastic, and yielding inelastic ranges of the material. Each specimen was loaded to approximately 75% of its predicted yield load four consecutive times, and then reloaded past yield into the inelastic zone. The divider method was then used to obtain data points for the remainder of the force-strain curve up to failure.

Calculation of the modulus of elasticity for the steel reinforcement specimens was obtained by averaging the last three, of the first four, force-strain plots and dividing by the nominal area of the respective bar size.

From the data obtained from the tensile tests, the yield stress, ultimate stress and modulus of elasticity are given in Table 6.6. The average values of the modulus of elasticity for the 1/4 in. diameter plain bar, and the No. 2, No. 3 and No. 4 deformed bars were: 27.9, 27.0, 28.8 and 27.5 x 10^6 psi respectively. These average values for the modulus of elasticity were used in the reduction of the experimental data. The average values of yield stress, as calculated from the test data of Table 6.6, for the 1/4 in. diameter plain bar and the No. 2, No. 3 and No. 4 bars were 47, 38, 61 and 70 ksi respectively. Typical load-strain curves for the steel reinforcement tests are shown in Fig. 6.7.

6.6 Temperature and Humidity Measurements

Continuous temperature recordings were made from the initial casting of the bottom slab and girder webs, until loading to failure of the reinforced concrete box girder bridge model. During an extended period of air conditioning system malfunctioning in the laboratory, June 29 to October 2, 1972, the average temperature in the laboratory was 75°F with a variation of only $\pm$ 2°F except for a maximum increase of 10°F above average at midday for a short period of three days. After October 2, 1972 the air conditioning system functioned properly and records show temperatures of 70°F $\pm$ 1°F throughout the remainder of the experimental program. Humidity measurements were not taken during the experimental program, however, previous experience in the laboratory indicated that a practically constant condition of 50 $\pm$ 5% humidity existed in the laboratory. The temperature record for the bridge model from initial casting to final load test to failure is shown in Fig. 6.8.

TABLE 6.6 SUMMARY OF TENSILE TESTS ON STEEL REINFORCEMENT

No.	Bar Size No.	Nominal Area Sq. in.	Measured E_s x 10^6 psi	Yield Stress σ_y x 10^3 psi	Ultimate Stress σ_u x 10^3 psi
1	¼" ϕ	0.05	27.6	47.4	78.1
2	¼" ϕ	0.05	26.9	46.8	74.3
3	¼" ϕ	0.05	28.8	46.8	77.8
4	¼" ϕ	0.05	27.9	48.9	78.6
5	¼" ϕ	0.05	28.3	42.8	75.2
6	2	0.05	25.9	38.0	65.6
7	2	0.05	26.6	38.0	65.6
8	2	0.05	28.4	37.0	65.5
9	2	0.05	27.4	39.0	66.6
10	2	0.05	26.7	37.0	66.6
11	3	0.11	28.6	63.6	95.8
12	3	0.11	28.3	60.9	92.7
13	3	0.11	27.6	59.1	93.6
14	3	0.11	28.5	60.0	94.7
15	3	0.11	29.6	61.8	96.0
16	3	0.11	30.7	60.0	93.4
17	3	0.11	29.6	63.1	93.1
18	3	0.11	28.5	60.0	93.6
19	3	0.11	30.6	63.1	94.4
20	3	0.11	30.1	62.9	95.6
21	3	0.11	27.6	60.0	93.4
22	3	0.11	28.7	61.8	93.8
23	3	0.11	28.9	62.7	95.3
24	3	0.11	27.3	60.0	93.3
25	3	0.11	27.9	61.8	93.3
26	4	0.20	27.7	70.5	99.9
27	4	0.20	28.0	71.0	99.9
28	4	0.20	27.6	70.5	99.5
29	4	0.20	27.6	70.0	98.5
30	4	0.20	28.1	73.0	100.6
31	4	0.20	27.4	70.5	99.6
32	4	0.20	27.7	69.0	102.0
33	4	0.20	26.8	70.0	99.5
34	4	0.20	26.9	71.0	99.9
35	4	0.20	26.5	60.0	99.5
36	4	0.20	26.9	70.5	100.4
37	4	0.20	28.2	72.0	99.9

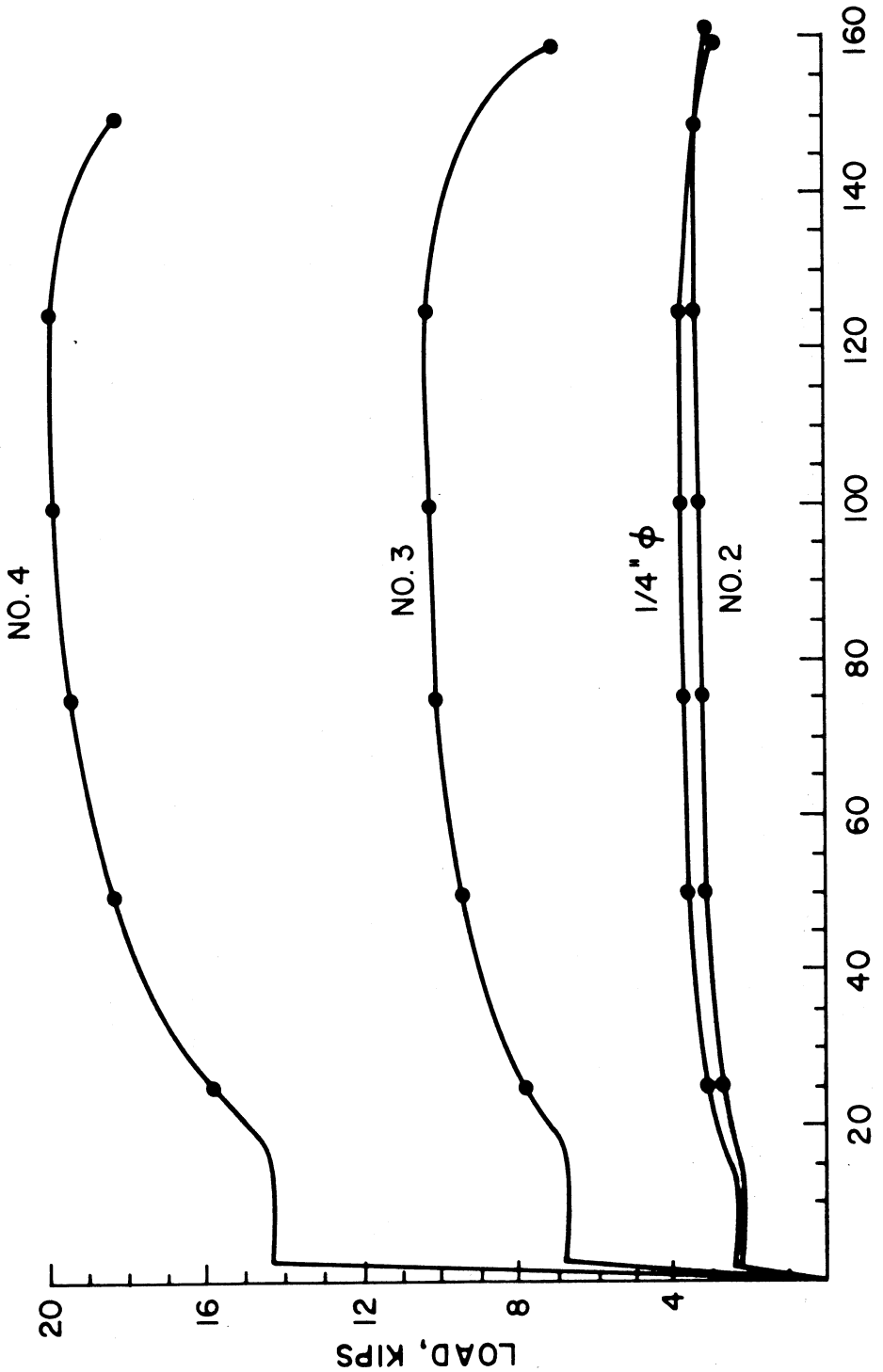

FIG. 6.7 TYPICAL LOAD-STRAIN CURVES FOR REINFORCING STEEL

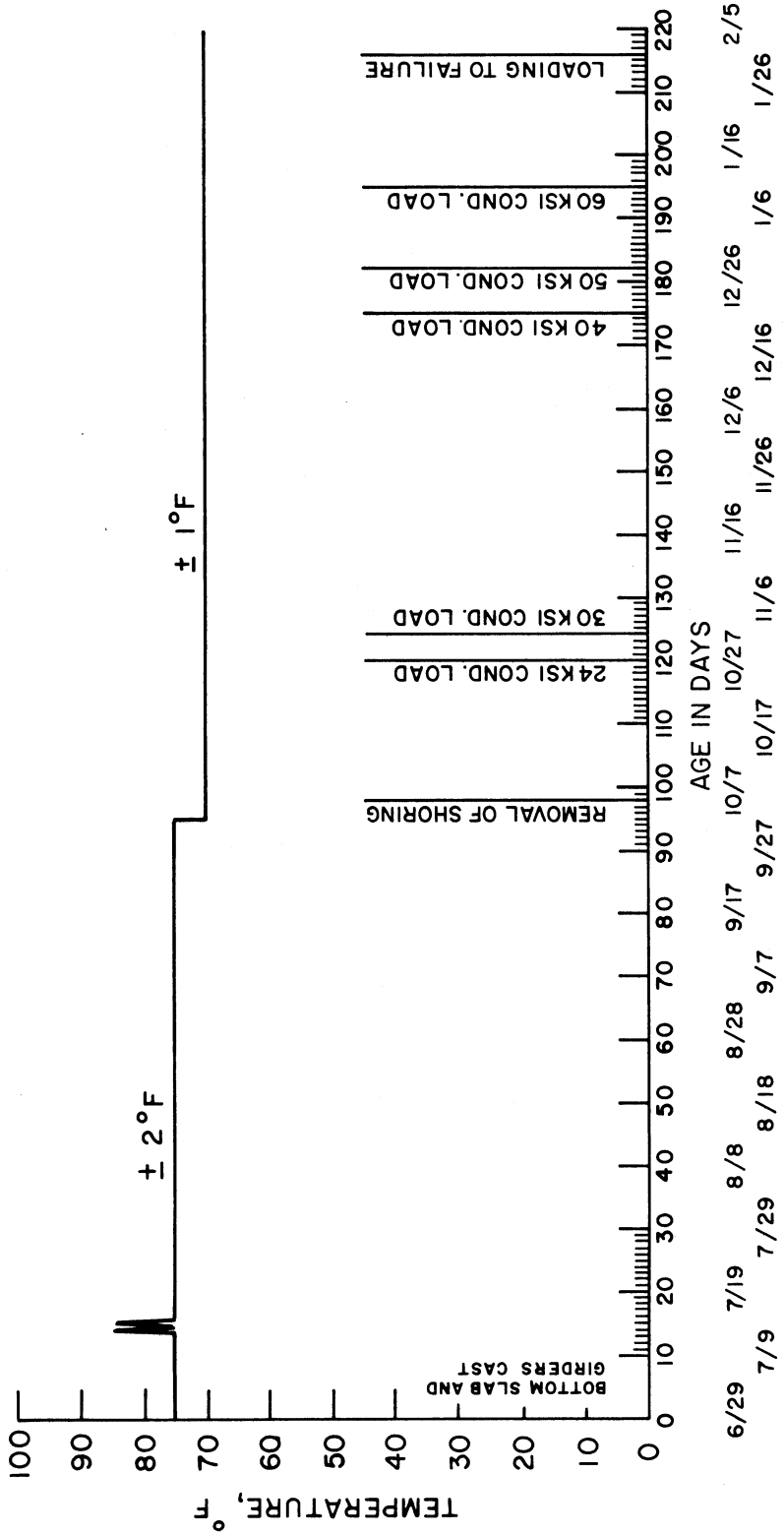

FIG. 6.8 TEMPERATURE RECORD FOR BRIDGE MODEL FROM INITIAL CASTING TO FAILURE

7. SUMMARY AND CONCLUSIONS FOR VOLUME I

The present volume is the first of a three volume sequence on the "Structural Behavior of a Curved Two Span Reinforced Concrete Box Girder Bridge Model." The material included in each volume is as follows:

Vol. I - Design, Construction, Instrumentation and Loading

Vol. II - Reduction, Analysis and Interpretation of Results

Vol. III - Detailed Tables of Experimental and Analytical Results

The construction, instrumentation and testing of the model in the Structures and Engineering Materials Laboratory, Davis Hall, University of California, Berkeley over the period March 22, 1972 to February 2, 1973 has been described in detail in the present volume. The model was 72 ft. long along the longitudinal centerline, 12 ft. wide and 1 ft. 8 9/16 in. in depth. It had a radius of curvature in the horizontal plane of 100 ft. It was a two span continuous structure and had four cells, a center bent with a circular column support, two end diaphragms and a mid-span diaphragm in one span only.

The model was a 1:2.82 scale replica of a typical prototype California box girder bridge. The radius of curvature was selected as being the maximum encountered in highway design in California. The scale of 1:2.82 was the smallest that allowed the use of standard reinforcing steel and concrete, as well as proper simulation of prototype behavior. The scale was selected so that a No. 11 deformed bar in the prototype was replaced by a No. 4 deformed bar in the model.

The curved bridge model was similar in all respects, except horizontal curvature, to a straight bridge model tested previously in 1970 and reported on in detail in References 9, 10 and 11. Experience gained

in the early test program on the straight bridge proved invaluable and resulted in very few difficulties being encountered in the construction, instrumentation and testing of the curved bridge model.

The loading frames and loading system used worked very satisfactorily. The instrumentation, designed to record all measurements electronically, consisted of load cells for the reactions, potentiometers for the deflections, strain meters for the concrete strains, and weldable waterproofed strain gages for the steel strains, all of which proved to be very reliable. The data acquisition system used in the investigation can be strongly recommended for its ease of handling, speed and stability. It permitted the acquisition of data from 192 channels, for each of which, the computer scanned each gage five times and averaged the readings in a matter of a few minutes. Four hundred and fifty sets of scanner readings of the 192 channels were required during the test program in which 135 different loading combinations were applied to the bridge. Output from the data acquisition system computer in the form of paper tape was then fed into a CDC 6400 computer for further reduction, analysis and interpretation of results. These results are discussed in detail in Vols. II and III.

8. ACKNOWLEDGEMENTS

This investigation was sponsored by the Division of Highways, Department of Transportation, State of California, and the Federal Highway Administration, United States Department of Transportation.

The contents of this report reflect the views of the authors who are responsible for the facts and the accuracy of the data presented herein. The contents do not necessarily reflect the official views or policies of the State of California or the Federal Highway Administration. This report does not constitute a standard, specification, or regulation.

The planning, preparation, construction, supervision, testing, control, analysis and data reduction for a research project of the scope and size of the curved box girder bridge model of the present study necessitate the cooperative assistance and teamwork of all involved.

From the State of California Division of Highways, G. D. Mancarti, Assistant Bridge Engineer and R. E. Davis, Senior Bridge Engineer of the Research and Development Section, maintained a close and keen interest in the project in all its stages.

R. M. Stephen, S.E.M. Laboratory Manager, actively participated in the preliminary planning, design, instrumentation and contruction of the box girder bridge model, and deserves special thanks for his assistance and interest.

Of primary importance to the success of the project were the hard work and enthusiasm of the various Research Assistants, Students and Staff working for different periods on the research investigation.

Special acknowledgement should be given to A. Horeis, Graduate Research Assistant, who participated in all phases of the research program

from its inception to the publication of the final reports.

J. Ho, A. F. Kabir, Y. J. Kang, C. S. Lin and S. Shankar, Graduate Research Assistants, worked on various phases of the investigation especially on analytical studies, computer programming and reduction of experimental data.

L. Elfgren, a postdoctoral student from Chalmers University of Technology, Sweden, who spent six months in Berkeley, was very helpful during the critical testing portion of the program. He also contributed greatly to the analysis and interpretation of the ultimate strength behavior of the bridge during its final loading to failure.

As always, the S.E.S.M. Laboratory staff provided excellent support. D. Wasley gave frequent and valuable help in the running of the S.E.S.M. Data Acquisition System. J. G. Foster, E. Cleave, A. D. Lawrence and A. Costa enabled full utilization of the skills and resources of the Mechanical and Electronics shops. R. Parsons as Mechanician and T. Brennan as Electronics Technician contributed toward the fabrication and preparation of the test set-up and instrumentation.

Finally acknowledgement is due to the drafting staff composed of A. Klash, G. Feazell and A. Pereda and the typing staff composed of I. Blowers. P. Ward, L. Larson and L. Tsai for their assistance in the production of the final reports.

9. REFERENCES

1. Scordelis, A. C., "Analysis of Simply Supported Box Girder Bridges," Structural Engineering and Structural Mechanics Report No. SESM 66-17, University of California, Berkeley, October 1966 (PB 175 646).

2. Scordelis, A. C., "Analysis of Continuous Box Girder Bridges," Structural Engineering and Structural Mechanics Report No. SESM 67-25, University of California, Berkeley, November 1967 (PB 178 355).

3. Scordelis, A. C., and Meyer, C., "Wheel Load Distribution in Concrete Box Girder Bridges," Structural Engineering and Structural Mechanics Report No. SESM 69-1, University of California, Berkeley, January 1969 (PB 183 923).

4. Willam, K. J., and Scordelis, A. C., "Analysis of Orthotropic Folded Plates with Eccentric Stiffeners," Structural Engineering and Structural Mechanics Report No. SESM 70-2, University of California, Berkeley, February 1970 (PB 191 051).

5. Meyer, C., and Scordelis, A. C., "Computer Program for Prismatic Folded Plates with Plate and Beam Elements," Structural Engineering and Structural Mechanics Report No. SESM 70-3, February 1970 (PB 191 050).

6. Meyer, C., and Scordelis, A. C., "Analysis of Curved Folded Plate Structures," Structural Engineering and Structural Mechanics Report No. UC SESM 70-8, University of California, Berkeley, June 1970 (PB 193 535).

7. Willam, K. J., and Scordelis, A. C., "Computer Program for Cellular Structures of Arbitrary Plan Geometry," Structural Engineering and Structural Mechanics Report No. UC SESM 70-10, University of California, Berkeley, September 1970 (PB 196 143).

8. Meyer, C., "Analysis and Design of Curved Box Girder Bridges," Structural Engineering and Structural Mechanics Report No. UC SESM 70-22, University of California, Berkeley, December 1970 (PB 197 289).

9. Bouwkamp, J. G., Scordelis, A. C., and Wasti, S. T., "Structural Behavior of a Two Span Reinforced Concrete Box Girder Gridge Model, Volume I," Structural Engineering and Structural Mechanics Report No. UC SESM 71-5, University of California, Berkeley, April 1971 (PB 199 187).

10. Scordelis, A. C., Bouwkamp, J. G., and Wasti, S. T., "Structural Behavior of a Two Span Reinforced Concrete Box Girder Bridge Model, Volume II," Structural Engineering and Structural Mechanics Report No. UC SESM 71-16, University of California, Berkeley, October 1971 (PB 210 431).

11. Scordelis, A. C., Bouwkamp, J. G., and Wasti, S. T., "Structural Behavior of a Two Span Reinforced Concrete Box Girder Bridge Model, VolumeIII" Structural Engineering and Structural Mechanics Report No. UC SESM 71-17, University of California, Berkeley, October 1971.

12. Meyer, C., and Scordelis, A. C., "Computer Program for Non-Prismatic Folded Plates with Plate and Beam Elements," Structural Engineering and Structural Mechanics Report No. UC SESM 71-23, University of California, Berkeley, December 1971.

13. Lin, C. S., and Scordelis, A. C., "Computer Program for Bridges on Flexible Bents," Structural Engineering and Structural Mechanics Report No. UC SESM 71-24, University of California, Berkeley, December 1971 (PB 210 171).

14. Godden, W. G., and Aslam, M., "Model Studies of Skew Box Girder Bridges," Structural Engineering and Structural Mechanics Report No. UC SESM 71-26, University of California, Berkeley, December 1971.

15. Comartin, C. D., and Scordelis, A. C., "Analysis and Design of Skew Box Girder Bridges," Structural Engineering and Structural Mechanics Report No. UC SESM 72-14, University of California, Berkeley, December 1972.

16. Godden, W. G., and Aslam, M., "Model Studies of Curved Box Girder Bridges," Structural Engineering and Structural Mechanics Report No. UC SESM 73-5, University of California, Berkeley, March 1973.

17. Scordelis, A. C., Davis, R. E., and Lo, K. S., "Load Distribution in Concrete Box Girder Bridges," ACI Proceedings of First International Symposium on Concrete Bridge Design, Toronto, Canada, April 1967, ACI Publication SP-23, 1969.

18. Scordelis, A. C., and Davis, R. E., "Stresses in Continuous Concrete Box Girder Bridges," ACI Proceedings of Second International Symposium on Concrete Bridge Design, Chicago, April 1969, ACI Publication SP-26, 1971.

19. Scordelis, A. C., "Analytical Solutions for Box Girder Bridges," Proceedings, Conference on Modern Developments in Bridge Design and Construction, Cardiff, Great Britain, April 1971.

20. Bouwkamp, J. G., Scordelis, A. C., and Wasti, S. T., "Structural Behavior of a Reinforced Concrete Box Girder Bridge," Proceedings, Conference on Modern Developments in Bridge Design and Construction, Cardiff, Great Britain, April 1971.

21. Willam, K. J., and Scordelis, A. C., "Analysis of Eccentrically Stiffened Folded Plates," Proceedings of IASS Symposium on Folded Plates and Prismatic Structures, Vienna, September 1970.

22. Meyer, C., and Scordelis, A. C., "Analysis of Curved Folded Plate Structures," Journal of the Structural Division, Proceedings of American Society of Civil Engineers, Volume 98, No. ST1, January 1972.

23. Willam, K. J., and Scordelis, A. C., "Cellular Structures of Arbitrary Plan Geometry," Journal of the Structural Division, Proceedings of American Society of Civil Engineers, Volume 98, No. ST 7, July 1972.

24. Godden, W. G., and Aslam, M., "Model Studies of Skew Multicell Girder Bridges," Journal of the Engineering Mechanics Division, Proceedings of the American Society of Civil Engineering, Volume 99, No. EM 1, February 1973.

25. Scordelis, A. C., Bouwkamp, J. G., and Wasti, S. T., "Study of AASHO Loadings on a Concrete Box Girder Bridge," Highway Research Record No. 428, Highway Research Board, Washington, D. C., 1973.

26. Scordelis, A. C., Bouwkamp, J. G., and Wasti, S. T., "Structural Response of a Concrete Box Girder Bridge," Journal of the Structural Division, Proceedings of the American Society of Civil Engineers, Volume 99, No. ST 10, October 1973.

27. Bouwkamp, J. G., Scordelis, A. C., and Wasti, S. T., "Ultimate Strength of a Concrete Box Girder Bridge," Journal of the Structural Division, Proceedings of the American Society of Civil Engineers, Vol.100, No. ST 1, January 1974.

28. Davis, R. E., Kozak, J. J., and Scheffey, C. F., "Structural Behavior of a Concrete Box Girder Bridge," Highway Research Record No. 76, Highway Research Board, Washington, D. C., 1965.

29. "Standard Specifications for Highway Bridges," American Association of State Highway Officials, [AASHO], Eleventh Edition, Washington, D. C., 1973.

30. Sanders, W. W., and Elleby, H. A., "Distribution of Wheel Loads on Highway Bridges," National Cooperative Highway Research Program Report 83, Highway Research Board, Washington, D. C., 1970.

Copies of most of the research reports [1-14] in the above reference list have been placed on file with the U. S. Department of Commerce and may be obtained on request for cost of reproduction by writing to the following address:

National Technical Information Service
Operations Division
Springfield, Virginia 22151

The accession number (shown in parenthesis in the reference list) should be specified when ordering a particular report.

APPENDIX A

Detailed Design Drawings of Bridge Model

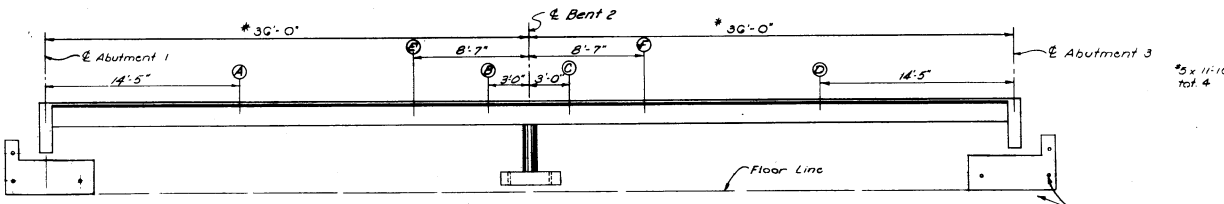

ELEVATION

1/4" = 1'-0"

○ Indicates reference locations

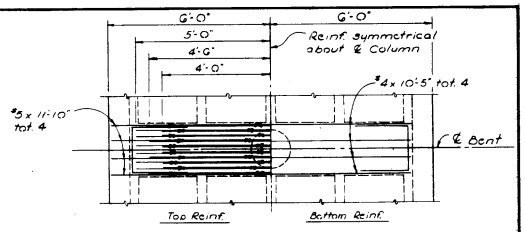

PLAN

Note:
All reinf. #5 for Top Reinf.
Denotes bundled bars

2" ϕ Pipe Sleeve

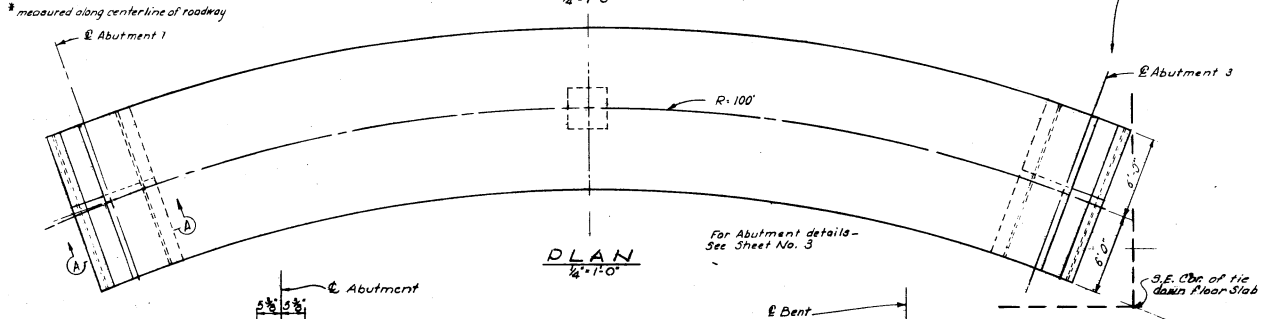

PLAN

1/4" = 1'-0"

For Abutment details - See Sheet No. 3

S.E. Cor. of tie down Floor Slab

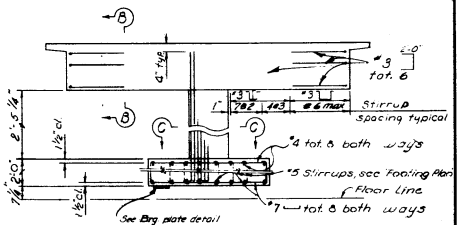

ELEVATION

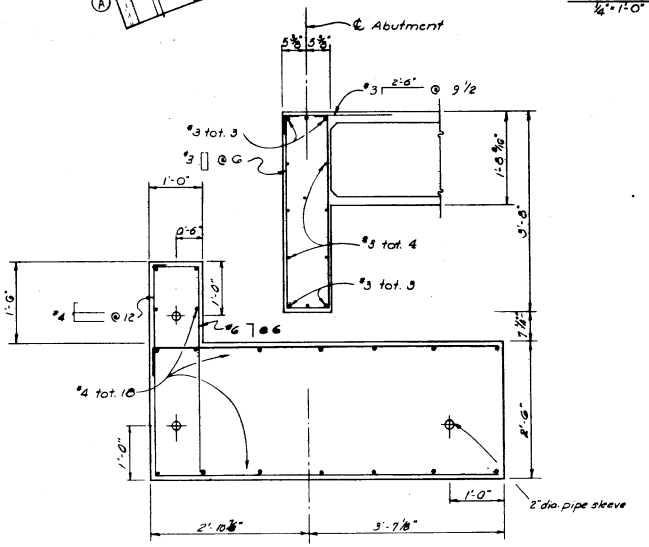

SECTION A-A

1" = 1'-0"

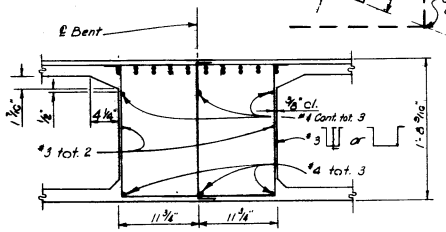

SECTION B-B

1 1/2" = 1'-0"

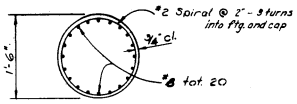

SECTION C-C

1" = 1'-0"

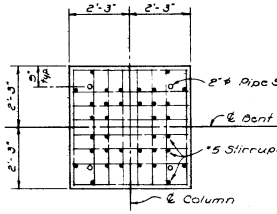

FOOTING PLAN

BENT DETAILS

1/2" = 1'-0"

PROFESSOR OF CIVIL ENGINEERING — REGISTERED CIVIL ENGINEER NUMBER 11868

BRIDGE DEPARTMENT	DESIGN SECTION	UNIVERSITY OF CALIFORNIA, BERKELEY COLLEGE OF ENGINEERING DEPARTMENT OF CIVIL ENGINEERING DIVISION OF STRUCTURAL ENGINEERING AND STRUCTURAL MECHANICS
Project Engineer	James E. Bouwkamp	
DESIGN	by R.S. Wilson 9/69	TWO-SPAN BOX GIRDER MODEL
	Checked E. Nielsen 10-69	
DETAILS	by S. Yamaguchi 10-69	
	Checked E. Nielsen	SHEET 1 OF 4
QUANTITIES	by	
	Checked	

WO 624123
CU 14030

A-1

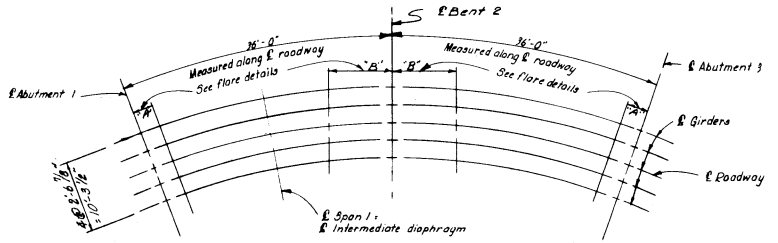

GIRDER LAYOUT
1/8 = 1'-0"

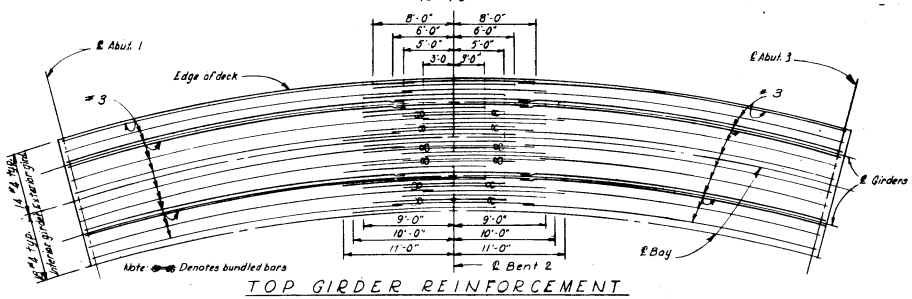

TOP GIRDER REINFORCEMENT
No Scale

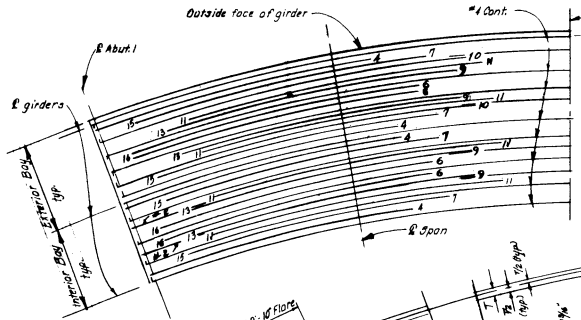

Note: All girder reinforcement #4 unless noted otherwise. Numbers at ends of bars indicate distance in ft. from ℄ Span.

BOTTOM GIRDER REINFORCEMENT
No Scale

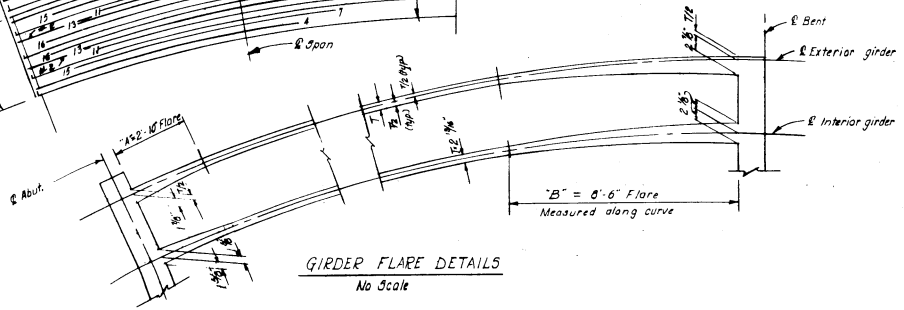

GIRDER FLARE DETAILS
No Scale

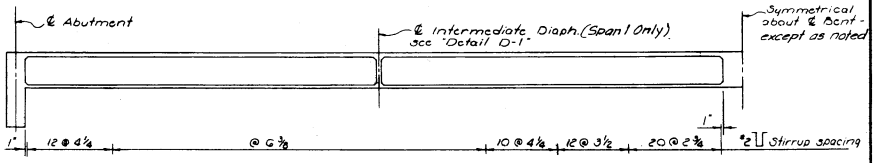

PART LONGITUDINAL SECTION
3/8" = 1'-0"

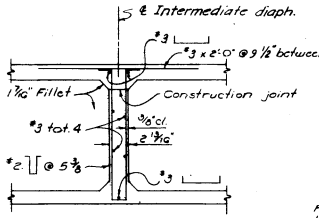

DETAIL D-1
1 1/2" = 1'-0"
(Span 1 Only)

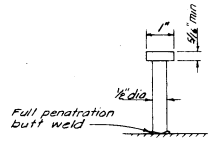

STUD CONNECTOR
No Scale

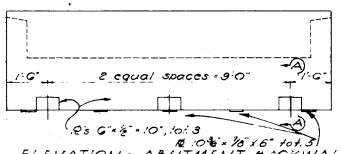

ELEVATION - ABUTMENT BACK WALL
1/2" = 1'-0"

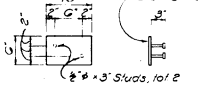

BEARING PLATE DETAILS
1" = 1'-0"

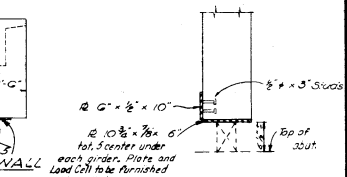

SECTION A-A
1" = 1'-0"

PROFESSOR OF CIVIL ENGINEERING — REGISTERED CIVIL ENGINEER NUMBER 11552

BRIDGE DEPARTMENT DESIGN SECTION		
Project Engineer	James E. Taylor	
DESIGN	In K.J. Watanabe 7/69	
	Chkd. G. Swanson	
DETAILS	In S. Yamaguchi 12-69	
	Chkd. G. Swanson	
QUANTITIES	In	
	Chkd.	

UNIVERSITY OF CALIFORNIA, BERKELEY
COLLEGE OF ENGINEERING
DEPARTMENT OF CIVIL ENGINEERING
DIVISION OF STRUCTURAL ENGINEERING AND STRUCTURAL MECHANICS

TWO-SPAN BOX GIRDER MODEL

SHEET	OF
2	4

A-2

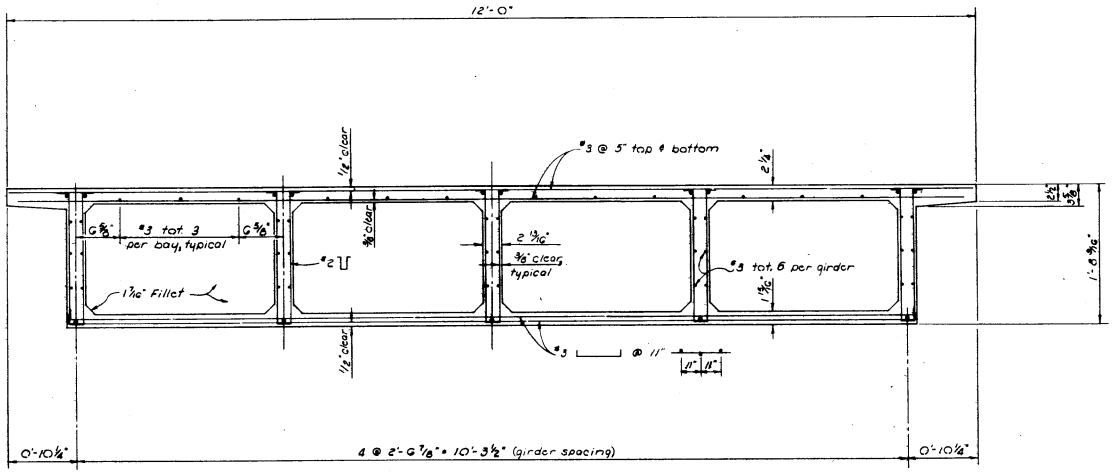

TYPICAL SECTION
1½" = 1'-0"

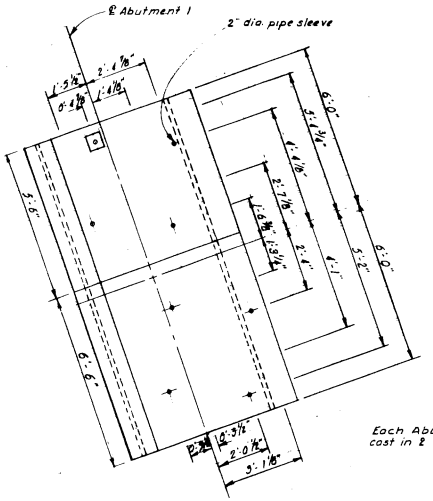

WEST ABUTMENT
½" = 1'-0"

Note: For main girder reinforcement see Sheet 2 of 4

Each Abutment will be cast in 2 sections

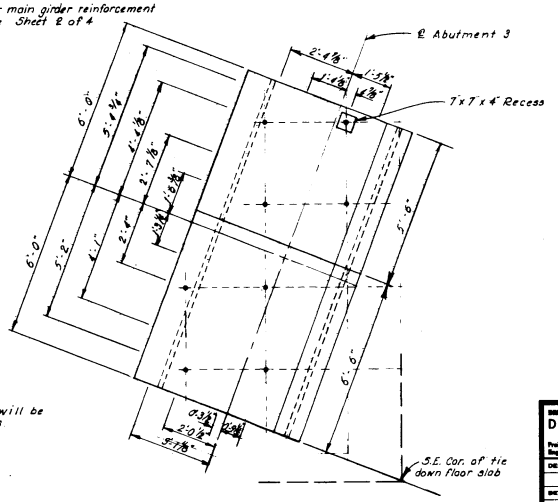

EAST ABUTMENT
½" = 1'-0"

GENERAL NOTES

Design: AASHO dated 1969 with revisions and as supplemented by Bridge Planning and Design Manual

Live Loading: H S20-44 and alternative

Reinforced Concrete: f_s = 24,000 p.s.i., except
f_s = 20,000 p.s.i. in transverse deck slabs and stirrups
f_c = 1,300 p.s.i., except
f_c = 1,200 p.s.i. in transverse deck slabs.
n = 10

Structural Steel: f_s = 20,000 p.s.i.

PROFESSOR OF CIVIL ENGINEERING — REGISTERED CIVIL ENGINEER NUMBER 11986

BRIDGE DEPARTMENT
DESIGN SECTION
Project Engineer: J. E. Culvi
DESIGN — In: R.S. Watanabe 9/69 — Checked: T. Davidson
DETAILS — In: S. Yamaguchi 10-69 — Checked: T. Davidson
QUANTITIES — In: — Checked:

UNIVERSITY OF CALIFORNIA, BERKELEY
COLLEGE OF ENGINEERING
DEPARTMENT OF CIVIL ENGINEERING
DIVISION OF STRUCTURAL ENGINEERING AND STRUCTURAL MECHANICS

TWO-SPAN BOX GIRDER MODEL

SHEET 3 OF 4

WO
CU

Disregard prints bearing earlier revision dates →

REVISION DATES (PRELIMINARY STAGE ONLY)

A-3